



Towards autonomous mapping in agriculture: A review of supportive technologies for ground robotics

Diego Tiozzo Fasiolo, Lorenzo Scalera*, Eleonora Maset, Alessandro Gasparetto

Polytechnic Department of Engineering and Architecture, University of Udine, via delle Scienze, 206, 33100, Udine, Italy



ARTICLE INFO

Article history:

Received 10 January 2023
Received in revised form 30 June 2023
Accepted 22 August 2023
Available online 23 August 2023

Keywords:
Mobile robotics
Agriculture
Localization
Mapping
Path planning
Artificial intelligence

ABSTRACT

This paper surveys the supportive technologies currently available for ground mobile robots used for autonomous mapping in agriculture. Unlike previous reviews, we describe state-of-the-art approaches and technologies aimed at extracting information from agricultural environments, not only for navigation purposes but especially for mapping and monitoring. The state-of-the-art platforms and sensors, the modern localization techniques, the navigation and path planning approaches, as well as the potentialities of artificial intelligence towards autonomous mapping in agriculture are analyzed. According to the findings of this review, many examples of recent mobile robots provide full navigation and autonomous mapping capability. Significant resources are currently devoted to this research area, in order to further improve mobile robot capabilities in this complex and challenging field.

© 2023 The Author(s). Published by Elsevier B.V. This is an open access article under the CC BY license (<http://creativecommons.org/licenses/by/4.0/>).

1. Introduction

Nowadays, the research interest in precision agriculture is growing since global warming, climate change, and population increase are demanding the production optimization, waste minimization, and sustainability enhancement. Climate change is indeed increasing weather fluctuations, natural disasters, and desertification, thus making agriculture production more challenging (Abbass et al. [1]). The agricultural demand is also stressed by the population increase, which is expected to grow from 7 to 10 billion in 2050, as predicted by the United Nations (Searchinger et al. [2]). Moreover, the 70% of the world population is supposed to live in urban areas by 2050, leading to a lack of rural workers (Phasianam et al. [3]). As a result, the demand for automation is growing, and novel strategies and technologies are needed not only to optimize farming productivity, but also for monitoring and inspecting plants and crops (Oliveira et al. [4]).

Mobile robotics can be of extreme importance in the context of precision agriculture [5,6] to automate different tasks (e.g., harvesting, weeding, sowing, and planting), and to boost production yield, while minimizing the waste of resources (e.g., water, nutrients, and pesticides), as stated by Elsayed et al. [7]. Sensorized mobile robotic solutions are increasingly used also for mapping and monitoring, since they can detect with high accuracy the spatial heterogeneity of agricultural terrains and crops.

Traditional remote sensing techniques adopted to perform mapping in agriculture are generally based on images taken by

satellites [8–10], aircrafts [11], and unmanned aerial vehicles (UAVs) [12,13]. Alongside these technologies, which can mainly provide data from a top view, ground mobile robots are starting to be used for monitoring and mapping in the complex operational context of agriculture. Robotic solutions, indeed, can acquire data from crops and plants at a close range and from different viewpoints, are less weather dependent than airborne platforms, are not subjected to strict legislative regulations, and have a higher payload with respect to UAVs.

In this work, we provide a critical review of the supportive technologies for ground mobile robots for autonomous mapping in the challenging field of agriculture, by building on the work by Tiozzo et al. [14]. This article differs from existing reviews in terms of its focus: autonomous mapping applications in agriculture. With *autonomous mapping* we refer to the ability of a mobile robotic system to acquire data and build a map of the surrounding environment without external intervention. More in detail, the mapping application is here focused on the monitoring and inspection of real-world agricultural crops and plants. We consider as *supportive technologies* both hardware (platforms and sensors), and software (localization, path planning, and artificial intelligence methods) supporting the purpose of mapping in agriculture. In this survey, we propose to address the following research questions:

- What are the state-of-the-art hardware technologies for autonomous robotic mapping in agriculture?
- What are the modern localization and mapping approaches for mobile robotics in agriculture?

* Corresponding author.

E-mail address: lorenzo.scalera@uniud.it (L. Scalera).

- What are the path planning strategies for autonomous navigation in agriculture?
- How is artificial intelligence applied for robotic mapping and monitoring purposes in agriculture?
- What are the future developments and challenges to improve autonomy and reliability of robotic platforms in agriculture?

Several works assessing mobile robotics for agriculture can be found in the literature. However, to the best of our knowledge, the existing reviews are either out of the topic of this paper, out of date, or narrow in scope. Table 1 presents the review papers written on mobile robotics in agriculture over the last five years, which are more related to the topic of this article. A broad introduction to robotics applications for monitoring and phenotyping in precision agriculture is provided in [15–17], referring to the technologies developed in the last 20 years. The three aforementioned publications cover destructive measurements for plant inspection (e.g., leaf picking by robotic arms) in addition to mobile robotic systems. On the contrary, in the work by Sishodia et al. [18] particular focus is given to non-destructive techniques through remote sensing technologies. While mobile robots are briefly mentioned in [18], the majority of the methods described in that article are designed to work with data from sensors installed in the field or from aerial and satellite systems.

Robotic platforms exploited for field operations are described in [4,19–21], focusing, however, on multipurpose robots that were not primarily designed for inspection and monitoring. Insights on sensors needed by robotic platforms to perform monitoring tasks can be found in [22,23], with special focus on the work by Guo et al. [24] that applies light detection and ranging (LiDAR) technology for three-dimensional observations. Although centered on sensing technologies, these articles provide little information on how to build a three-dimensional map, especially when employing robots as mobile mapping systems. Furthermore, simultaneous localization and mapping (SLAM) methods used by mobile robots in agriculture and forestry are discussed in [25–27]. However, these papers cope with the SLAM problem only for navigation, with no discussion on the issues posed by the complex operational context and no explanation on how the obtained map can be useful for agricultural purposes.

The problem of autonomous navigation for mobile robots in agriculture is addressed in the work by Santos et al. [28], and expanded by Li et al. [29] for navigation in orchards, and by Hrabar et al. [30] for vineyards. Moreover, an overview of crop row navigation techniques is given by Bonadies et al. [31]. Please note that these publications are confined to strategies suited to a specific scenario, and do not provide insights on their applicability in other environments. The availability of similar navigation techniques for unmanned aerial vehicles and quadrupedal robots is reported in the works [12,32], respectively.

The aforementioned articles discuss what characteristics a mobile robot needs to be autonomous, but they do not furnish details about how to use the onboard sensors for monitoring and mapping. Furthermore, computer vision techniques in agricultural automation are explored by Tian et al. [33], but only the image acquisition methods and sensors are classified, dealing marginally with image-based deep learning algorithms. Future uses of deep learning in agricultural production management based on large-scale data are discussed by Darwin et al. [34], and additional information on the use of artificial intelligence techniques in precision agriculture can also be found in the works cited in [6,35,36]. These studies are helpful for understanding the challenges that artificial intelligence techniques need to face in different agricultural scenarios. However, there is a lack of information on the advantages and disadvantages of mobile robots as well as

discussion regarding the viability of the suggested methods on these platforms.

Finally, the literature reports works in which the importance of big data and Internet of Things applications to optimize agricultural production is stressed, as in [1,2,5]. In the latter three studies, though, terrestrial, aerial sensors and satellites take precedence over autonomous mobile platforms.

In this review, we cover the aspects that should be considered in the development of an autonomous mobile robot for inspections in agricultural environments. Moreover, we describe real-world operations in complex and challenging scenarios. The main contributions of this work are: (a) a comprehensive categorization and comparison of hardware systems that characterize a mobile robotic mapping platform to be used in agriculture; (b) a discussion on standard localization techniques and cutting-edge alternatives to handle the challenges posed by complex agricultural scenarios; (c) an extension to the mapping problem to include the information useful for phenotyping purposes; (d) an overview of how classic path planning methods need to be extended and modified to ensure their robustness even in these challenging environments; and (f) a selection of artificial intelligence (AI) methods for agricultural perception, which have been tested by mobile robots in the field. As a conclusion, we identify current trends, highlight unexplored paths in the literature, and suggest future research directions.

Fig. 1 summarizes the proposed classification of fundamental aspects to be considered for autonomous mobile robotic mapping. First, the robotic platform requires computing capabilities and onboard sensors to gather geometric, visual, and spectral data from the surrounding scenario. To georeference the collected data and produce a map of the environment, a robust and accurate localization strategy should be applied. Moreover, the robot needs reliable path planning strategies for autonomous navigation purposes. Finally, thanks to AI, the robot can recognize and classify objects in the explored environment.

This article is structured as follows. In Section 2, the methodology adopted for the literature review is presented. In Section 3, robotic platforms and sensors for autonomous mapping in agriculture are described. Section 4 deals with the localization problem and the reconstruction of maps for monitoring purposes in agriculture. Global and local path planning approaches, as well as exploration strategies adopted in agricultural environments are addressed in Section 5. Section 6 discusses recent applications of data-driven pattern recognition approaches, mainly based on images and three-dimensional geometric data, to agricultural monitoring and mapping tasks. Section 7 highlights future trends and research directions. Finally, the conclusions are given in Section 8.

2. Methodology

We consulted the Scopus database and analyzed the scientific articles published from January 2012 to December 2022. The following combinations of words were used in searching within article titles, abstracts, and keywords: “agriculture” AND “artificial intelligence” AND “mapping” (140 papers found), “agriculture” AND “artificial intelligence” AND “mobile robot” (15 papers), “agriculture” AND “autonomous” AND “navigation” (480 papers), “agriculture” AND “localization” AND “mapping” (149 papers), “agriculture” AND “mobile robot” (391 papers). A total number of 1175 works, including multiple counts of the same paper, were found. A paper belonging to different queries is counted in all the queries. Uniqueness is then checked by importing the results from Scopus to the Mendeley Desktop software v.1.19.8 and removing duplicates with the appropriate tool. A total of 1031 unique papers was found.

Table 1

Review papers and their focus on the topic of mobile robotics in agriculture over the last five years.

Author	Year	Ref.	Focus of the review
Monitoring			
Ammoniaci et al.	2021	[15]	Monitoring techniques and data processing for precision viticulture
Atefi et al.	2021	[16]	Robotic technologies for plant phenotyping
Botta et al.	2022	[17]	Perception and tasks in precision agriculture
Sishodia et al.	2020	[18]	Applications of remote sensing in precision agriculture
Platforms and sensors			
Duckett et al.	2018	[19]	Robotics in Agri-Food industries
Fountas et al.	2020	[20]	Robotic platforms for field operations
Guo et al.	2020	[24]	LiDAR sensor observations of agricultural environments
Magalhães et al.	2022	[22]	Active perception for fruit harvesting robots
Oliveira et al.	2021	[4]	Advances in agricultural robotics
Tardaguila et al.	2021	[23]	Smart applications and digital technologies in viticulture
Vougioukas et al	2019	[21]	Advances in agricultural robotics
Localization			
Aguiar et al	2021	[25]	Simultaneous localization and mapping in agriculture and forestry
Ding et al.	2021	[26]	Simultaneous localization and mapping in agriculture
Navigation and path planning			
Bonadies et al.	2019	[31]	Crop row navigation methods
Ferreira et al.	2022	[32]	Localization, mapping, and path planning for quadruped robots in vineyards
Gao et al.	2018	[27]	Localization, mapping, and path planning for wheeled robots in agriculture
Gyagenda et al	2022	[12]	UAV navigation techniques
Hrabar et al.	2021	[30]	Autonomous navigation in vineyards
Li et al.	2021	[29]	Autonomous navigation in orchards
Santos et al.	2020	[37]	Path planning for ground robots in agriculture
Artificial intelligence			
Darwin et al.	2021	[34]	Recognition of bloom in crop images using deep learning models
Linaza et al.	2021	[35]	Data-driven artificial intelligence applications for precision agriculture
Pathan et al.	2020	[36]	Artificial cognition for applications in smart agriculture
Subeesh et al.	2021	[6]	Precision agriculture using artificial intelligence and internet of things
Tian et al.	2020	[33]	Computer vision in precision agriculture
Other			
Abbass et al.	2022	[1]	Climate change impacts and sustainable mitigation measures
Goel et al.	2021	[5]	Internet of things and data-driven technology in smart agriculture
Searchinger et al.	2019	[2]	Solutions for sustainable food production

The trend of the number of published articles over the years according to the keyword search is shown in Fig. 2 (a paper belonging to different combinations of keywords can be counted multiple times). As it can be seen from the figure, the trend of research articles including localization and mapping issues, and particularly the use of mobile robots in agriculture, is fast increasing, with most of the papers published within the last four years. The green line of the graph, which refers to the keywords search “agriculture” AND “artificial intelligence” AND “mobile robot”, is rather stationary. This shows that mobile robots in agriculture are still not considerably relying on artificial intelligence technologies, which have been instead increasingly applied in several fields in the last decade.

From the total number of publications retrieved, we then selected only the ones that pertain to autonomous mapping. Even though not all the robotic solutions discussed in this article are capable of accurately reconstructing an agricultural environment in 3D, they are still mentioned if they implement novel techniques for localizing the robot, navigating in the field, or extracting information from the acquired data that could make the mobile robot more autonomous during a mapping session. Works addressing the use of mobile robots to specifically perform agricultural tasks such as harvesting or pruning are not included, unless the robot is equipped with particularly useful sensors and capabilities for mapping and monitoring.

The works analyzed in this review are chosen to limit the scope of the paper to wheeled and tracked mobile robots.

Quadrupedal robots can be also adopted for agricultural monitoring tasks, as stated by Ferreira et al. [32], but are not included in this survey. The outcome of the whole shortlisting process was the selection of 148 articles.

3. Hardware technologies

In this section, the hardware technologies currently available for mapping and surveying agricultural environments are reviewed. We describe mobile robotic platforms, sensors, and embedded computers to be used onboard.

3.1. Robotic platforms

Robotic platforms, also referred to as unmanned ground vehicles (UGVs), are designed with diverse kinematic solutions to better adapt to rough agricultural terrains. These solutions comprise: tracked skid-steered (Fig. 3(a)), wheeled skid-steered (Fig. 3(b)), four-wheel steering (Fig. 3(c)), and Ackermann steering (Fig. 3(d)) vehicles. Tracked skid-steered vehicles (e.g., Gao et al. [38]) are mainly used to avoid getting stuck due to sinking in soft ground, since tracks, compared to wheels, reduce sinkage and increase traction. On the contrary, tracked mobile robots are not utilized in wheat fields or similar crops, to prevent the compaction of plants. To clarify, both tracked and wheeled skid-steered are differentially driven solutions. The Ackermann steering geometry

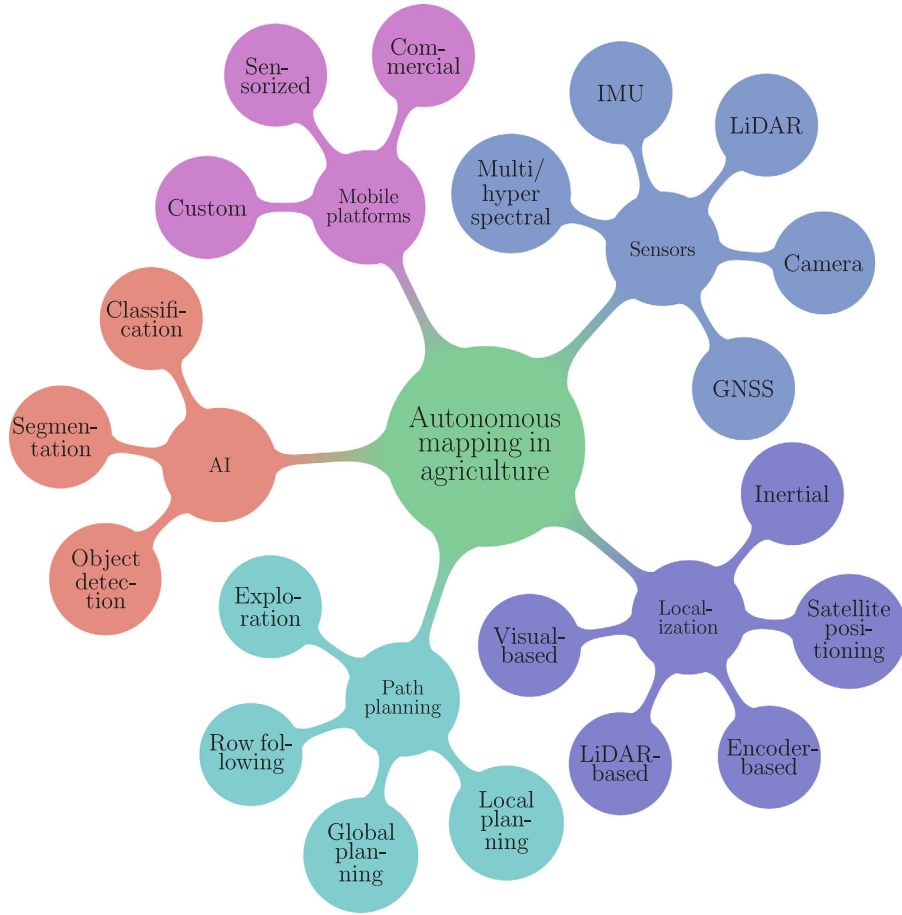


Fig. 1. Overview of the topics covered in this survey.

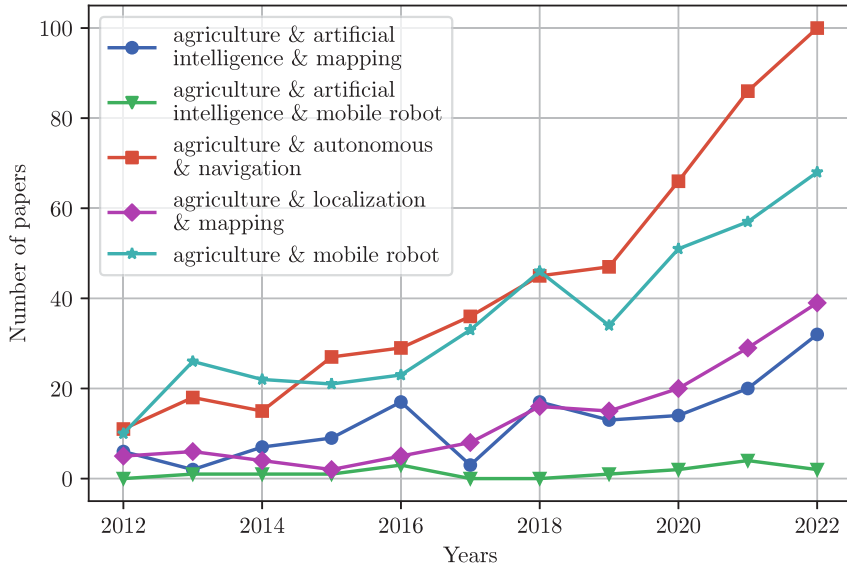


Fig. 2. Number of papers over the year of publication, from January 2012 until and including December 2022, database Scopus.

is widespread (e.g., [39–42]), as it overcomes the need for wheels to slip sideways when performing a curve. Skid-steered solutions (e.g., [43,44]) and four-wheel steering solutions (e.g., [45–48]) are advantageous in small or cluttered environments. For these reasons, skid-steered and four-wheel steering kinematic solutions are frequently employed in under-canopy (Manish et al. [49]) and greenhouse navigation (Baek et al. [50]).

Robotic platforms can be divided into three main categories: custom mobile robots, such as the platforms designed in [49,53–56] (Fig. 4(a), 4(c), 4(g), 4(h), and 4(i)), sensorized agricultural machines, like the ones developed in [57,58] (Figs. 4(b) and 4(d)), and commercial solutions, including those described in [59–61] (Figs. 4(e) and 4(f)).

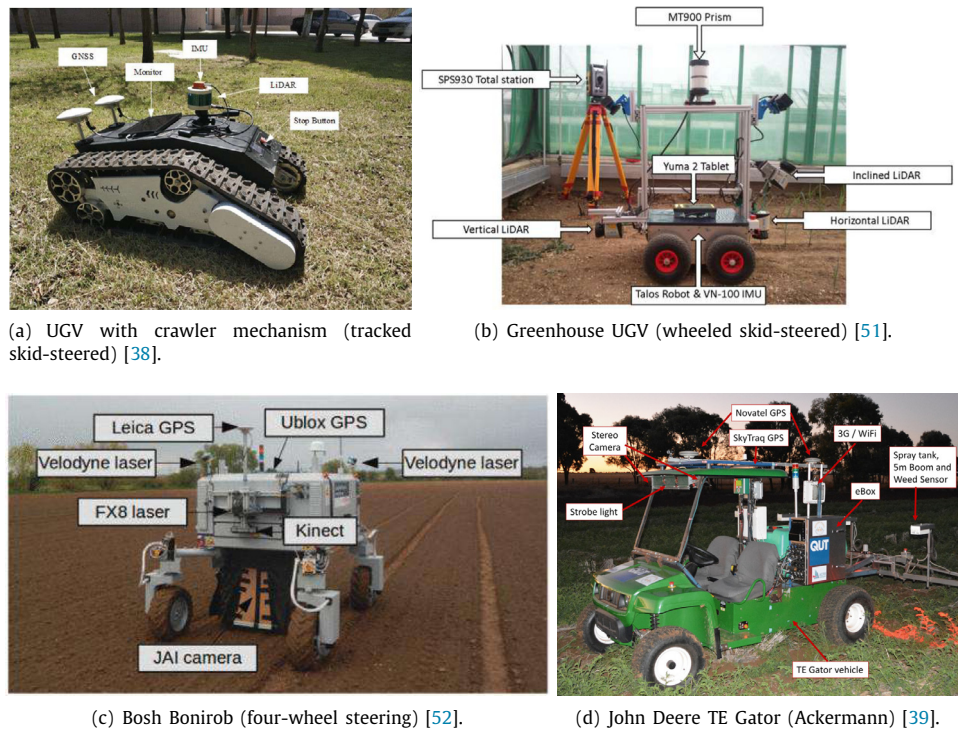


Fig. 3. Examples of robotic platforms with different kinematic solutions and sensor suites.

An example of a custom mobile robot used for fruit monitoring in precision agriculture is shown in the work by Beloiev et al. [62]. That robotic platform is built with 3D printed components and exploits the Ackerman steering solution. Another interesting custom robot (Fig. 4(a)) is RobHortic [53]. It uses proximal sensors to inspect the presence of pests and diseases in horticulture crops, while being controlled remotely. Thanks to a calibrated artificial illumination system, its measurements are unaffected by natural light. Furthermore, PhenoBot [63] introduces the innovation of carrying sensors on a telescoping and self-balancing mast to collect agricultural data at various heights. The mast is placed between the front and the rear part of PhenoBot, which are connected by an articulated steering joint. Moreover, Pire et al. [55] present the robot used to acquire the Rosario dataset, which contains stereo images and data from localization sensors captured in soybean fields. That robotic system features four batteries that are charged by photovoltaic cells placed at the top of the vehicle, as is shown in Fig. 4(h).

The second category includes agricultural vehicles and tractors equipped with drive-by-wire systems and sensors. Examples of these machines are reported in Figs. 3(d) and 4(d). In the work by Ball et al. [39], an electric John Deere TE Gator with Ackermann steering, shown in Fig. 3(d), is made completely autonomous by means of a RoPro Design interface. Furthermore, in the work by Kai et al. [64], an electric-driven agricultural tracked robot is equipped with an Advantech MIC-7700 industrial computer as control unit.

The third group considers commercial mobile robots utilized to map agricultural areas. These systems are described in Table 2, including dimensions, weight, travel speed, and driver information. One of the most widespread platforms is the Husky A200 by Clearpath Robotics (Fig. 4(f)), used, for example, in [65–67]. The Husky A200 is a medium-sized UGV, available with a sensor suite integrated directly by the manufacturer, comprising Global Navigation Satellite System (GNSS) receiver, LiDAR sensor, stereo camera, and inertial measurement unit (IMU). A smaller

solution from Clearpath Robotics is Jackal (see e.g., [68,69]). Both these robots are provided with an onboard computer with the Robot Operating System (ROS) preinstalled, for out-of-the-box autonomous capabilities. Similar solutions are developed by AgileX Robotics, as for instance the Scout 2.0 used in Jiang et al. [70], which, contrary to the Husky robot, is equipped with suspensions and features four-wheel drive with independent motors (the Husky model has only two motors).

The commercial robots previously mentioned are sensorized mobile platforms designed for generic outdoor applications. Other companies build solutions specifically for agriculture. Among them, Thorvald (Fig. 4(e)), described by Fentanes et al. [46], can quickly be customized to adapt to a particular environment, such as a greenhouse, an open field, or a vineyard. Another interesting robot is Bonirob (Fig. 3(c)), developed by Bosch, Amazone, and the Osnabrück University of Applied Sciences [52]. Bonirob features a complete sensor suite and proved to be capable of building a large scale agricultural dataset, which details can be found in the work by Chebrolu et al. [52]. Moreover, Bonirob provides high maneuverability thanks to its four-wheel steering kinematic solution and makes use of visual servoing and a penetrometer to detect soil compaction.

The results of the literature review are summarized in the pie charts shown in Figs. 5 and 6. The 54.1% of mobile robotic platforms are customized solutions built for agricultural tasks, 31.7% are sensorized machines (e.g., tractors), and the remaining 14.2% are commercial robots. Regarding the kinematics solutions, the most widespread is the wheeled skid-steered (44.0% of the considered systems), followed by the Ackermann steering (35.7%). Four-wheel steering (11.4%), and tracked skid-steered robots (8.9%) are less common.

3.2. Sensors

In the following, the onboard sensors that can be used by a robotic platform to survey agricultural areas and crops are



Fig. 4. Examples of mobile robotic platform solutions.

Table 2
Commercial robotic platforms employed in the papers analyzed in this review.

Commercial robot	Kinematics [mm]	Dimensions [mm]	Weight [Kg]	Max speed [m/s]	Programming language	ROS	Ref.
AgileX Scout 2.0	Wheeled skid-steered	930 × 699 × 349	68	1.5	C++	✓	[70]
Bosh Bonirob	Omnidir.	1500 × 1000 × 500	400	2.22	C++, Python	✓	[52,71–75]
Clearpath Husky A200	Wheeled skid-steered	990 × 670 × 390	50	1	C++, Python, Matlab	✓	[37,43,60,65–67,76–85]
Clearpath Jackal	Wheeled skid-steered	508 × 430 × 250	17	2	C++, Python, Matlab	✓	[68,69,86,87]
CoroWare Explorer	Wheeled skid-steered	230 × 210 × 160	n.r.	0.6	C	✓	[88]
Robotnik Summit-XL	Wheeled skid-steered	720 × 614 × 416	65	3	C++, Python	✓	[89,90]
Saga Robotics Thorvald	Omnidir.	1500 × 1350	n.r.	n.r.	C++, Python	✓	[46,91,92]
Sterela Air-cobot	Wheeled skid-steered	1450 × 800 × 1200	230	2	n.r.	n.r.	[93]
Traxxas X-Maxx	Ackermann	518 × 417 × 419	4.2	13.5	n.r.	✗	[42,82,94]
Oz Naio Technologies	Wheeled skid-steered	1300 × 470 × 830	150	0.5	C++, Python	✓	[93,95]

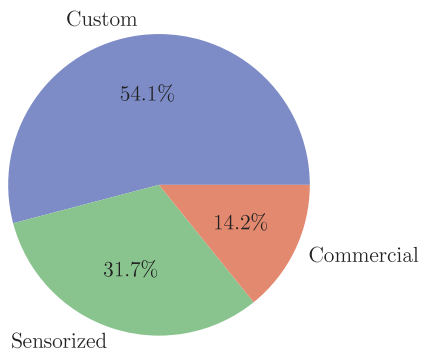


Fig. 5. Pie chart of the mobile robotic platforms classification.

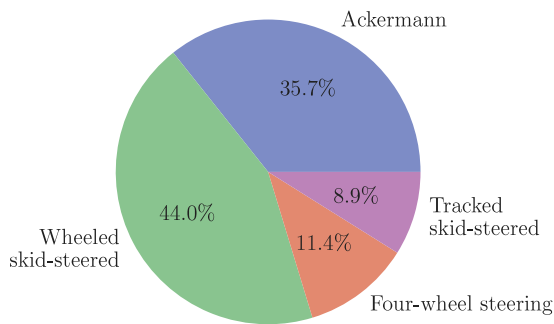


Fig. 6. Pie chart of the kinematics solution classification.

described. [Tables 3, 4](#) and [5](#) list the published specifications of the most common LiDAR, visual and spectral sensors used by mobile platforms in agriculture.

3.2.1. Direct georeferencing systems

Localization sensors are used for autonomous navigation and for the direct georeferencing of the acquired data. These systems are mainly based on GNSS and IMU technologies.

Nowadays, satellite-based localization systems are quite mature and cheap. Thus, GNSS receivers have found numerous applications in agriculture (e.g., tractor autonomous navigation [[96](#)]). In more detail, GNSS estimates the 3D absolute position (e.g., with respect to the world geodetic system WGS84) of the receiver by measuring the range from at least four satellites. The most well-known and employed GNSS constellation is the Global Positioning System (GPS), operated by the United States Department of Defense [[97,98](#)]. One of the main drawbacks of GNSS positioning lies in the low reliability in densely vegetated areas, due to multipath propagation of the signals that reduces the position accuracy when compared to clear sky conditions (Kaarinen et al. [[99](#)]).

In addition to the absolute position, by mounting three antennas on a mobile platform, it is possible to retrieve the 6-degree-of-freedom (DOF) pose of the robot, typically with an update rate of 1 Hz (Hirokawa et al. [[100](#)]). In [[57,101](#)], the authors estimate the vehicle yaw using methods based on multiple onboard GNSS receivers.

In agricultural applications, the attitude (roll pitch, yaw) of the robot is more often derived using a 9-DOF IMU, as discussed by Lan et al. [[102](#)]. The latter is a device that integrates a tri-axial accelerometer (measuring linear accelerations), gyroscopes (measuring angular rate), and a magnetometer (commonly used as a heading reference). IMU sensors typically output data at a rate of up to 1 kHz. However, in slowly moving systems, IMU data are usually acquired at lower frequencies to reduce the drift [[49,103](#)].

The size and weight of IMUs, together with their low power consumption, make them ideal for the integration even in a small robotic platform. Anyway, when mounting a 9-DOF IMU, it must be taken into account that a locally disturbed magnetic field might introduce inaccuracies in the orientation detected by the magnetometer. The amplitude of the disturbance is determined by the relative location and orientation of the measuring equipment in relation to ferromagnetic materials, permanent magnets, and strong currents (Vitali et al. [[104](#)]). Additionally, extrinsic calibration (the process of aligning and recording the reference frames) should be performed to estimate the position of the IMU relative to the center of rotation of the robot or the sensor (e.g., LiDAR) to which the IMU is coupled. Otherwise, the position, velocity and acceleration readings are inconsistent and cannot be used for sensor coupling.

3.2.2. LiDAR sensors

Geometric information on vegetation is mainly retrieved by means of LiDAR sensors, which allow to reconstruct the map of the surrounding scenario in the form of a point cloud. The LiDAR working principle is based on the measurement of the time taken by a laser pulse sent by the sensor and reflected by the environment to come back to the instrument. This approach to retrieve range measurements is implemented through micro-electro-mechanical systems or optical phased arrays. LiDAR sensors usually employed in agriculture are either spindle-type (a 360° field of view is guaranteed by a optomechanical rotating system) or hybrid solid-state (that achieve deflection through an internal moving mirror). Moreover, LiDAR systems can be distinguished in 2D (28.1% of the considered works, [Fig. 7](#)) or 3D (16.7%) according to whether they have a single laser ring that performs measurements on a plane, or multiple rings. As shown in [Table 3](#), the most widespread commercial solutions among the 2D and 3D LiDAR devices are the SICK LMS 111 and the Velodyne VLP16, respectively.

The high measurement range of LiDAR sensors (e.g., up to 100 m for the common Velodyne VLP16) enables their use for mapping in both closed environments, such as greenhouses [[41, 50,51,70,81,87,105](#)], and outdoor scenarios, such as vineyards [[37,47,66,76–78,82,83,90,91,101,103,106–115](#)] and orchards [[38,40,44,79,80,88,95,116–120](#)].

2D LiDAR sensors are useful for localization and collision avoidance, such as in the presence of moving humans or dynamic barriers in the robot environment [[37,41,47,83,121–124](#)]. To extend their applicability to build 3D point clouds, 2D LiDAR sensors must be mounted in a way that the laser plane is placed orthogonal to the robot trajectory ([Fig. 8](#)), as in [[56,101,107, 113,118,125–127](#)]. However, 3D LiDAR devices constitute a more suitable solution for map reconstruction. In fact, these sensors directly provide a dense point cloud of the surroundings and have a larger field of view (FoV) in comparison to 2D LiDAR devices ([Table 3](#)). The main limitation of LiDAR solutions in outdoor environments arises when performing the survey in rainy conditions, as raindrops may reflect or refract laser beams, resulting in noisy and inaccurate point clouds (Wichmann et al. [[128](#)]).

In these conditions, radar has advantages as a robotic perception modality with respect to LiDAR, since it is less susceptible to dust, fog, rain, and snow (Wichmann et al. [[128](#)]). For instance, the PELICAN radar tested by Rouveure et al. [[129](#)] provides a view of 360° of the surroundings in a range of 5 : 100 m. However, this kind of radar can only build 2D images of the surrounding environment. Besides, radars have better penetration in vegetation than LiDAR sensors and cameras, and can detect occluded targets (Cheng et al. [[130](#)]).

Table 3

Overview of the LiDAR sensors integrated in the robotic platforms covered in this review. The * indicates hybrid solid-state LiDAR sensors.

LiDAR sensor model	Resolution [deg]	FoV [deg]	Scan rate [Hz]	Measurement range [m]	Accuracy [mm]	Ref.
2D LiDAR sensor						
HOKUYO URG-04LX-UG01	0.36°	240°	55	0.02 : 5.6	±30	[82]
HOKUYO UST-20LX	0.25°	270°	200	0.06 : 20	±40	[105]
HOKUYO UTM-30LX	0.25°	270°	200	0.01 : 30	±50	[43,44,47,54,88,90,91,120,126,131]
SICK LMS 111	0.25° / 0.5°	270°	25/50	0.5 : 20	±30	[40,58,65,66,123,127,132–137]
SICK LMS 151	0.25° / 0.5°	270°	25/50	0.5 : 50	±12	[124]
SICK LMS 200	0.25° / 0.5° / 1°	180°	75	0 : 80	±15	[106,125]
SICK LMS 291	0.25° / 0.5° / 1°	180°	75	0 : 80	±35	[136]
SICK LMS 511	0.1667°	190°	100	0.2 : 80	±50	[51,135,138]
SICK TIM 310	1°	270°	15	0.05 : 4	±30	[115]
SICK TIM 561	0.33°	250°	15	0.05 : 10	±20	[122]
SICK TIM 781	0.33°	270°	15	0.05 : 25	±60	[41]
3D LiDAR sensor						
HOKUYO YVT-X002	n.r.	210° × 40°	20	0.3 : 25	±100	[139]
Nippon Signal FX-6*	n.r.	50° × 60°	8/16	0 : 16		[140]
Nippon Signal FX-8*	0.63° / 1.43° × 0.86° / 2.06°	60° × 50°	4/20	0.3 : 5	±50	[52]
Ouster OS1-16	0.1° : 0.2° × 2.075°	360° × 33.2°	10 : 20	0.8 : 120	n.r.	[141]
Robosense RS-LiDAR-32	0.1° : 0.4° × 0.33°	360° × 40°	5 : 20	0.4 : 200	±30	[142]
Velodyne VLP16	0.1° : 0.4° × 2°	360° × 30°	5 : 20	0 : 100	±30	[38,45,49,52,64,72,73,87,91,105,117,141,143]
Velodyne HDL32E	0.1° : 0.4° × 1.33°	360° × 40°	5 : 20	1 : 100	±20	[57]
Velodyne HDL64E	0.08° × 0.04°	360° × 26.8°	5 : 14	0 : 120	±20	[144,145]

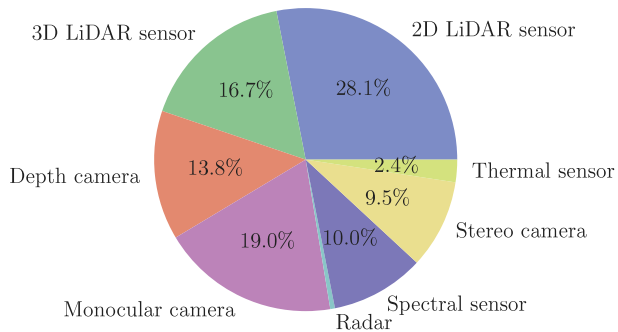


Fig. 7. Pie chart of the onboard sensors. Many platforms use more than one sensor at the same time.

3.2.3. Visual sensors

Visual sensors offer RGB images that can be used for localization, obstacle avoidance, and mapping. Moreover, a live video transmitter and a camera system installed on the robot are beneficial for manual piloting and viewing the robot in operation [146,147].

As summarized in Fig. 7, visual sensors include monocular (19.0% of the analyzed papers), stereo (9.5%), and depth cameras (13.8%). Stereo cameras comprise two image sensors, perceiving depth simulating human binocular vision. In low-textured scenes, depth accuracy of the stereo vision can be improved using infrared (IR) patterns, as with the Intel RealSense D435 exploited in [41,45,62,68,148–150] (Table 4). Aghi et al. [68] use the RGB-D images from that camera to implement a local motion planner for autonomous navigation in vineyards, whereas the camera is used for 3D reconstruction by Vulpi et al. [150]. However, it is worth noting that camera sensors making use of IR light are most likely applied for indoor navigation, as the maximum measurable depth is low and the technology is sensitive to sunlight.

Depth cameras provide range values by means of structured light or time-of-flight (ToF) sensors. Among depth cameras, one

of the most widespread devices in agricultural scenarios is the Kinect V2, used for instance in [43,52,89–91,105,151–153]. For instance, the Kinect V2 is used as a mobile laser scanner by Rosell-Polo et al. [152] and adopted by Matsuzaki et al. [151] to perceive the types of obstacles for autonomous navigation purposes.

In the context of mapping, monocular cameras can be used to create a 3D reconstruction of the surrounding area using a structure-from-motion (SfM) approach, which integrates pictures collected from many viewpoints (Sylvain et al. [154]). In addition, a multi-camera system, composed of many sensors externally calibrated, can be employed to gain a broader field of view, as in [39,150]. Nowadays, a 360° field of view can be obtained through commercial systems, such as the Giroptic 360CAM mounted on the sensorized tractor in the work by Kragh et al. [57] to acquire a dataset with both static and moving obstacles, or the Ladybug3 camera (Fig. 4(i)) used by Underwood et al. [56] as a support for obstacle avoidance and crop row detection. However, no examples of omnidirectional or wide-field-of-view vision systems for visual odometry in agriculture are found in the literature.

Visual sensors are usually compact and operate adequately in textured environments. For outdoor applications, it must be taken into account that they are not suited for bad weather conditions or low light scenes, as stated by Patricio et al. [155]. Moreover, the measurement range of ToF cameras is considerably smaller than that of LiDAR sensors.

3.2.4. Spectral sensors

The spectral response of vegetation depends on the absorption of electromagnetic radiation by the pigments, and it represents an important indicator, in the context of agriculture, for characterizing the state of health of the plants (Bannari et al. [161]). To this end, analyzing the visible part of the light spectrum is not sufficient, and one should resort on the disparity in reflectance between the red and near-infrared (NIR) bands, as well as on the spectral reflectance in the transition zone (the so-called *red edge*) to gain important information regarding the vegetation status (French et al. [135]).

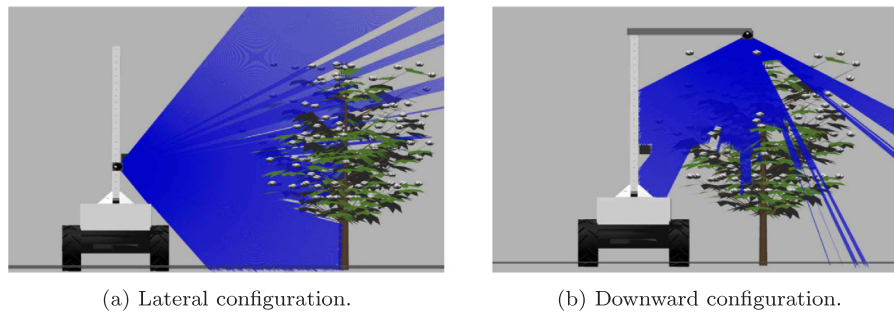


Fig. 8. Example of 2D LiDAR configurations adopted to build 3D maps [44].

Table 4

Overview of the visual sensors integrated in the robotic platforms covered in this review.

Visual sensor model	Technology	Resolution [pixel]	Pixel size [μm]	Fps [Hz]	Depth range [m]	Ref.
Monocular camera						
Canon EOS 600D	CMOS	5184 × 3456	4.29	3.7	x	[53]
Flir Blackfly S GigE	CMOS	720 × 540	6.9	291	x	[81]
Grasshopper3 GS3-U3-23S6C-C	CMOS	1920 × 1200	5.86	163	x	[45]
IDS UI-5240CP Rev.2	CMOS	1280 × 1024	5.30	60	x	[39]
Imaging Source DFK 21BUC03	CMOS	744 × 480	6	76	x	[116]
Logitech C920 PRO HD	CMOS	1080 × 720	3.98	30	x	[57,122,156]
Logitech Pro 9000	CMOS	1600 × 1200	n.r.	5	x	[88]
Mako G-125C	CCD	1292 × 964	3.75	30	x	[76]
Nikon D80	CCD	3872 × 2592	n.r.	5.89	x	[66]
Sony A7R	CMOS	7360 × 4912	4.88	60	x	[49]
Stereo camera						
FireWire Bumblebee2	CCD	640 × 480/1024 × 768	7.4/4.65	48/18	n.r.	[133]
Multisense S21 CMV2000	CMOS	1024 × 544	n.r.	10	1.5 : 50	[57]
Stereolabs ZED	CMOS	1920 × 1080/1280 × 720/ 672 × 376	2/4/8	30/60/100	0.5 : 25	[47,55,157,158]
Stereolabs ZED2	CMOS	2208 × 1242 : 672 × 376	2	15 : 100	0.3 : 20	[159]
360 camera						
Giroptic 360CAM	n.r.	1920 × 960/3840 × 1920	n.r.	25	x	[57]
Point grey Ladybug3	CCD (×6)	1616 × 1232 (each sensor)	4.4	16	x	[56]
Depth camera						
ifm O3M150	ToF	64 × 16	n.r.	50	n.r.	[160]
Intel RealSense D435/D435i	IR pattern	RGB 1920 × 1080, D 1280 × 720	1.4	30	0.3 : 3	[41,45,61,62,68, 148–150]
Intel RealSense L515	ToF	RGB 1920 × 1080, D 1024 × 768	n.r.	30	0.25 : 9	[62]
KinectV2	ToF	RGB 1920 × 1080, D 512 × 424	n.r.	30	0.5 : 4.5	[43,52,89–91, 105,151–153]

Specific spectral cameras are therefore built to capture visible and NIR wavelengths, usually exploited to compute vegetation indexes, i.e., combinations of image bands that enhance vegetation properties. The NDVI (Pettorelli et al. [162]), for instance, is the normalized difference between the reflectance in the red visible (670 nm), and in the NIR (780 nm) [163]. An area without vegetation gives NDVI values close to 0, whereas values close to 1 are found in correspondence of high density of leaves or healthy canopies. Moreover, the normalized difference red edge (NDRE), computed considering NIR and red edge wavelengths (730 nm), is sensitive to leaf chlorophyll content, plant vigor, and stress detection (Thompson et al. [163]). Several vegetation indexes are discussed by Poccas et al. in [164], where the authors analyze the use of each indicator for a variety of crop species and offer details on their benefits and drawbacks. Furthermore, the work by Dong et al. [165] provides instructions on how to adopt red-edge measurement to estimate leaf density using the leaf area index.

In 10.0% of the considered papers (Fig. 7), spectral sensors are taken into account, allowing to collect the data employed for vegetation index calculation. The radiometric resolution is the key parameter for the classification of spectral cameras into multispectral (less than 20 narrow bands), or hyperspectral (hundreds

of narrow bands). To obtain a radiometrically trustful reflectance map, multispectral cameras are provided with a light sensor that measures the incoming radiation from the sun. This information is subsequently exploited for the radiometric calibration of the captured images, that makes it possible to compare images taken with different illumination conditions. The light sensor, also known as sun or sky sensor, must be installed on the mobile robot looking upward and apart from active sensors to prevent interference (e.g., LiDAR sensors), as in [56,110,160].

Among the applications of mobile robots equipped with multispectral cameras, we can cite the work by Clamens et al. [89], where a multispectral camera is used in a vineyard to generate NDVI colored images. In [53,123], crop field images are acquired with the sensor pointing downward, the NDVI index is computed and thresholding is then applied to identify pixels that belong to vegetation, as shown in Fig. 9. Furthermore, the robot Bonirob (Fig. 3(c)), which features a four-channel multispectral camera onboard, is used to detect plants and assess the crop status by Fawakherji et al. [71], and to gather an open-access dataset of multispectral images by Chebrolu et al. [52]. The multispectral cameras employed in the aforementioned studies have a number of channels ranging from 4 to 8, as summarized in Table 5.

Table 5

Overview of the spectral sensors integrated in the robotic platforms covered in this review.

Spectral sensor model	Resolution [pixel]	Number of bands	Spectral range [nm]	Ref.
Multispectral camera				
JAI AD-130GE	1280 × 960	4	400 : 1000	[52,71]
Parrot Sequoia	1280 × 960	4	530 : 810	[123]
Silios Technologies CMS-V	1280 × 1024	8	550 : 830	[53,89]
Hyperspectral camera				
InSpectral-VNIR Infaimon SL	n.r.	133	410 : 1130	[53]
Resonon Pika II	n.r.	230	400 : 900	[56,144]
Thermal camera				
ThermaCAM FLIR P640	640 × 480	1	780 : 1000	[110,160]
Teledyne FLIR A65	640 × 512	1	750 : 1300	[57]
UDOO MIPI 5MP IR AF	2592 × 1944	1	780 : 1000	[42,82]
Agriculture-specific sensor				
Ag Leader Optrx Crop ^a	n.r.	n.r.	670 : 780	[108,118,134]
Apogee SI-131	1 × 1	1	800 : 1400	[135]
Apogee SI-421	1 × 1	1	800 : 1400	[110,160]
Crop Circle ACS-435	n.r.	3	670/730/780	[135]
SRS Meter Group ^b	n.r.	4	532 : 810	[137]

^aThe Optrx Crop sensor directly outputs NDVI and NDRE index values.^bThe central wavebands of SRS Meter Group are specific for NDVI and PRI indexes.

Hyperspectral cameras are adopted to capture data in orchards and crop fields in [53,56,96,144], respectively. The radiometric resolution of these sensors is remarkably higher than multispectral devices. For instance, the camera used in [56,144] is sensitive to wavelength in the range 400 : 900 nm, with a resolution of approximately 2 nm. The storage speed of the data logger, which needs to be sufficient to prevent data loss during acquisition, is one of these sensors main bottlenecks. For this reason, even though the InSpectral-VNIR device has a greater resolution, Cubero et al. [53] capture only 133 bands in the domain of 410 : 1130 nm.

Due to the large amount of data collected, post processing, and dimension reduction are often required to retrieve relevant information with both multispectral and hyperspectral cameras. In contrast, a solution for real-time processing is offered by spectroradiometers, which are sensors that collect sections of the light spectrum necessary for vegetative index calculations. They are employed, for example, by the robot Vinescout in a vineyard in [110,160]. The work by French et al. [135] describes the use of spectroradiometers for cotton phenotyping, whereas Perez-Ruiz et al. [137] present a comparable sensor to determine NDVI and Photochemical Reflectance Index (referred to as PRI and obtained with the 532 : 570 nm light spectrum) values on wheat canopies. However, in [135,137], the data are not analyzed online, and a post processing step is performed. Please note that sensors able to estimate crop health in real-time thanks to NDVI and NDRE indices are already available on the market. The Optrx Crop sensor, exploited for example in [108,118,127,134,166], is among them.

Moreover, thermal cameras (used only in 2.4% of the considered research works) allow one to obtain further information on vegetation, such as water state and stress. In particular, a review of current and potential uses of thermal sensors in precision agriculture can be found in the article by Khanal et al. [167].

Finally, the research work by Cubero et al. [53] shows that the NIR channel can be captured using standard digital RGB cameras. More in detail, replacing the red filter with a NIR one on a Canon EOS 600D camera provided equivalent findings to those achieved from multispectral cameras, and may be efficiently applied to crop health monitoring.

3.3. Cutting-edge embedded computers

Autonomous mapping is a task that requires perception, localization, and motion planning methods. Additionally, more advanced intelligence capabilities based, for example, on artificial neural networks can improve the mapping results, as will be explained in Section 6. To run those algorithms, the robot must be equipped with adequate computing power, provided by cutting-edge embedded computers. Common hardware solutions employed by mobile robots in the agricultural context are mainly based on Intel Core processors [38,41,46,51–53,64,65,75,84,86,117,136,139,140,147,168–174], often coupled with NVIDIA graphic boards [81,105,107,114,123,148,151,158,175–177]. ARM-based computing units are nowadays achieving computing capabilities that are suitable to accomplish several tasks, as demonstrated in [70,178]. Common ARM-based solution are Raspberry Pi and UDOO models, exploited in [62,111,131,179], respectively. As the size and weight of the computer are crucial factors in the design of mobile robots, Mini ITX motherboards, used in [43,60,133], are often an excellent alternative to ARM architectures.

In the last years, the advances in the computing power of embedded systems gave birth to the concept of Edge AI, which consists of running trained AI models on embedded computers online. In this context, Intel offers a family of hardware accelerators, used for instance by Zhang et al. [178], which are compatible with typical embedded computers such as the Raspberry Pi. To give an example, the Raspberry Pi 3 B+ can be improved with Neural Compute Sticks hardware accelerators (Figs. 10(a) and 10(b)). Similarly, the new hardware model Raspberry Pi 4 is used with the Google Coral USB accelerator by Simoes et al. [180].

Moreover, NVIDIA provides a family of embedded computers with dedicated GPU. Among the NVIDIA boards, one can find the Jetson TK1 and TX2, used respectively in [47,87,181], as well as the Jetson Nano (Fig. 10(c)), exploited in [50,76,149,182], and the Jetson AGX Xavier (Fig. 10(d)), used by Mazzia et al. [183]. The latter can be considered one of the most powerful solution among the computers used by mobile robots analyzed in this survey. The Jetson Nano is instead a cheaper solution designed with the goal of lowering the board dimensions and cost, while increasing energetic performance. Moreover, the recent Raspberry Pi 4, equipped with a ARM Cortex-A72 CPU, has a performance closer to the Jetson Nano. More detailed specifications of embedded systems

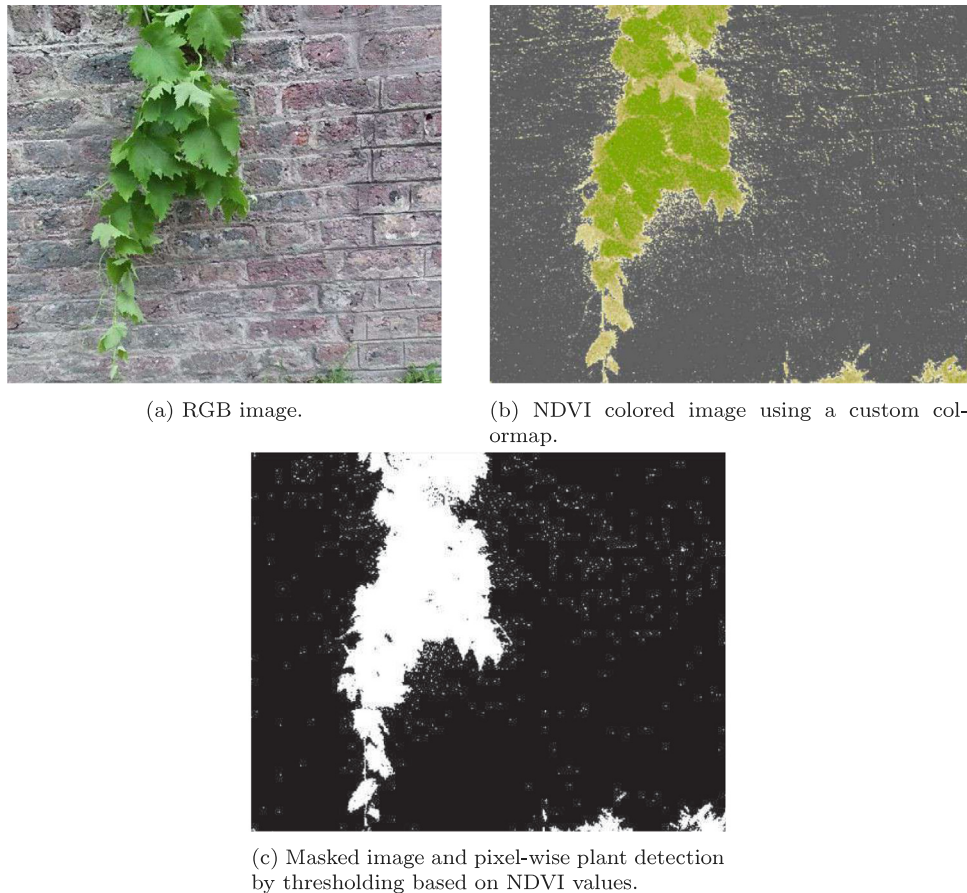


Fig. 9. Example of multispectral image processing [89].

and hardware accelerators can be found in the article by Mazzia et al. [183].

4. Localization and mapping

In this section, methods for locating a mobile robot in its surrounding environment and thus to georeference the acquired data are described, together with the types of map that can be built, useful for phenotyping tasks. An overview of advantages and disadvantages of localization methods is shown in Table 6, whereas mapping applications covered in this review are summarized in Table 7.

4.1. Robot localization

The localization algorithms are required to estimate the robot pose throughout the mapping session. Generally, in indoor scenarios the robot moves on a surface that can be considered planar: estimating its 2D position over the ground plane and its yaw is thus sufficient for navigation. However, agricultural terrain cannot always be considered planar and, for mapping purposes, it is mandatory to retrieve the sensor position and orientation in a three-dimensional space, i.e., the localization algorithm must output 6-DOF poses.

On the one hand, incremental localization techniques are based on data giving the robot pose in a local frame, compatible

with the prior positions. On the other hand, global localization methods provide poses in a known, fixed frame (Panigrahi et al. [184]). The localization based on wheeled odometry, used in an orchard in the work by Bayar et al. [40], is the simplest incremental approach, but inaccuracies and drift increase over time. This is related to wheel slip, which is difficult to measure and variable in real-world agricultural contexts. On the contrary, global methods can rely on GNSS standalone solutions, described in Section 4.1.1, or on the coupling of the satellite-based approach with IMUs, as illustrated in Section 4.1.2.

In addition, the literature reports a variety of techniques for robot localization that exclude wheel-to-surface contact. The most notable are visual odometry (VO) and LiDAR odometry (LO), described in Sections 4.1.3 and 4.1.4, respectively. Commonly, approaches exploiting visual or LiDAR data can be considered SLAM algorithms. With SLAM, we refer to the problem of retrieving the pose of the robot, while concurrently reconstructing a 2D or 3D model of the surroundings. The pie chart shown in Fig. 11 summarizes the most common localization methods employed in the papers covered in this review.

Furthermore, methods based on alternative data sources that can be found in the literature are reported in Section 4.1.5. Finally, Section 4.1.6 provides examples of how multiple techniques can be combined to cover the drawbacks of each standalone method.

4.1.1. Global navigation satellite system

As introduced in Section 3.2.1, robot localization can be directly performed using a single GNSS receiver (as in the 4.5% of



Fig. 10. Examples of cutting-edge embedded computers [183].

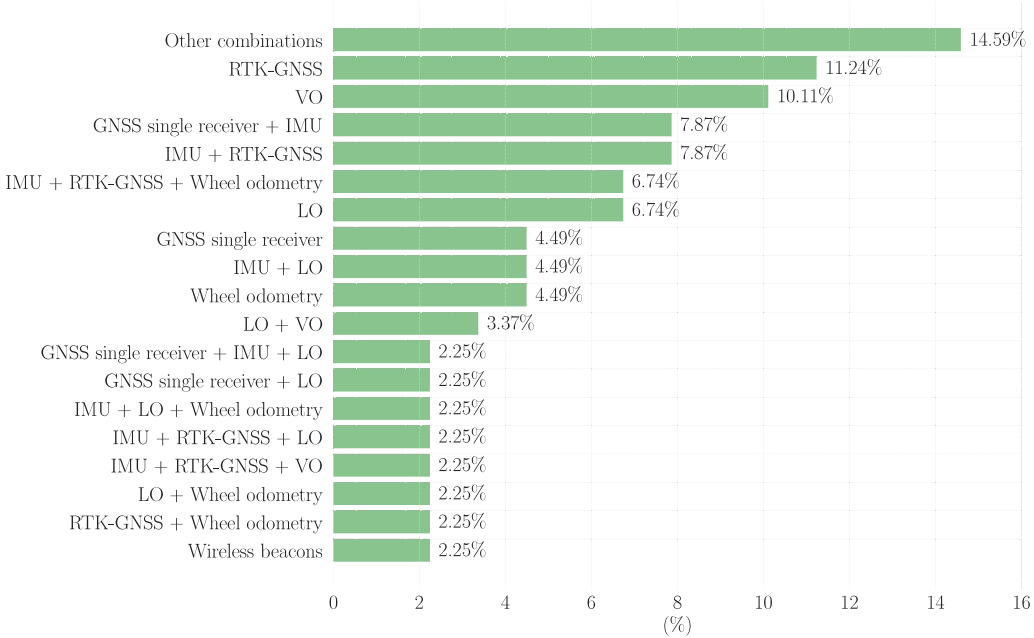


Fig. 11. Bar plot of the localization approaches reported in Table 7 (in this figure IMU stands for IMU-based localization).

the considered systems, Fig. 11). This approach is implemented on a robotic platform by Fentanes et al. [46], and tested for mapping an uncultivated field, a crop field, and for water status monitoring in a vineyard by Krus et al. [58], Saiz Rubio et al. [110], and Fernandez Novalez et al. [160], respectively. However, the accuracy provided by this system is significantly influenced by the data acquisition and processing. When using a single receiver, indeed, the estimated 3D coordinates can be affected by errors of up to a few meters. To achieve centimeter-level accuracy, differential GNSS techniques can be employed. In this case, one receiver (the *reference station*) is located in a precisely known and fixed position and provides the onboard receiver (also called *rover*) with corrections. The latter can be implemented in real

time (from which the term *Real-Time Kinematic-GNSS*) thanks to a communication radio link, or in post-processing mode.

The RTK-GNSS is exploited for localization in orchards [125,126,171], in cotton fields [135,138], in corn fields [63], and in vineyards [90,107,108,152]. Moreover, the RTK-GNSS approach is coupled with wheel odometry for localization in an orchard (Daglio et al. [134]), and in a carrot field (Cubero et al. [53]). Obviously, the installation of receivers in the surrounding environment constitutes a drawback of the method, because of the cost of using multiple sensors and the need to place the reference station in a known location. Nevertheless, a cost-effective solution is represented by GNSS correction service providers based on networks of ground reference stations, available world wide.

Finally, in agricultural sites, it should be considered that vegetation could cause signal blockage (as in indoor environments) and multi-path reflection (Lan et al. [102]), decreasing the availability of the system (the total amount of time in which the receiver reports a solution over the whole test duration) and limiting its applicability.

4.1.2. Inertial measurement unit

Inertial measurement units exploit the so-called *dead reckoning* to calculate the current pose of a moving object, i.e., the result is obtained using the previously determined pose and integrating subsequent estimates of acceleration, speed, and heading direction over elapsed time. In long measurement sessions, retrieving the position of the robot only by means of dead reckoning can lead to a *drift*, which is the difference between where the UGV is really located and where the UGV assumes to be (Table 6). Particularly with vibrations, and double integration, the position estimates become quickly useless. Furthermore, it should be noted that the measured signals are related to the unknown true values by scale factors and biases, which are functions of temperature. Therefore, due to the variability of weather conditions, sensor bias could be problematic in agricultural scenarios. For these reasons, in agriculture IMUs are never used for dead-reckoning by themselves.

The use of IMUs coupled with other sensors is widespread in mobile robotics for agriculture (found in 47.2% of the considered robots, Fig. 11), since IMUs directly provide the orientation of the robot, which is generally not available by means of a satellite-based positioning solution. IMU also fills the gap between two GNSS measurements over time, thanks to the higher update rate. By integrating GNSS measurements, it is possible to reduce the trajectory estimation drift that the dead reckoning approach typically experiences. Thus, the coupling of IMU and GNSS may overcome the drawbacks of both solutions alone.

The literature reports applications of the IMU coupled with a single GNSS receiver for the localization in vineyards [106,143], orchards [144], crop fields [75,93], uncultivated fields [45,57,172], and for under canopy localization [49]. Moreover, the RTK-GNSS approach is combined with an IMU to perform localization among crop rows [48,96], in vineyards [114,185], orchards [159], maize fields [140], and gardens [176]. Finally, it is worth citing examples of wheel odometry integrated to the RTK-GNSS - IMU localization solution for applications in an uncultivated field [39], in a citrus groove [43], in a garden [186], in a vineyard [111], and in orchards [118,119].

As a consequence of the vehicle vibrations, very noisy path estimations are generally provided by IMUs in rough terrains (unless special filters are used, as in the work by Gao et al. [186]). As a result, visual- and LiDAR-based approaches mentioned below are frequently preferred.

4.1.3. Visual-based localization

Nowadays, visual odometry represents one of the most widespread solutions for localization (exploited in 21.3% of the works considered in this article, Fig. 11), with the goal of retrieving the pose of the camera by analyzing the captured image sequence. Plug-and-play VO solutions are also available on the market, thanks to cameras that directly integrate algorithms able to output the sensor poses, as the one employed by Smitt et al. [148] in a greenhouse, by de Silva [61] in a crop field, and by Belov et al. [62] in an orchard.

In general, the VO methods can be divided into two classes: appearance- and feature-based. Appearance-based approaches rely on photometric consistency to match two subsequent images. These methods are computationally more onerous and often

require GPU-based processing (Debeunne et al. [187]). Consequently, feature-based approaches are favored for application on robotics and autonomous systems.

Feature-based methods involve extracting local keypoints (such as corners, lines, and blobs) and their descriptors from each image, matching or tracking them across consecutive image frames by comparing the identified features. Matches established across multiple images are then used to estimate the camera motion. For instance, a feature-based method is applied in [67,82] for localization in vineyards and in [72] in a crop field. A commonly used algorithm for feature extraction and matching is the so-called SIFT (Scale-Invariant Feature Transform), that is invariant to scale, rotation, and illumination of images (Se et al. [188]). A VO method based on SIFT features and tested in a peanut field can be found in the work by Dong et al. [189]. Alternatively, template matching can be employed, as in [156]. This approach entails finding the location of a template window, extracted from an image, in the subsequent picture.

Several open-source feature-based VO algorithms are available online and are tested in real-word agricultural scenarios. ORB-SLAM and its variants (e.g., ORB-SLAM2) [190,191] are among the most used, due also to their ability of correcting the accumulated drift of the estimated trajectory by exploiting loop closure (i.e., the recognition of regions already visited). This is identified through the bag-of-words algorithm, which counts how often a visual feature occurs in a picture and converts such image into a histogram of the so-called codewords, i.e., representatives of similar features. The comparison among images is thus performed thanks to the histograms stored in the database, simplifying the process of place recognition and loop closure detection. ORB-SLAM is tested, for example, in crop fields [192], and orchards [175,193]. The robustness of this method is improved in the latest version of the algorithm, ORB-SLAM3, released in December 2021 [194], and tested on the Rosario dataset by Cremona et al. [195]. ORB-SLAM3 combines information from camera and IMU, improving the localization estimations significantly.

Another widespread VO framework is Real-Time Appearance-Based Mapping (RTAB-Map [196]), which supports inputs from RGB-D, stereo and, additionally, LiDAR sensors. It combines two main algorithms: a loop closure detector and a graph optimizer. However, loop closure is exploited in a limited number of locations to achieve real-time performance in large-scale environments. RTAB-Map is employed in greenhouses in [41,105,151], and in vineyards in [47], where the authors combine the VO module of RTAB-Map, wheel odometry, and LiDAR data to enhance the results.

The previously mentioned approaches are compared by Hroob et al. [91] in a virtual vineyard, where the trajectory generated using RTAB-Map proves to be the most accurate in a scenario with multiple loop closures, with the robot traversing multiple vine rows in a zig-zag pattern before going back to its starting point. Instead, ORB-SLAM2 fails this task. Comelli et al. [197] carry out a similar work with the Rosario dataset [55], and state that the analyzed algorithms perform poorly in terms of accuracy and robustness compared to the urban or indoor situations where they are often evaluated.

To conclude, we would like to point out that the highly repetitive appearance of the environment, the strong vibration produced by the rough terrain, and the movement of the leaves caused by the wind can limit the performance of the VO algorithm [195]. To overcome these issues, other data sources are currently being investigated to solve the SLAM problem: LiDAR and radar, as it is reviewed in Sections 4.1.4 and 4.1.5.

4.1.4. LiDAR-based localization

In the literature, several SLAM algorithms based on the point clouds generated by LiDAR sensors can be found, an approach employed in 29.2% of the papers considered in this review (Fig. 11). Localization based on LiDAR sensors is beneficial since they are characterized by the independence from illumination, a FoV up to 360°, and long-range detection.

The extended Kalman filter (EKF) is a classical method for locating a robot using 2D LiDAR sensors (or the horizontal ring of a 3D LiDAR sensor). The filter prediction step retrieves the pose using dead reckoning, and the update step refines the pose estimate using the measured location of a recognized landmark (Thrun et al. [198]). This method permits the evaluation of the 3-DOF pose of the robot in the ground plane, and is particularly suited for mobile robots with limited computational capabilities. However, in real-world agricultural contexts, it is not always simple to extract features from the LiDAR data to be utilized as landmarks. This technique can therefore be exploited in environments characterized by clearly visible and separate stems, as in the orchard in [79,136], or when crop rows are easily detectable and lines can be used as landmarks, as is the case of vineyards in [66]. Furthermore, the lack of robustness of this method may be overcome by employing artificial reflecting targets as landmarks [65,120], or by coupling calibrated images and LiDAR measurement and searching for distinctive features in the image frames, as tested in orchards by Cheein et al. [133].

An alternative solution is offered by the Rao-Blackwellized particle filter, whose details are explained in [199,200]. This technique relies on the whole bi-dimensional horizontal scan, and is exploited in virtual agricultural environments in [80,122,145,153] and in greenhouses in [41,70,87]. However, it was designed for navigation in structured areas, and it is therefore not employed in real-world outdoor agricultural contexts, which are usually unstructured.

More recent LiDAR SLAM systems directly exploit three-dimensional point clouds, thus being applicable in many scenarios with fewer limitations. In state-of-the-art algorithms, the SLAM problem is generally solved on the front-end by scan matching. This approach finds the optimal 6-DOF transformation that minimizes the overall distance between two point clouds, using, e.g., Gauss–Newton based methods such as the Levenberg–Marquardt optimizer [201]. As the correspondences between points belonging to subsequent scans are unknown, they need to be guessed, and the problem is solved iteratively, as in the most popular approach for point cloud alignment, the Iterative Closest Point (ICP) algorithm [202]. For example, ICP is tested in vineyards to refine the localization output of a particle filter by Aguiar et al. [77], and to improve GNSS–IMU localization in [103].

Furthermore, LiDAR SLAM algorithms often store the map and the path of the robot in a graph structure, with nodes corresponding to the poses of the robot, and edges representing spatial constraints between contiguous nodes (e.g., the estimated transformation among the two point clouds). Thus, a back-end optimization stage is generally performed, using ad-hoc libraries (e.g., GTSAM [203]) to minimize the sum of errors over all constraints, as tested in a greenhouse in the work by Ohi et al. [81]. Moreover, loop closure can be handled in a similar manner to reduce the trajectory drift.

To speed up the computation, 3D LiDAR SLAM is usually executed using downsampled point clouds obtained, for example, as the set of centroids of voxels of predefined dimension. Subsequently, features (e.g., points belonging to planes or edges) can be extracted from the voxelized point cloud, as in the approaches implemented by the LiDAR Odometry and Mapping (LOAM) [204] and the Lightweight and Ground Optimized LOAM (LeGO-LOAM) [205] algorithms. For instance, LOAM is used in [84]

to locate a robot developed to recognize the position of flowers in a greenhouse. Moreover, two similar algorithms (referred to as LIO-SAM [206] and Static Mapping [207]) are compared by Hroob et al. [91] in a virtual vineyard, with findings indicating the estimate of an appropriate path shape, but significant drift accumulation.

Most of the state-of-the-art SLAM solutions (e.g., RTAB-Map, LOAM, LeGO-LOAM, LIO-SAM) can integrate data provided by additional sources, as it is described in more detail in Section 4.1.6. For instance, the IMU can be used to roughly estimate the motion of the robot between two subsequent LiDAR scans (Zhang et al. [204]).

The literature suggests that algorithms based on the aforementioned LiDAR SLAM methods, but specifically modified to be used in agriculture, outperform the original formulations. For instance, LeGO-LOAM inspired versions, optimized for orchards, are proposed in [38,64]. Gao et al. [38] compare the modified algorithm with LOAM, LeGO-LOAM, and LIO-mapping [208] to demonstrate its better performance. Furthermore, an algorithm specifically implemented for vineyards is compared with LeGO-LOAM by Aguiar et al. [78]. An updated version of LOAM is optimized for maize fields by Dong et al. [142], where only points belonging to stalks are used for scan matching. The stalk segmentation is performed by discarding ground points and then applying clustering algorithms on the remaining points.

As a further alternative, LiDAR SLAM can be performed using the NDT (Normal Distribution Transform [209]) representation of the 3D point clouds, as in [210]. This method associates a normal distribution with voxels, which is used to model the probability of measuring a point inside it. NDT is computationally less onerous than ICP-based scan matching, but does not degrade the SLAM result. Examples of robots using the NDT approach are found in [73,139], but are only tested in artificial outdoor scenarios that do not mimic an agricultural environment.

Please be aware that all of the discussed methods may perform poorly in environments with long corridors, leading to frequent scan matching failures and inaccurate robot location estimates. Moreover, they are usually not employed in agricultural fields with low plant heights.

4.1.5. Other localization methods

Alternative data sources for localizing a mobile robot in agriculture are radars, ultrasonic sensors, and wireless beacons (devices that broadcast their identifier). These devices are adopted to measure landmarks so that the EKF-based localization described in Section 4.1.4 can be performed.

The radiation pattern of radars makes them robust to the variations in pitch and roll of the robot in natural and non-flat environments (Rouveure et al. [129]). In the article by Radcliffe et al. [211], an ultrasonic sensor pointing sideways is exploited to retrieve the distance of the robot with respect to a fixed cardboard. Moreover, measurements from four HC-SR04 ultrasonic sensors are used together with GNSS and IMU for localization in a vineyard in [212].

Furthermore, wireless beacons (i.e., solutions based on Time Difference Of Arrival (TDOA) approach, such as DecaWaves) provide localization with 30 cm of accuracy and are immune to weather and illumination conditions [213]. For instance, in the work by Duarte et al. [94], the range and angle between landmarks and the receiver are estimated using radio frequency-based beacons. Moreover, a mobile robot based on ultra-wideband positioning is tested in a greenhouse with four fixed beacons installed, as illustrated by Yao et al. [214]. Such methods can constitute a cheap alternative to LiDAR-based approaches, but they are less accurate with respect to the solutions listed in Section 4.1.4 [213,214]. Moreover, ultrasonic sensors and wireless beacons are suited only for small-scale areas.

Garrido et al. [51] use a markedly different method to localize the robot in a greenhouse: a 360-degree prism is mounted on top of the vehicle shown in Fig. 3(b), and it is tracked by a total station by measuring ranges and angles both in the horizontal and vertical planes. Although accurate, this solution is expensive and can be used only in the surroundings of the total station.

4.1.6. Data fusion

All the localization methods previously described have their own advantages and drawbacks, as summarized in Table 6. A multi-sensor fusion strategy offers significant benefits over the use of a single data source. Firstly, by combining multiple sensor data, it is possible to obtain a higher temporal resolution than the one achievable with some sources (see, e.g., the low update rate of GNSS systems, highlighted in Section 3.2.1). Moreover, this should help in reducing the effect of noise in sensor measurements and possibly fill gaps in individual sensor data. It is worth noting that data acquired from different sensors are associated to different reference frames, making the transformation into a common reference system a crucial processing step (Fung et al. [215]).

Multi-sensor fusion is historically handled by Bayesian filters, such as Kalman filters. One of the characteristics of Kalman filters is that the estimated confidence should grow when numerous sources are used, due to the properties of multivariate Gaussians multiplication. Different sensor configurations merged by means of the EKF are reported in Table 7, whereas examples of the use of Kalman filters on direct georeferencing systems are found in [44,45,75,86,88,111,114,186,216,217]. Moreover, VO is coupled with wheel odometry in [82], and with LO in [47] to localize the robot in a vineyard and an orchard, respectively. An alternative formulation to the EKF is the extended information filter (EIF), used by Cheein et al. [133] to fuse LO and VO. The EIF could be useful to avoid numerical problems in case of large uncertainty in sensor readings and motion prediction models. An EIF is also used to generate pose estimates from RTK-GNSS, IMU, and the RealSense T265 tracking camera in Vulpi et al. [150]. In addition, the literature describes agriculture case studies in which the EKF is used to increase LO [64,66,73,79,136,145] and VO [73,157] reliability using direct georeferencing systems.

Since the pose estimate of Bayesian filters depends not only on current measurements, obtained through various sensors such as GNSS, but also on the previous iteration of the algorithm, often an error accumulation can occur. This leads to the requirement of a different approach, such as the so-called factor graph. A factor graph is a bipartite graph that connects factors to variables. The variables denote the unknowns in the estimation task, and the factors represent the probabilistic information acquired through measurement or previous knowledge of those variables. Thus, unlike classical Bayesian filters, a factor graph encodes probabilistic information for every robot pose throughout the survey, not just the latest pose estimate. This permits the use of loop-closure constraints to prevent errors from accumulating when the robot revisits an area of the environment that has already been explored. The mathematical definition of factor graphs is beyond the scope of this article, for further details we refer the reader to [218–220]. For example, a factor graph is used to fuse VO, RTK-GNSS, and IMU data in peanut fields in [189], LO, RTK-GNSS, and IMU data in orchards in [38], and LO, IMU, and wheel odometry in vineyards in [84].

Furthermore, in LO algorithms based on data provided by rotating 3D LiDAR sensors (described in Section 4.1.4), the acquired point clouds are often paired with data from an IMU even more tightly [221]. In fact, readings of linear acceleration and angular velocities are used to retrieve the motion of the LiDAR sensor during a 360° scan, and to perform the undistortion of the point cloud, i.e., to correct the 3D coordinates of the points to take into

Table 6

Advantages and disadvantages of localization methods.

Method	Advantages	Disadvantages
RTK-GNSS	<ul style="list-style-type: none"> • Accurate positioning • No drift over time 	<ul style="list-style-type: none"> • Low update rate • Only position available with one receiver • Base station required • Not working in indoor environments • Not working with vegetation causing signal blocking
IMU	<ul style="list-style-type: none"> • High update rate • Low power consumption • Low size and weight 	<ul style="list-style-type: none"> • Drift over time • High noise in rough terrain • Dependent on the initial state • Sensitive to magnetic interference • Calibration required
Visual odometry	<ul style="list-style-type: none"> • High update rate (hardware and software dependent) • Loop closure enabled • Low power consumption • Low size and weight • Cheap 	<ul style="list-style-type: none"> • Sensitive to weather and illumination • Sensitive to rapid changes in viewing angle
LiDAR odometry	<ul style="list-style-type: none"> • High update rate (software dependent) • Loop closure enabled • Independent from illumination • Up to 360° Fov • Long range detection 	<ul style="list-style-type: none"> • Sensitive to rain • High power consumption • Bad performance in long corridors

account the changing of the sensor position during a single scan [204]. Otherwise, in the absence of IMU data, undistortion can be applied by assuming linear motion of the LiDAR between two successive acquisitions [196].

In summary, it can be said that sensor fusion is crucial for precise robot localization in real agro-ecosystems. Every sensor has disadvantages that may be solved by coupling it with another data source, either in a loose manner using Kalman-based filters or more tightly, using a factor graph.

4.2. Mapping in agriculture

This section discusses the types of maps (summarized in Table 7) built by mobile robots for inspection and monitoring purposes in agriculture. In the context of plant phenotyping, 3D models can be used when a detailed assessment of the canopy morphology is desired. In order to achieve this, SLAM methods, mentioned in Section 4.1, can be applied to build a complete point cloud of the surveyed environment. For instance, LiDAR SLAM algorithms are used to generate maps in [73,78,81,84,114], even though the obtained models are mostly exploited for navigation purposes. The literature review carried out in this paper reveals that half of the research works analyzed are focused on retrieving maps not only for autonomous navigation, but also for monitoring. Furthermore, depending on the required map accuracy, a refinement stage can be necessary to enhance the map built by online SLAM methods. Please note that not all robotic platforms rely on a SLAM algorithm able to produce the map online (as in [44,49,51,56,58,107,125,126,138,140,143,152,179]). In these cases, an offline data processing step is needed. Alternatively to LiDAR data, the 3D model can be built also by using

SfM with RGB images captured by a single camera moving along the row, as in the work by Jay et al. [154]. However, visual sensors for mapping are less common than LiDAR devices. In fact, as highlighted in [222], a 3D reconstruction based on SfM is negatively affected by slight displacements of the plants during data acquisition, caused, e.g., by wind moving the leaves.

The original point cloud data can contain a high number of noisy points and outliers, resulting from inaccuracies in sensor readings, motion-induced distortions and improper scans registration. Since they can have a significant impact on the subsequent assessment of canopy properties, a post-processing step is advisable before producing the final outputs.

The statistical outlier removal filter (SOR) is a common method to refine the point cloud. It initially calculates the average distance between each point and its neighbors. Then, it rejects the points that are farther than the average distance plus a specified multiple of the standard deviation. SOR can be used in a variety of environments, without crop restrictions, as shown by the authors of [64,135] in wheat fields and orchards, respectively.

An alternative outliers removal strategy is implemented by the random sample consensus algorithm (RANSAC) [223]. The fundamental idea of RANSAC is that the dataset consists of “inliers” (data whose trend can be described by a set of model parameters), and outliers are data that do not match the model. RANSAC is used, for instance, by Gao et al. [38] to remove noisy points from an orchard point cloud. RANSAC also assumes that it is possible to estimate the parameters of a model that best fits the data given a set of inliers. Thus, it is also useful to detect the ground and remove points that belong to it, as those points are useless for phenotyping. Considering a plane model to be fitted, RANSAC is used for ground removal in [44,51,64,138–140]. Alternatively, points belonging to the ground may be identified using the cloth simulation filter (CSF) [224], which makes it possible to achieve high precision without configuring a multitude of algorithm settings, as in the work by Gao et al. [38]. In the CSF, the point cloud is first flipped along the altitude axis. Then, the digital surface model of the ground is found simulating the physics of a piece of cloth leaning on the terrain due to gravity. The CSF is better suited for real-world agricultural scenarios where the ground is rarely considered planar.

The effects of the above mentioned filters are depicted in Fig. 12. The portion of the whole point cloud (Fig. 12(a)), obtained by a mobile robot running a LiDAR SLAM algorithms, is first filtered with the CSF to exclude ground-related points (Fig. 12(b)). Subsequently, the SOR filter is applied for further refinement (Fig. 12(c)).

Mesh surfaces, as an alternative to point clouds, can be used to obtain a continuous representation of the vegetation structure, allowing volume information to be retrieved. Widespread triangulation methods, exploited for shape reconstruction from a dense, unorganized set of data points, are the convex hull algorithm and its generalization, the alpha-shape method, whose outcomes are shown in Fig. 13. The convex hull approach, that consists of determining closed curves that include the line segments linking each pair of points inside the curve, is exploited in the literature to represent the geometry of vineyards [103,143] and orchards [44,124,125,217]. Furthermore, the alpha-shape approach is used in [64,107,125] for vineyards and orchards, respectively.

The reconstructed model can also be represented as a 3D occupancy grid, discretizing the environment with a grid of small regular geometries (square cells). Based on the number of points contained in each cell, the occupancy grid stores probabilistic data indicating whether it is occupied or not. For example, the literature reports agricultural environments depicted with 3D occupancy grid in [101,113,159,179].

To evaluate the health state of plants and its spatial variation, geometric maps should additionally include spectral information,

as done in [41,47,67,77,105,148,151,152,174,175,189,192]. In particular, the robots in [41,105,151] use the Visual SLAM module of RTAB-Map (described in Section 4.1), for building maps in greenhouses. Furthermore, Aguiar et al. [76] developed and tested an open-source algorithm (VineSLAM) specifically for photorealistic reconstruction of vineyard corridors. RGB features can also be combined to assign a Green-Red Vegetation Index (GRVI) to each point of the 3D map, as in the work by Vulpi et al. [150].

When utilized for plant condition assessment, visual and spectral information is often represented in the form of orthophotos or mosaics, as illustrated in [53,56,60,108,123,140,160]. Bi-dimensional maps representing georeferenced NDVI index values are produced, for instance, for carrot [53] and wheat [137] fields, vineyards [108,143], and orchards [56]. Moreover, maps of the NDRE and the PRI indexes are provided in [108,137].

The maps in [53,56,137] are retrieved from measurements taken with the spectral sensor looking downward. However, lateral configurations of the sensing device enable a more thorough assessment of the vegetation status when the plants are arranged in rows. This configuration is adopted to create a water stress status map of an orchard in [110,160], combining multiple vegetative indexes with the method proposed in Ihuoma et al. [225]. Moreover, in the work by Clamens et al. [89] the robot successfully creates images of grapevines with superimposed NDVI index (Fig. 9) by means of calibrated multispectral and depth cameras, while the mobile platform developed in [119,127,166] manages to assemble a 3D point cloud maps with NDVI values.

Starting from the 3D reconstruction, summary metrics are frequently computed to directly evaluate quantitative properties of vegetation. Among them, the canopy height can be derived straightforwardly from the normal to the ground. In fact, knowing the height of plants can be useful, e.g., in pesticide or water dosages (Fernández-Novales et al. [160]). In scenarios characterized by a homogeneous plant density, such as cotton [135,138] and wheat [132,137] fields, it is common to produce maps representing the height distribution of plants. Moreover, height maps of orchards (Fig. 13) are reported in [44,56,125,126].

Volume measurements are preferred for estimating growth and predicting yields of plants arranged in rows, such as vineyards and orchards. Given a representation of the environment as a point cloud, a suitable technique is the one employed in [112,126], in which the authors use prisms of adjustable lengths stacked vertically to approximate the plants shape and to compute the width and the volume of trees. Instead, when using meshes to represent the vegetation structure, the volume is directly recovered from the geometry boundaries, as done in [44,58,64,107,125,143]. Finally, in case the environment is known as a 3D occupancy grid, the volume is computed by simply summing the volume of each occupied cubic cell [101,113].

Another geometric parameter indicating plant growth is the Leaf Area Index (LAI), which relates the total leaf area to the total arable land area [226]. The literature reports case studies in which the LAI is derived from point clouds in vineyards [103,106,108], and in wheat fields [49,60].

5. Path planning strategies

Agricultural crops and terrains are challenging for autonomous UGV navigation, since these environments are highly variable and unstructured. The global and local path planning algorithms, which are tested in agriculture, are discussed in Sections 5.1 and 5.2. Section 5.3 describes the techniques specifically developed for autonomous navigation between parallel plant rows, whereas Section 5.4 surveys exploration strategies. An overview of path planning strategies for autonomous navigation in agriculture is shown in Table 8.

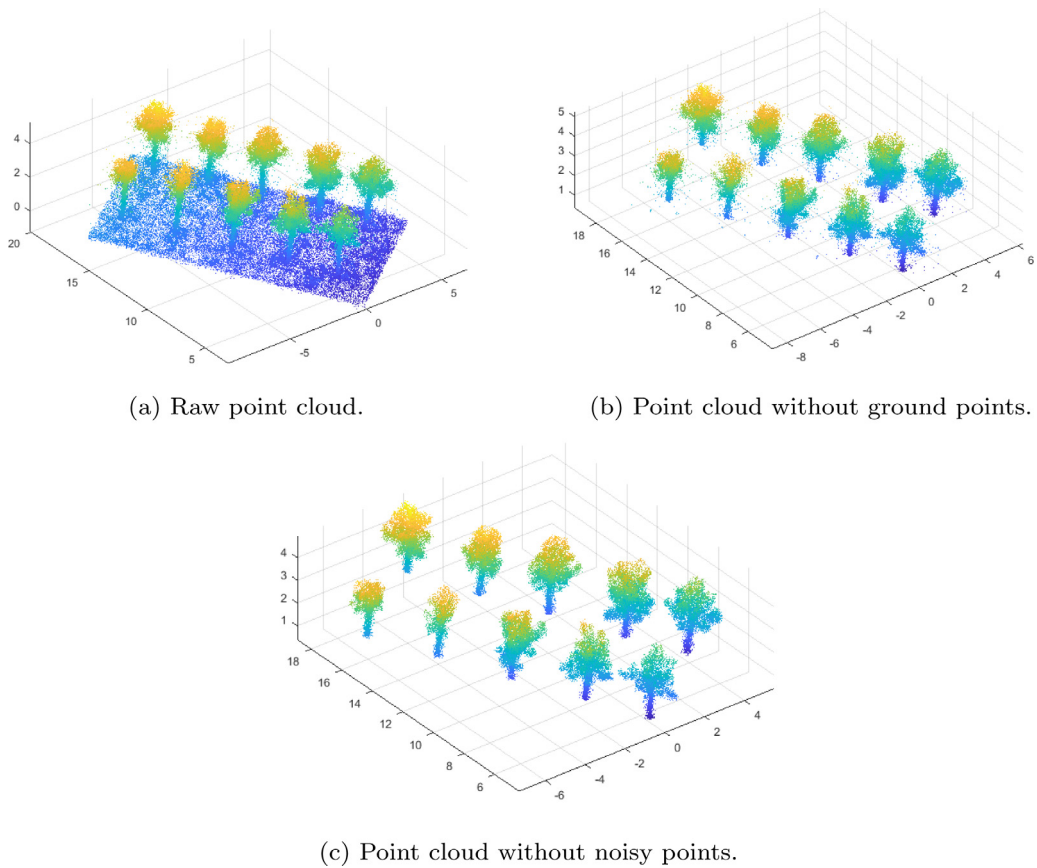


Fig. 12. Post processing of a point cloud obtained by means of LiDAR SLAM [38].

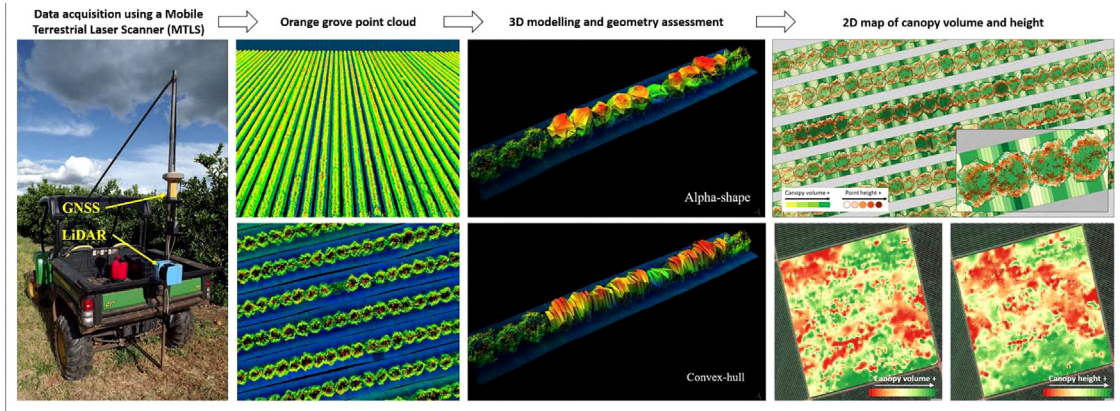


Fig. 13. Point cloud, mesh surface and 2D map of canopy volume and height of an orange grove [125]. (For interpretation of the references to colour in this figure legend, the reader is referred to the web version of this article.)

5.1. Global path planning

With the term *global path planning* we refer to the methods exploited to find a feasible and collision-free path towards a goal point, when obstacles in the environment are known a priori [28]. Therefore, after the route has been defined, the robot navigates using a localization and path following strategy.

A simple solution is to exploit GNSS way points that generally need to be previously collected teleoperating the robot in the field, as in [44,53,56,62,90,110,114,117]. This method is appropriate for open fields where the GNSS signal is not blocked by vegetation. When used in vineyards or orchards, GNSS way-point

based navigation is generally coupled with a row following algorithm (Section 5.3). In contrast, GNSS way-point based navigation cannot be used to define routes in indoor environments such as greenhouses.

Since the surroundings of a robot in greenhouses are more structured, autonomous navigation may be accomplished using indoor-developed path planning algorithms. Once a representation of the working area is provided, goal points that must be reached by the robot can be manually selected. The path planner then calculates the path to the goal.

For instance, in the work by Ohi et al. [81], the path is obtained by discretizing the greenhouse environments by means of a Voronoi diagram. Otherwise, probabilistic approaches may

Table 7

Overview of the localization methods and the mapping applications described in the papers covered in this review.

Author	Year	Ref.	Environment	Localization method	Mapping application	Feature extraction
Aguiar et al.	2021	[77]	Vineyard	LO (ICP with Particle Filter refinement)	3D reconstruction (RGB features)	
Aguiar et al.	2022	[78]	Vineyard	LO	3D reconstruction	
Arita et al.	2016	[139]	Garden	LO (Normal Distribution Transform)	Tree measurement	Semiplane extraction Ground detection (RANSAC)
Astolfi et al.	2018	[145]	Vineyard (Gazebo)	GNSS + IMU + LO + Wheel odometry (fused with EKF)		
Ball et al.	2016	[39]	Uncultivated field	IMU + RTK-GNSS + Wheel odometry		
Bayar et al.	2015	[40]	Orchard	Wheel odometry		
Beloev et al.	2021	[62]	Controlled	VO	Crop detection and mapping	Crop detection (CNN)
Bietresato et al.	2016	[127]	Controlled	Wheel odometry	3D reconstruction, volume measurement	
Bietresato et al.	2016	[166]	Controlled	IMU + RTK-GNSS + Sonar	3D reconstruction with NDVI information	
Blanquart et al.	2020	[132]	Wheat field		Height and density measurement	
Blok et al.	2019	[65]	Vineyard	LO (Particle filter and KF)		
Cerrato et al.	2021	[86]	Vineyard	IMU + RTK-GNSS (fused by EKF)		
Chakraborty et al.	2019	[143]	Vineyard	IMU	Volume and height measurement	
Chen et al.	2021	[175]	Orchard	VO	3D reconstruction (RGB features)	Fruit detection (CNN)
Cheein et al.	2014	[124]	Olive groove	GNSS + LO	3D reconstruction (mesh)	
Choudhary et al.	2021	[41]	Greenhouse	LO + VO	3D reconstruction (RGB features)	
Clamens et al.	2021	[89]	Vineyard		Multispectral images and point cloud co-registration	
Colaco et al.	2017	[125]	Orange crop	RTK-GNSS	3D reconstruction, volume measurement	
Comelli et al.	2019	[197]	Rosario dataset	VO	Visual SLAM comparison	
Cubero et al.	2020	[53]	Carrot field	RTK-GNSS + Wheel odometry	Pests and diseases detection (NIR and NDVI)	
Daglio et al.	2019	[134]	Apple trees	RTK-GNSS + Wheel odometry	Flower charge estimation	
Darwin et al.	2021	[34]	Rosario dataset	VO	Visual SLAM comparison	
Dogru et al.	2018	[79]	Orchard	IMU + RTK-GNSS + LO (fused by EKF)		
Dong et al.	2017	[189]	Peanut field	IMU + RTK-GNSS + VO (fused by factor graph)	3D reconstruction (RGB feature)	SIFT feature
Dong et al.	2022	[142]	Maize field	IMU + LO	3D reconstruction	Ground detection and stalk segmentation
Duarte et al.	2016	[94]	Controlled	Wireless beacons		
Eiffert et al.	2021	[45]	Uncultivated field	GNSS + IMU (fused by EKF)		
Emmi et al.	2021	[93]	Different crops fields		Topological map	Crop detection (CNN)
Fei et al.	2022	[171]	Orchard	RTK-GNSS		
Fentanes et al.	2018	[46]	Pasture field	GNSS	Soil exploration and compaction mapping	
Fernandez-Novalez et al.	2021	[160]	Vineyard	GNSS	Vineyard water status monitoring	
Freitas et al.	2012	[136]	Orchard	LO + Wheel odometry (fused by EKF)		
French et al.	2016	[135]	Cotton field	RTK-GNSS	Cotton phenotyping (NIR and thermal info)	
Gai et al.	2021	[63]	Corn field	RTK-GNSS		
Gan et al.	2018	[43]	Citrus grove	IMU + RTK-GNSS + Wheel odometry		

(continued on next page)

be used, in which a sample way point is selected and approved at each iteration if it does not result in a collision with an obstacle. In the probabilistic roadmap (PRM) method, used by Zhang et al. [178], the generation process is based on a uniform probability distribution and stops when an adequate number of

connected components is achieved or after the maximum number of iterations is reached.

The algorithms based on roadmaps are called multi-query [228], since given the network of paths, solutions can be found to navigate to other goal points in the sampled space. In order to identify

Table 7 (continued).

Author	Year	Ref.	Environment	Localization method	Mapping application	Feature extraction
Gao et al.	2021	[38]	Orchard	IMU + RTK-GNSS + LO (fused by factor graph)	3D reconstruction	Plane detection (Cloth Simulation Filter and RANSAC)
Gao et al.	2022	[186]	Garden	IMU + RTK-GNSS + Wheel odometry (fused by EKF, autoencoder NN)		
Garrido et al.	2015	[51]	Greenhouse, maize rows	IMU + Total station (ICP registration)	3D reconstruction	
Habibie et al.	2017	[80]	Orchard (Gazebo)	LO	Bi-dimensional map with fruit location	Fruit detection
Hroob et al.	2021	[91]	Vineyard	IMU + LO + VO		
Imperioli et al.	2018	[72]	Crop rows	GNSS + VO + Wheel odometry (fused by factor graph)	SLAM comparison	
Iqbal et al.	2020	[44]	Orchard (Gazebo)	GNSS + LO (fused by EKF)	3D reconstruction, volume and height measurement	
Iqbal et al.	2020	[217]	Controlled	IMU + RTK-GNSS + Wheel odometry (fused by EKF)	3D reconstruction	
Lv et al.	2022	[157]	Open field	GNSS + IMU + VO + Wheel odometry (fused by EKF)		
Jiang et al.	2022	[70]	Greenhouse	IMU + LO + Wheel odometry		
Kai et al.	2021	[64]	Orchard	IMU + LO (fused by EKF, loop closure capable)	3D reconstruction	Ground detection (RANSAC)
Kragh et al.	2015	[172]	Uncultivated field	GNSS + IMU		
Kragh et al.	2017	[57]	Uncultivated field	GNSS + IMU		
Krus et al.	2020	[58]	Different crops	GNSS	3D reconstruction, volume measurement	Ground detection (RANSAC)
Le et al.	2019	[73]	Building garden	IMU + LO (NDT, fused by EKF, loop closure capable)	3D reconstruction	Ground and object segmentation (LeGO-LOAM)
Lowe et al.	2021	[103]	Vineyard	GNSS + IMU + LO	Density measurement	Ground detection and rows segmentation
Mammarella et al.	2022	[212]	Vineyard	GNSS + IMU + Ultrasonic sensors (fused by EKF)		
Manish et al.	2021	[49]	Wheat fields	GNSS + IMU	3D reconstruction	
Martínez-Casasnovas et al.	2017	[126]	Olive orchard	RTK-GNSS	Volume measurement	
Marden et al.	2014	[66]	Vineyard	GNSS + IMU + LO (fused by EKF)		
Mark et al.	2017	[47]	Vineyard	LO + VO + Wheel odometry (fused by EKF)	3D reconstruction (RGB features)	
Mashhadani et al.	2020	[121]	Controlled (Gazebo)	LO		
Masuzawa et al.	2017	[105]	Greenhouse	LO + VO (loop closure capable)	3D reconstruction (RGB features)	Ground and object segmentation (LeGO-LOAM)
Matsuzaki et al.	2018	[151]	Greenhouse	VO	3D traversability mapping	Pixel wise labeling
Moral-Martinez et al.	2016	[106]	Vineyard	GNSS + IMU	LAI estimation	
Moreno et al.	2020	[107]	Vineyard	RTK-GNSS	3D reconstruction	
Narvaez et al.	2018	[174]	Garden		3D reconstruction (RGB features)	Terrain classification (SVD)
Navarro et al.	2016	[90]	Vineyard	RTK-GNSS		
Ohi et al.	2018	[81]	Greenhouse	IMU + LO	3D reconstruction (RGB features)	
Pagliari et al.	2022	[108]	Vineyard	RTK-GNSS	MMS and UAV 3D map comparison (NDVI and NDRE)	
Perez-Ruiz et al.	2020	[137]	Cultivars of wheat	Wheel odometry	Wheat phenotyping (NIR and NDVI)	
Reina et al.	2017	[67]	Vineyard and Olive grove	VO	3D reconstruction (RGB features)	
Reiser et al.	2017	[179]	Controlled	Wheel odometry	3D reconstruction	
Ristorto et al.	2017	[118]	Orchard	IMU + RTK-GNSS	3D reconstruction (NDVI information)	
Rosellpolo et al.	2017	[152]	Vineyard	RTK-GNSS	3D reconstruction (RGB features)	
Saiz-Rubio et al.	2021	[110]	Vineyard	GNSS	Vineyard water status monitoring	

(continued on next page)

Table 7 (continued).

Author	Year	Ref.	Environment	Localization method	Mapping application	Feature extraction
Santos et al.	2016	[111]	Vineyard	IMU + RTK-GNSS + Wheel odometry + Landmarks (fused by EKF)		
Santos et al.	2020	[82]	Steep slope vineyard	LO, + VO (fused by EKF)	3D reconstruction	Trunk detection
Sanz et al.	2013	[112]	Vineyard, orchard		Leaf area density estimation	
Shafeekhani et al.	2017	[60]	Maize crop		Maize phenotyping (eye-in-hand)	
Shalal et al.	2015	[88]	Orchard	IMU + Wheel odometry (fused by EKF)	Trunk mapping	
Shu et al.	2021	[192]	Soybean field	VO	3D reconstruction (RGB features)	
Siebers et al.	2018	[113]	Vineyards	GNSS + IMU + Wheel odometry	3D reconstruction, volume measurement	
Silwal et al.	2021	[114]	Vineyard	IMU + RTK-GNSS (fused by EKF)	3D reconstruction	Bud detection (R-CNN) and canes detection (SVM)
Skoczen et al.	2021	[176]	Garden	IMU + RTK-GNSS		
Smitt et al.	2021	[148]	Greenhouse	IMU + VO + Wheel odometry	3D reconstruction (RGB features)	Fruit segmentation (CNN)
Sun et al.	2018	[138]	Cotton field	RTK-GNSS	Height measurement	Ground detection (RANSAC)
Tagarakis et al.	2022	[159]	Orchard	IMU + RTK-GNSS	3D reconstruction	
Underwood et al.	2017	[56]	Orchard	IMU + RTK-GNSS	3D reconstruction (NIR and NDVI)	
Velasquez et al.	2016	[131]	Corn crop	LO		
Vidoni et al.	2017	[119]	Orchard	IMU + RTK-GNSS + Wheel odometry	Health status monitoring (NIR and NDVI)	
Vulpi et al.	2022	[150]	Vineyard	IMU + RTK-GNSS + VO (fused by EIF)	3D reconstruction (RGB features)	GRVI
Wendel et al.	2018	[144]	Mangoes orchard	GNSS + IMU		
Winterhalter et al.	2021	[75]	Crop rows	GNSS + IMU + yaw from row detection (fused by EKF)	Maturity estimation	Fruit detection (CNN)
Xue et al.	2014	[227]	Crop rows	Radar		
Yamasaki et al.	2022	[96]	Crop rows	IMU + RTK-GNSS		
Yang et al.	2019	[84]	Orchard/Vineyard	IMU + LO + Wheel odometry (fused by factor graph)	3D reconstruction	
Yao et al.	2021	[214]	Greenhouse	Wireless beacons (TDOA)		
Zaman et al.	2019	[156]	Orchard	VO		
Zhang et al.	2014	[120]	Orchard	LO + Wheel odometry		
Zhao et al.	2020	[193]	Orchard	VO		

the best solution, all the calculated feasible paths are represented with a graph in which way points (nodes) are connected by feasible primitives (edges), e.g., lattice planner [229]. By assigning weights to the edges, it is possible to optimize parameters like time, traveled distance, energy, and distance from obstacles with search algorithms like Dijkstra or A*, as in [70,81,87,121].

On the contrary, the rapidly exploring random tree (RRT) method, exploited by Choudhary et al. [41], attempts to solve a specific instance of motion, hence it aims to look at just a subset of the environment pertaining to the specified path. Finally, genetic algorithms, inspired by natural selection, crossover, and mutation, can also be adopted to solve the global path planning problem in agriculture. For instance, the PRM strategy together with an algorithm referred to as the Non-dominated Sorting Genetic Algorithm are applied in [230] to determine the best routes for a mobile robot in a greenhouse. Tests performed by Pak et al. [87] demonstrate that the A* method is more suitable in greenhouses compared to Dijksta and RRT.

However, the literature describes several test cases in which indoor-developed algorithms are tested not only in greenhouses, but also for outdoor agricultural navigation. For example, the PRM and the lattice planner are used by Ball et al. [39] to provide kinematically feasible paths to an Ackermann steering robot, whereas Dijksta is tested on an omnidirectional robot in Eiffert et al. [45], both in an uncultivated field. Moreover, A* is used in an uncultivated field in [231] by an Ackermann steering robot,

and Dijkstra and A* are used to provide collision-free paths to a differential robot navigating in a vineyard by Mark et al. [47]. In addition, modified versions of the above-mentioned classical approaches, tailored to outdoor agricultural scenarios are found in the literature. For instance, the A* algorithm is extended for the navigation in steep slope vineyards to be aware of the center of gravity of the UGV and terrain slope, as well as to avoid soil compaction, in [37,82,83].

Traditional global path planners usually rely on prior knowledge of the environment (at least a 2D occupancy grid) in which the robot navigates. An occupancy grid map can be generated by means of onboard sensors or using 3D point clouds acquired during exploratory surveys by UAV, as in the work by Mammarella et al. [212]. However, sometimes a 3D map is required, e.g., in steep slope vineyards [82].

Lastly, when the robot must travel repeated pathways during continuous monitoring surveys, it may be practical to store the computed paths in a topological map. Topological maps constitute a set of locations that can be connected with each other. In this case, they can be represented as graphs, where nodes are associated with exact locations, whereas edges represent possible physical paths between these locations. Topological maps differ from graph search-based global path planners in that edges are represented by complete point-to-point paths rather than primitives. For instance, Santos et al. [111] use a topological map with nodes representing vine rows to improve the localization

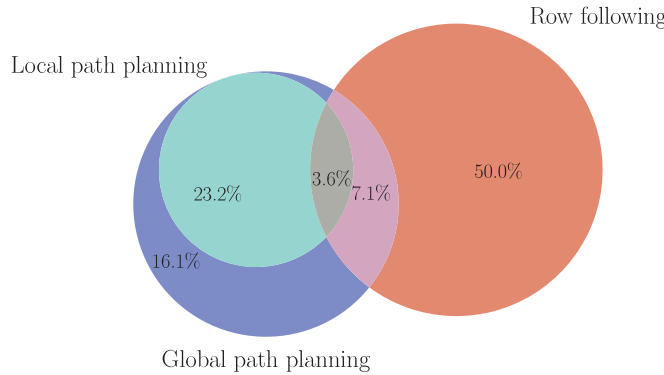


Fig. 14. Venn diagram reporting the percentage of mobile robots considered in this work that exploit each navigation capability.

and navigation. Furthermore, in the work by Emmi et al. [93], a topological map that stores the gateway, alleyway, and lane end locations is used to improve navigation in a broccoli field. Finally, in [81], the map is used to store paths to flowers in a greenhouse.

5.2. Local path planning

Local path planning is required to deal with uncertainties and inaccuracies in the knowledge of the environment as well as to avoid obstacles whose movements are unknown. The objective of local path planners for obstacle avoidance is to change the global path and provide collision-free velocities to control the robot.

Widespread approaches of local path planning include the artificial potential field (tested in a virtual greenhouse by Harik et al. [122], and in an open field to avoid bumps in the ground by Ball et al. [39]), and the dynamic window approach (DWA) [232], which relies on a cost function evaluated in the robot local area using range measurements to define the risk of collision. The DWA planner, for each iteration, generates samples of linear and angular velocities to be sent to the robot. Then, the resulting paths are simulated so as to eliminate those that would lead to a potential collision. The best local path is determined by weighing the proximity of obstacles and the global path. DWA is used in greenhouses in [70,81,87], and vineyards in [86].

An alternative solution is the elastic band (E-band) method exploited in [41], to navigate in a greenhouse. More in detail, the E-band algorithm considers the global path as an elastic band on which two forces are acting, an internal contraction force simulating the tension in a stretched elastic and a repulsive force to repel the band from the obstacles [233]. Furthermore, Choudhary et al. [41] use the Reeds-Shepp curve methods [234], since their robot is provided with an Ackermann steer. Reeds-Shepp is suitable for robots with non-holonomic constraints operating in limited spaces such as greenhouses, vineyards and orchards rows, as it generates various combinations of switch-back trajectories with high computational efficiency.

Please note that the above-mentioned collision avoidance methods rely only on range measurements on a plane and do not account for the 3D geometry of the object or any potential obstacles below or above the plane. To overcome this limitation, Santos et al. [83] use 3D LiDAR data and project points within a certain height range over a plane to take into account every possible collision of the robot. Moreover, in the work by Santos et al. [83] global paths are modified with an approach based on Bézier curves. To sum up, only 25.9% of the considered mobile robots integrate local path planning strategies, as shown in Fig. 14.

5.3. Row following

Path planning methods aimed at making the UGV follow the row can be used for autonomous navigation in environments characterized by crop rows. Moreover, a global path planning algorithm is no longer necessary if the robot detects the end of the row and engages a U-turn path to enter in the following line (as performed in [173] exploiting the detection of AprilTag coded targets).

Row following can be accomplished by estimating the pose of the robot between the rows and by sending velocity commands with the aim of keeping it on the centerline. For instance, the robot navigates based solely on lateral distance measurements between the plants and the robot itself in [60,109]. However, EKF and particle filters (Section 4.1.4) provide the basis for more reliable solutions using the distance from the centerline and yaw as state variables, as demonstrated in [39,40,65,75,136,235].

In general, the challenge to be addressed involves using sensor data and computer vision algorithms to locate a roadway for the robot. The lane lines can be found by using LiDAR, depth, or RGB sensors. Once the position of the crop edges on the left and right sides of the robot is found, a center point identifying the location of the row center is calculated. The error between the determined center point and the predefined setpoint in front of the robot is fed through standard control loops in all of the test cases described in this section (with the exception of case [131], which uses a fuzzy logic controller) to determine the wheel velocities required to move the robot to the center, thereby reducing the error to zero.

Regarding LiDAR-based approaches for the row following, a popular practice is to project the measured points on a horizontal plane to generate two clouds that can be fitted with lines (Fig. 15(a)) using, e.g., the RANSAC algorithm. RANSAC-based line detection is exploited in vineyards [66,90], and orchards [117]. RANSAC is also used to detect crop row lines on depth images by Zhang et al. [120] and RGB images (pre-processed with the Sobel operator) by Zhang et al. [116]. Moreover, an algorithm similar but more efficient than RANSAC, referred to as PEARL, is described by Isack et al. [236]. PEARL is tested for navigation in an orchard using LiDAR sensor data by Malavazi et al. [95]. Alternatively, the least square line fitting is applied to point clouds in [44,237], and tested in a real agricultural scenario by Gasparino et al. [54]. Planes can also be used as mathematical models to fit crop rows, as done for navigation in corn fields by Gai et al. [63].

Moreover, a method based on the row-sensing template, which is the expected observation of a depth sensor when it is properly aligned with the centerline, is used by Fei et al. [171]. Similar approaches can be applied also to data provided by LiDAR sensors. For instance, in [238], the mobile robot uses 2D laser scanners and approximates the vineyard rows by square pattern. Despite the approach proposed in [238] is not tested with a real agricultural robot, the simulated environment is realistic since it is designed from a real point cloud of the vineyard acquired with a terrestrial laser scanner. Finally, the robot in [158] navigates by finding the tree trunks by detecting their shadows, which are materialized by concavities in the point cloud obtained with the depth sensor pointing forward.

Generally, using the Hough transform [239] on images, it is possible to identify the lines that follow the crop row edges. The image should be first converted to binary applying an algorithm for edge detection. Canny edge detection [240], for instance, may be used to discern edges from the remainder of an image. The result of the Canny edge detection method is a binary picture with the edges of objects represented by white pixels and the remaining portion of the image represented by black pixels. Once the edges of the crops within the picture have been identified, the

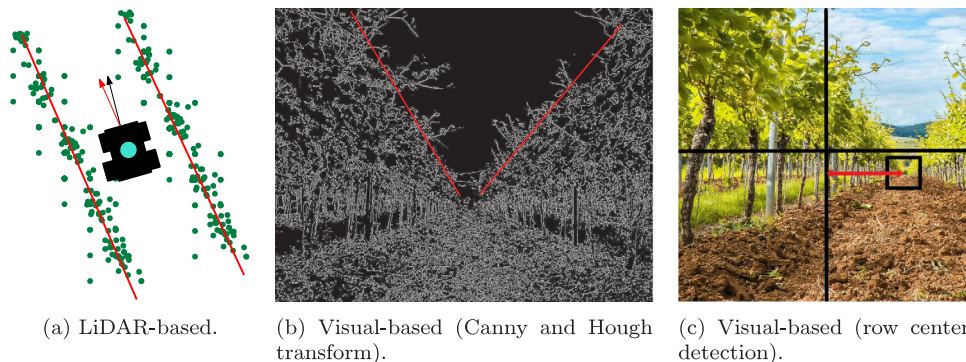


Fig. 15. Representations of row following methods.

Hough transform may be used to calculate the equation of the lane lines (Fig. 15(b)), as in [43,169,241,242]. Hough transform is also applied to LiDAR data to track the robot pose among crop rows in [141]. Moreover, a method to improve the outcome of the Hough transform by considering multiple crop rows is presented in [141]. Alternatively, Radcliffe et al. [211] propose an approach to navigate in vineyards by detecting the sky with a color mask and using the centroid of that region of interest as the row center point. Ruangurai et al. [243] demonstrate that a principal component analysis-based method provides better results than the Hough- and RANSAC-based on paddy field images.

Choosing a smaller area inside the picture to conduct the Hough transform might increase efficiency, since lines are prevented from being computed in incorrect areas of the image. In addition, utilizing filters to eliminate noise from the photo or isolating green masks before running the Canny edge detection may enhance the result for the specific image (Bonadies et al. [31]). However, image preprocessing and the Hough transform settings are specific to the scenario. Thus, the development of an algorithm that works in agriculture does not ensure the robustness of the method in different scenarios. More innovative approaches (discussed in Section 6) fall into the field of AI, and are used for row following by the authors of [68,69,86,181].

Most advanced row following algorithms also include a solution to detect the end of the row to make the robot engage the next one [40,120,136,168,173,235]. Row-end detection methods exploit drastic changes in the data distribution acquired by the sensor compared to those sensed inside the row.

As summarized in Fig. 16, LiDAR-based row following is the predominant strategy (50.0% of the considered works), followed by visual-based (38.9%), and depth-based (11.1%) methods. To wrap up this section, the path-planning architectures for mobile robots in agriculture include global, local, and row-following algorithms. Nevertheless, only the 3.6% of the considered robotic systems include all these three navigation strategies (Fig. 14).

5.4. Exploration

In the context of mapping in agriculture, with *exploration* we refer to the autonomous motion of the robot towards an unknown part of the environment, which has not been already mapped. Furthermore, the process of exploration aims at gathering data from an environment in order to reduce uncertainty about its boundaries (Bajcsy [245]). When the surrounding environment is not completely explored yet, the ground robot, localized in the currently mapped environment through SLAM, should choose the next way point towards unknown areas. The decision is influenced by factors such as the effort required to reach the destination (e.g., distance) and the gain proportionate to the difference in the quantity of information provided by the

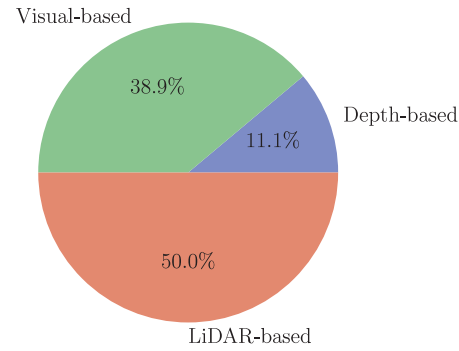


Fig. 16. Pie chart of the row following strategies.

map before and after navigating to the desired destination (Lluvia et al. [246]).

In this context, frontiers (areas at the boundary of explored space) can be used for autonomous way point identification [247,248]. Computer vision methods such as edge detection and region extraction can be applied to search for frontiers (Keidar et al. [249]). Moving to successive frontiers, the robot grows its world knowledge (using SLAM) until no more borders are discovered and the environment has been considered fully explored. This method is used for example in the work by Al-Mashhadani et al. [121], but it has not been tested in a real agricultural environment yet.

Furthermore, Dornhege et al. [250] extend the notion of frontier-based exploration to 3D environments by adding the concept of unknown 3D volumes. Another example is given by Senarathne et al. [251], who describe a 3D exploration method based on the idea of surface boundaries. In a 3D occupancy grid, a surface boundary can be defined as a voxel of a mapped area having at least one of its six sides exposed to unmapped space. However, no test cases of mobile robots using the aforementioned 3D exploration methods to build maps in agricultural scenarios are reported in the analyzed works.

In addition, the literature describes exploration methods that aim to direct the robot to a way point that maximizes the amount of new information gained from the environment. Among these approaches, the next-best-view algorithm is used in an open field by Fentanes et al. [46], and described by Bircher et al. [252]. In next-best-view methods, the way point selection can be improved by taking into account the traveling distance and the expected battery level once the navigation task is completed. An algorithm of this kind is proposed and tested both in a digital twin and in a real strawberry orchard by Polvara et al. [253].

Table 8

Overview of the state-of-the-art path planning methods for autonomous navigation in agriculture.

Author	Year	Ref.	Environment	Kinematics	Path planning strategies
Adhikari et al.	2020	[181]	Crop rows	Ackermann	Row following (visual-based)
Aghi et al.	2020	[68]	Vineyard	Wheeled skid-steered	Row following (visual-based)
Aghi et al.	2021	[69]	Vineyard	Wheeled skid-steered	Row following (visual-based)
Ball et al.	2016	[39]	Uncultivated field	Ackermann	Global (Lattice planner ROS [229]); local (Artificial potential field); row following (Visual-based)
Bayar et al.	2015	[40]	Orchard	Ackermann	Row following (LiDAR-based) with U-turn
Beloev et al.	2021	[62]	Controlled ^a	Wheeled skid-steered	Global (GNSS way points); local (depth-based obstacle avoidance)
Blok et al.	2019	[65]	Vineyard	Wheeled skid-steered	Row following (LiDAR-based)
Cerrato et al.	2021	[185]	Vineyard	n.r.	Global (custom algorithm: Adaptive Row Crops Path Generator (ARC-PG))
Cerrato et al.	2021	[86]	Vineyard	Wheeled skid-steered	Global (GNSS way points); local (DWA); row following (visual-based)
Chen et al.	2021	[169]	Greenhouse	Tracked skid-steered	Row following (visual-based)
Choudhary et al.	2021	[41]	Greenhouse	Ackermann	Global (RRT*,A*); local (E-band and Reeds-Shepp curve)
Cubero et al.	2020	[53]	Carrot field	Wheeled skid-steered	Global (GNSS way points)
Dang et al.	2022	[235]	n.r.	n.r.	Row following (LiDAR-based) with U-turn
Danton et al.	2020	[237]	Controlled	Ackermann	Row following (LiDAR-based)
Eiffert et al.	2021	[45]	Uncultivated field	Omnidirectional	Global (PRM, Dijkstra); local (RNN based obstacle avoidance)
Fei et al.	2022	[171]	Orchard	n.r.	Row following (depth-based)
Fentanes et al.	2018	[46]	Pasture field	Omnidirectional	Exploration (Next-Best-View)
Freitas et al.	2012	[136]	Apple orchard	Ackermann	Row following (LiDAR-based)
Gai et al.	2021	[63]	Corn and sorghum field	Wheeled skid-steered	Row following (depth-based)
Gan et al.	2018	[43]	Citrus grove	Wheeled skid-steered	Row following (visual-based)
Gasparino et al	2020	[54]	Maize field	Ackermann	Row following (LiDAR-based)
Guzman et al.	2016	[90]	Vineyards	Wheeled skid-steered	Global (GNSS way points); row following (LiDAR-based)
Harik et al	2018	[122]	Greenhouse (Gazebo)	Wheeled skid-steered	Global (GNSS way points); local (Artificial potential field)
Hu et al.	2021	[244]	Crop rows	n.r.	Row following (visual-based)
Iberraken et al.	2022	[238]	Vineyard (Gazebo)	Omnidirectional	Row following (LiDAR-based)
Iqbal et al.	2020	[44]	Orchard (Gazebo)	Wheeled skid-steered	Global (GNSS way points); row following (LiDAR-based)
Jeon et al	2022	[231]	Uncultivated field	Ackermann	Global (A*)
Jiang et al.	2022	[70]	Greenhouse	Wheeled skid-steered	Global (Dijkstra); local (DWA)
Li et al.	2022	[173]	Crop rows	Wheeled skid-steered	Row following (visual-based) with U-turn
Liang et al.	2022	[242]	Open field	Ackermann	Row following (visual-based)
Mahmud et al.	2019	[230]	Greenhouse	Omnidirectional	Global (Genetic algorithm)
Malavazi et al.	2018	[95]	Orchard	n.r.	Row following (LiDAR-based)
Mammarella et al.	2022	[212]	Vineyard	Four-wheel steering	Global (RRT*); local (DWA)

(continued on next page)

Exploration algorithms, while generally providing a highly irregular path, could be useful in the first mapping session when the robot has no prior knowledge of its surroundings. In subsequent mapping operations, the classical global path planners can be applied to retrieve optimal paths, allowing the robot to navigate autonomously. Moreover, since drift caused by frequent changes in the robot direction can result in inaccurate maps, it

may be advantageous to balance exploration and place revisiting operations, as mentioned by Holz et al. [254]. To this end, active loop-closure techniques, such as in the work by Stachniss et al. [255], should be included in the exploration strategy. Active loop-closure requires the robot to revisit previously traversed loops in order to reduce uncertainty in pose estimates and obtain more accurate maps.

Table 8 (continued).

Author	Year	Ref.	Environment	Kinematics	Path planning strategies
Mao et al.	2022	[117]	Orchard	Wheeled skid-steered	Global (GNSS way points); row following (LiDAR-based)
Marden et al.	2014	[66]	Vineyards	Wheeled skid-steered	Row following (LiDAR-based)
Mark et al.	2017	[47]	Vineyard	Four-wheel steering	Global (GNSS way points); local (E-band)
Masuzawa et al.	2017	[105]	Greenhouse	Wheeled skid-steered	Person following
Nehme et al.	2021	[141]	Crop rows	Ackermann	Row following (LiDAR-based)
Ohi et al.	2018	[81]	Greenhouse	Wheeled skid-steered	Global (Voronoi diagram, Dijkstra); local (DWA)
Pak et al.	2022	[87]	Greenhouse	Wheeled skid-steered	Global (Dijkstra, RRT, A*); local (DWA)
Peng et al.	2022	[168]	Orchard	Ackermann	Row following (depth-based)
Petiteville et al.	2018	[158]	Orchard	Ackermann	Row following (depth-based)
Radcliffe et al.	2018	[211]	Orchard	Wheeled skid-steered	Row following (visual-based)
Ruangurai et al.	2022	[243]	Paddy field	Ackermann	Row following (visual-based)
Riggio et al.	2018	[109]	Vineyard	Wheeled skid-steered	Row following (LiDAR-based)
Saiz-Rubio et al.	2021	[110]	Vineyard	Wheeled skid-steered	Global (GNSS way points)
Santos et al.	2016	[111]	Vineyard	Ackermann	Row folowing (LiDAR-based)
Santos et al.	2019	[37]	Vineyards	Wheeled skid-steered	Global (A* with COM-based weights); local (A*)
Santos et al.	2020	[82]	Vineyards	Wheeled skid-steered	Global (A* with COM-based weights); local (A*)
Santos et al.	2022	[83]	Vineyards	Wheeled skid-steered	Global (A* with COM-based weights); local (Bezier curves-based approach)
Shafiekhani et al.	2017	[60]	Maize crop	Wheeled skid-steered	Row following (LiDAR-based)
Sharifi et al.	2015	[241]	Orchard	n.r.	Row following (visual-based)
Silwal et al.	2021	[114]	Vineyard	Ackermann	Global (GNSS way points)
Underwood et al.	2017	[56]	Orchard	Omnidirectional	Global (GNSS way points)
Velasquez et al.	2016	[131]	Corn crop	Wheeled skid-steered	Row following (LiDAR-based)
Zhang et al.	2014	[120]	Orchar	Ackermann	Row following (LiDAR-based) with U-turn
Zhang et al.	2012	[116]	Orchard	Ackermann	Row following (visual-based)
Zhang et al.	2022	[178]	Greenhouse	Wheeled skid-steered	Global (PRM)

^aEnvironment with artificial features designed to test the algorithm.

6. Applications of artificial intelligence

In autonomous inspections, the abilities that a robot can learn using artificial intelligence approaches can be useful for improving the robustness and safety of autonomous navigation, as well as retrieving data for phenotyping. In fact, the robot must be able to distinguish between data that are useful for plant monitoring. In order to associate semantic information to data gathered by sensors, in this section we focus the review on data-driven pattern recognition approaches. In particular, as shown in Fig. 1, the main tasks covered in this paper regarding artificial intelligence are classification, segmentation, and object detection, mainly based on images and LiDAR data.

Through data classification, the robot can gain a better understanding of its surroundings, which is the basis for real-time decision support systems. The classification problem is concerned with assigning acquired data to predetermined classes. Regarding the classification task, popular methods are Support Vector Machine (SVM) and Convolutional Neural Network (CNN). On one hand, a SVM is a machine learning technique that conducts supervised learning for data group categorization. On the other hand, CNN are deep artificial neural networks that are typically employed for image recognition and processing, due to their ability to identify patterns in images.

For example, in order to perform the appropriate guiding or control actions, the mobile robot must be cognitively capable of

comprehending the surrounding terrain type and its features. The literature reports research works in which SVMs are used to classify the type of terrain by means of RGB-D images in the work by Narvaez et al. [174]. In addition, the classifier proposed by Reina et al. [67] benefits from a multi-modal ground representation that incorporates exteroceptive (RGB) and proprioceptive (wheels torque, slip, and acceleration) data inside an SVM-supervised framework. CNNs can also be used for classification in the agricultural domain, for example, to discriminate diseased plants from healthy ones (Metre et al. [256]). However, to the best of our knowledge, there are no examples in the literature of agricultural mobile robotic systems able to directly classify diseased plants. Nevertheless, a CNN is used for the estimation of fruit ripening level using hyperspectral images by Wendel et al. [144].

Unlike classification models, which label an image with its most representative element, segmentation algorithms provide pixel-by-pixel information on a specific object. The precise contours of an item within an image are identified using segmentation, as shown in Fig. 17(a). Segmentation is generally achieved using CNNs with a particular architecture called encoder-decoder (Fig. 18). To obtain a more accurate interpretation of the data, the encoder is tasked with extracting information from groups of neighboring pixels. The decoder must then restore the original resolution of the image and identify each pixel according to the class to which it belongs. The literature reports robots capable of performing segmentation on images of sweet peppers

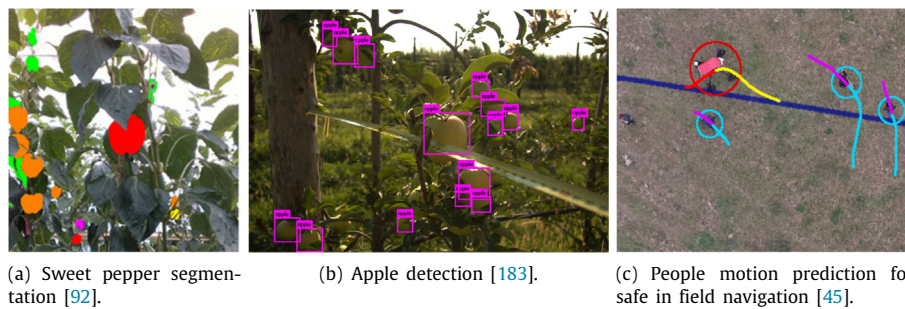


Fig. 17. Examples of applications of CNN (a), (b), and RNN (c).

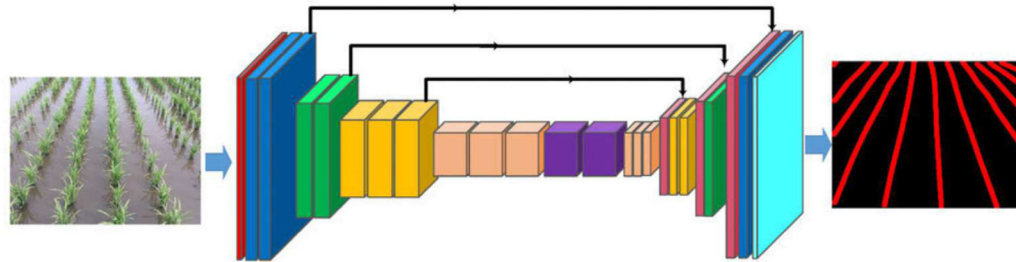


Fig. 18. Example of encoder-decoder CNN architecture for image segmentation [181].

in a greenhouse (Fig. 17(a)) in [92,148,257], and sugar beets in [92,257]. Moreover, by using encoder-decoder architectures for segmentation, the image preprocessing for row following can be made more robust to the variability of illumination and field context (Fig. 18), as demonstrated in [61,181].

The segmentation through encoder-decoder CNNs can be performed also on point clouds, assigning labels to each point (Maset et al. [258]). For example, in the work by Matsuzaki et al. [151], the robot is able to segment points belonging to leaves or branches. Alternatively, SVM may be used for this task. The work by Kragh et al. [172] shows an example of segmenting a point cloud to distinguish between terrain and vegetation-related features.

Furthermore, object detection and recognition architectures are common in agriculture since they can identify and locate one or more types of plants within an image. Object detection is a computer vision task that recognizes items in images and is typically performed using CNNs. While classification is related, it is more specific in that it detects distinct objects within an image and uses bounding boxes to determine their locations (Fig. 17(b)). Regarding agricultural applications of object detection, the literature reports mobile robots capable of locating tomatoes [62], passion fruits, lychees, and pineapples [175], apples [183], broccoli, cabbage [93,123], vine trunks [93,182], and vine shoots [114,177]. Moreover, a variant of an object detection CNN (R-CNN [259,260]) is used to find the number of leaves in a sugar beet field in [74], and to recognize weeds in a corn field [85].

In addition, object detection can be used to recognize people and obtain a semi-autonomous navigation strategy based on person following. In the work by Masuzawa et al. [105], for instance, a person-following approach is implemented on the mobile robot using the YOLOv2 CNN (Redmon et al. [261]). Assigning semantic value to the portions of pixels within images can be also useful for improving navigation strategies. Images from onboard cameras pointing forward can be used to recognize the position of the center of the row in a vineyard (Fig. 15(c)), as tested by Cerrato et al. [86].

Safety in navigation can be increased if CNNs are used to locate trunks or people (Fig. 17(c)) for obstacle avoidance, as

implemented by Aguiar et al. [76] and Skoczen et al. [176], respectively. More in detail, the robot by Aguiar et al. [76] uses a light version of YOLOv3 [262] (Tiny YOLO-V3) that permits boosting the frame rate at which inference can be carried out, reducing computational cost. Tiny YOLO-V3 represents a trade-off between accuracy and inference speed, overcoming the YOLOv3 inferior performance at inference stage on embedded computers. Furthermore, the SSD MobileNet 640 × 640, with transfer learning from the COCO 2017 database, is used as detection algorithm of peach trunks in orchard rows by Simoes et al. [180]. Details on the CNN architectures used in the aforementioned works can be found in the following articles [259–269].

Artificial neural networks can also be applied to automate the choice of way points on occupancy grid images (task also done with SVM by Santos et al. [270]), as described by Cerrato et al. [185]. Another category of neural networks that has been shown to be useful in obstacle avoidance are the so-called recurrent neural networks (RNNs). The RNNs, through an internal loop, are capable of keeping track of information about previous inputs. In the work by Eiffert et al. [45], for example, an RNN is used in an uncultivated field to increase safety in activities shared between humans and robots.

The methods previously described are supervised, i.e., they require training datasets that are usually manually labeled. An example is the one created by Kurtser et al. [149] to train neural networks for the recognition of grapes. However, manually collecting and annotating datasets (large enough to train a neural network) is a laborious task, especially in agricultural environments. For this reason, a technique called transfer learning is often adopted, such as in [76,81]. Transfer learning involves fine-tuning network layers or performing additional training with a small dataset to make it suitable for inputs other than those used for training. Furthermore, nowadays there are auto-labeling techniques that can be used to help with dataset creation, such as the one proposed by Matsuzaki et al. [271]. Auto-labeling solutions exploit neural networks that can learn from each annotation performed and offer tentative annotations for workers to eventually modify and confirm.

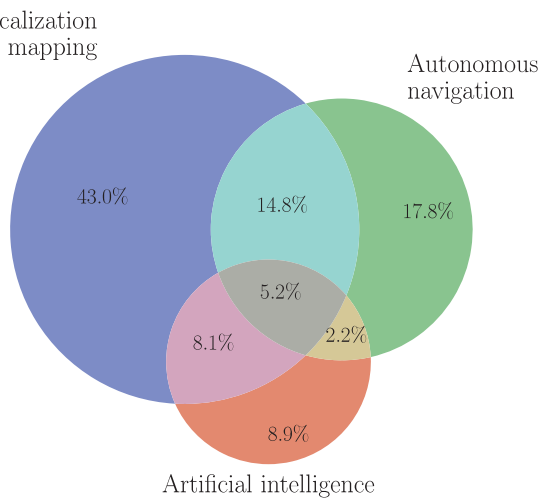


Fig. 19. Venn diagram reporting the percentage of mobile robots considered in this work that exploit each capability.

To summarize, AI techniques are integrated into 24.4% of the considered papers, permitting the solution of problems even beyond pure localization and mapping (e.g., object detection), as it is shown in Table 9. Fig. 2 highlights that the trend is growing since such kind of algorithms and dedicated hardware are spreading more and more in the last few years.

7. Future developments and challenges

According to the findings of this review, we can state that 20.0% of the considered mobile robotic solutions are capable of performing the mapping task autonomously, as shown in Fig. 19. This percentage is computed as the intersection of the two Venn diagrams representing localization and mapping and autonomous navigation approaches implemented in robotic platforms for mapping in agriculture. It is worth noting that this value is related to a time span of 10 years, and full navigation and mapping autonomy is more frequent in current robotic systems. This section looks at what the future holds for hardware technologies, localization and mapping methods, path planning, and artificial intelligence in this challenging and complex field.

Most agricultural robots use differential-type kinematics, which results in fewer constraints on the robot feasible trajectories. Furthermore, custom robots specifically designed for agricultural applications are commonly used. The use of modular commercial robots that adapt to the field to be analyzed, such as Thorvald, is becoming more common.

Among the most widely used sensors are the Velodyne VLP16 LiDAR sensor and the RealSense D435 depth camera. Multispectral cameras are also integrated into mobile robots to acquire proximity spectral images.

In terms of computational units, the Jetson by NVIDIA modules are cutting-edge, allowing for more efficient extraction of information from sensor data via parallel computing. Moreover, such modules permit to exploit CUDA features, that are necessary to run most the existing open-source AI algorithms. Among the Jetson solutions, future mobile robots for agriculture are expected to include the new Jetson Orin series for sensor management, which represents one of the cutting-edge commercial embedded computers, thanks to a 12-core CPU and a powerful GPU (Sipola et al. [273]).

To increase the autonomy and sustainability of agricultural mobile platforms, solar panels can be embedded as power sources [53,56,157]. The autonomy issue could be resolved in the future

by using alternative energy sources to supply low-power sensors, such as hydrogen fuel cells (Gonzalez et al. [274]).

Thanks to the new global wireless standard (5G), high-volume, real-time data streaming will also be available, and it is predicted that cloud storage will replace hard drives for data storage and management (Dharmasena et al. [275]). Swarm robotics and Internet of Things solutions could also be used to map large areas and solve the problem of low battery autonomy (Albiero et al. [276]). A system for autonomous agricultural tasks might alternatively consist of a main explorer robot and a secondary robot guided by a map provided by the master robot.

To the best of our knowledge, no study has been conducted in which a robot (or a fleet of mobile robots) creates a digital twin of a whole agricultural ecosystem from which simulations of plant growth patterns and plant health can be obtained using field-collected data. Furthermore, future developments may involve combining the 3D map with data that mobile robotic systems have not previously considered, such as plant temperature (which provides information about water stress), soil and plant moisture, soil carbon concentration, and greenhouse gases exchange.

In terms of localization, visual SLAM approaches have been found to be more common in open fields or fields defined by the presence of low crops. Conversely, LiDAR SLAM is increasingly being used in vineyards and orchards. In some instances, these LiDAR SLAM algorithms are tweaked to better fit agricultural contexts (e.g., in orchard by Gao et al. [38]). Cutting-edge visual and LiDAR SLAM algorithms (yet to be tested or poorly tested in agricultural scenarios) are reported in Table 10. Appearance-based VO is not used yet since it is onerous, although it could be tested in Jetson modules with GPU accelerators. LiDAR SLAM algorithms are mainly developed for indoor or road environments (e.g., KITTI), and use feature extraction techniques such as ground, edges, planes. As a result, more research is needed to determine whether extracting these characteristics is beneficial for agricultural contexts, or if better results can be obtained by retrieving alternative features or not using them at all. In addition, it is uncertain which scan matching approach is more accurate for agricultural LiDAR SLAM (NDT, point-to-plane ICP). To the best of our knowledge, a comparison using a ground truth from a terrestrial laser scanner has not been performed to evaluate the retrieved map yet.

The current state of the art for combining position estimations from several sensors is to use factor graphs rather than Kalman filters, which enables a more tight integration of the different sensors. Concerning the 3D reconstruction, recent applications see UAV-UGV collaboration to build a more complete 3D map by collecting data from multiple viewpoints [49,159]. Point clouds with vegetation indices, from multi/hyperspectral cameras, assigned to each point are not found in literature yet.

In terms of autonomous navigation, collaboration with drones or between multiple mobile robots could provide additional information to strengthen the knowledge and perception of the environment to be mapped. The effectiveness of multi-robot systems using a fleet navigation method could also be improved by implementing AI solutions and supervisory management strategies. Global path planning strategies could consider terrain characteristics for improving smoothness in the motion of the robot, thus reducing the noise in acquired data, especially when navigating in harsh agricultural soils. Future developments in the field of autonomous navigation in agricultural scenarios will consider more robust and AI-based solutions for row following and U-turn at the end of each row, as this problem is treated, for instance, in [40,120,136,168,173,235], but not consolidated yet.

Considering artificial intelligence, current research focuses mostly on the creation of lightweight architectures that can operate on embedded devices. However, the lack of labeled datasets

Table 9

Overview of the machine learning and deep learning techniques exploited by the mobile robotics systems covered in this survey.

Author	Year	Ref.	Method	Environment	Application
Adhikari et al.	2020	[181]	Encoder-decoder DNN	Crop rows	Row following
Aghi et al.	2020	[68]	CNN	Vineyard	Row following
Aghi et al.	2021	[69]	CNN (MobileNetV3 [269])	Vineyard	Row following
Aguiar et al.	2020	[76]	CNN	Vineyard	Trunk detection
Aguiar et al.	2021	[182]	CNN	Vinayard	Trunk detection
Ahmadi et al.	2021	[257]	Encoder-decoder DNN (U-Net [268])	Greenhouse, sugar beets field	Crop segmentation with a spatio-temporal module
Beloev et al.	2021	[62]	CNN (Faster R-CNN [259])	Controlled	Tomatoes detection
Cerrato et al.	2021	[185]	CNN	Vineyard	Way points generation for global path planning
Cerrato et al.	2021	[86]	CNN	Vineyard	Row following
Chen et al.	2021	[175]	CNN (EfficientNet [263])	Orchard	Fruit detection
Cruz et al.	2022	[123]	CNN	Crop rows	Cabbage detection
Eiffert et al.	2021	[45]	RNN	Uncultivated field	Motion prediction for obstacle avoidance
Emmi et al.	2021	[93]	CNN (YOLOv3 [262])	Crop field	Crop detection
Gao et al.	2022	[186]	Autoencoder NN	Garden	Data denoising for localization
Halstead et al.	2021	[92]	CNN (Mask R-CNN [260])	Greenhouse, sugar beets field	Crop and fruit segmentation and mapping
Hu et al.	2021	[244]	CNN (YOLOv4)	Crop rows	Row following
Kragh et al.	2015	[172]	SVM	Uncultivated field	Vegetation and terrain classification from point clouds
Masuzawa et al.	2017	[105]	CNN (YOLOv2 [261])	Greenhouse	People detection for person following
Matsuzaki et al.	2018	[151]	Encoder-decoder DNN	Greenhouse	Point cloud segmentation of branches and leaves
Matsuzaki et al.	2022	[271]	DNN	Greenhouse	Auto-labeling for semantic segmentation
Mazzia et al.	2020	[183]	CNN (YOLOv3-tiny [264])	Controlled	Apple detection and hardware comparison
Narvaez et al.	2018	[174]	SVM	Garden	Terrain classification
Ohi et al.	2018	[81]	CNN (Inceptionv3 [265])	Greenhouse	Flower detection
Reina et al.	2017	[67]	SVM	Vineyard and olive groove	Terrain classification
Santos et al.	2020	[82]	CNN	Vineyard	Trunk detection
Shu et al.	2021	[192]	Encoder-decoder DNN	Soybean field	Simulating RGB-D SLAM
Silva et al.	2021	[61]	Encoder-decoder DNN (U-Net)	Crop rows	Row following
Silwal et al.	2021	[114]	CNN (Faster R-CNN)	Vineyard	Bud detection
Simones et al.	2022	[180]	CNN (SSD MobileNet 640 × 640)	Orchard	Trunks detection
Skoczen et al.	2021	[176]	CNN (DeepLabv3+ [266])	Garden	Obstacle detection
Smitt et al.	2021	[148]	CNN (Mask R-CNN)	Greenhouse	Fruit segmentation
Wendel et al.	2018	[144]	CNN	Orchard	Estimating mangoes maturity
Weyler et al.	2021	[74]	CNN (Mask R-CNN)	Sugar beets field	Plants detection and leaves count
Yandun et al.	2021	[177]	CNN	Vineyard	Bud detection
Zaenker et al.	2021	[272]	CNN (Yolact [267])	Orchard	Sweet pepper segmentation and pose estimation
Zhang et al.	2021	[85]	CNN (Faster R-CNN)	Crop field	Crop detection

is often the bottleneck in the development and integration of AI methods. For this reason, recent research has also aimed at generating synthetic data (Fawakherji et al. [71]) to be used in the training of neural networks or AI-based tools to automate the labeling process (Matsuzaki et al. [271]). Finally the training process could be boosted by self-attention mechanisms (e.g., transformers [287]), which differently weight the significance of each part of the input data.

A further application of neural networks includes the extraction of information directly from multispectral images, which is not fully covered in the literature for autonomous mobile robots yet. Additionally, AI can be used to optimize the energy management of the robot and extend its autonomy in field operations. Finally, AI methods are expected to be applied for

increasing safety in human–robot collaboration tasks, especially in the context of motion prediction.

8. Conclusion

This paper examined the current supportive technologies for ground mobile robots used for autonomous mapping in agriculture. Unlike previous reviews, we described cutting-edge approaches and technologies for extracting information from agricultural environments, not just for navigation but also for mapping and monitoring. Advanced platforms and sensors, modern localization techniques, navigation and path planning methods, and the potentialities of artificial intelligence for autonomous mapping in agriculture have all been analyzed. This work revealed that mobile robotics in agriculture is a present and active field of

Table 10

Up-to-date open-source SLAM algorithms.

Algorithm	Ref.	Year	Approach	Github link	ROS	Tested in agriculture
DLO	[277]	2022	LiDAR, inertial	https://github.com/vectr-ucla/direct_lidar_odometry	✓	✗
DTAM	[278]	2011	Visual	https://github.com/akshitj1/dtam	✗	✓
DV-LOAM	[279]	2021	LiDAR, visual	https://github.com/kinggreat24/dv-loam	✗	✓
F-LOAM	[280]	2021	LiDAR	https://github.com/wh200720041/floam	✓	✗
hdl_graph	[210]	2019	LiDAR, inertial	https://github.com/koide3/hdl_graph_slam	✓	✗
LeGO-LOAM	[205]	2018	LiDAR, inertial	https://github.com/ RobustFieldAutonomyLab/LeGO-LOAM	✓	✓
LiODOM	[281]	2022	LiDAR	https://github.com/emiliofidalgo/liodom	✓	✗
LIO-SAM	[206]	2020	LiDAR, inertial	https://github.com/TixiaoShan/LIO-SAM	✓	✓
LOAM	[204]	2014	LiDAR	https://github.com/cedricxie/LOAM	✓	✓
LVI-SAM	[282]	2021	LiDAR, visual	https://github.com/TixiaoShan/LVI-SAM	✓	✓
LSD-SLAM	[283]	2014	Visual	https://github.com/tum-vision/lsc_slam	✓	✓
ORB-SLAM	[190]	2015	Visual	https://github.com/raulmur/ORB_SLAM	✓	✓
ORB-SLAM2	[191]	2017	Visual	https://github.com/raulmur/ORB_SLAM2	✓	✓
ORB-SLAM3	[194]	2021	Visual, inertial	https://github.com/UZ-SLAMLab/ORB_SLAM3	✓	✓
PL-VIO	[284]	2018	Visual, inertial	https://github.com/HeYijia/PL-VIO	✓	✗
RTAB-Map	[196]	2019	LiDAR or visual ^a	https://github.com/introlab/rtabmap_ros	✓	✓
Stereo DSO	[285]	2017	Visual	https://github.com/JiatianWu/stereo-dso	✗	✓
SVO	[286]	2014	Visual	https://github.com/uzh-rpg/rpg_svo	✓	✗

^aRTAB-Map provides multiple modules.

research driven by the need to optimize agricultural production, reduce waste, and improve sustainability, as dictated by climatic and social factors.

Declaration of competing interest

The authors declare that they have no known competing financial interests or personal relationships that could have appeared to influence the work reported in this paper.

Data availability

Data will be made available on request.

Acknowledgments

The first author acknowledges support from the National Ph.D. Programme in Artificial Intelligence of University of Naples Federico II (Naples, Italy). We thank the anonymous Reviewers who helped to improve the paper.

Funding

This study was carried out within the Agritech National Research Center and received funding from the European Union Next-Generation EU (Piano Nazionale di Ripresa e Resilienza (PNRR) – Missione 4 Componente 2, Investimento 1.4 - D.D. 1032 17/06/2022, CN00000022). This manuscript reflects only the authors' views and opinions, neither the European Union nor the European Commission can be considered responsible for them.

References

- [1] K. Abbass, M.Z. Qasim, H. Song, M. Murshed, H. Mahmood, I. Younis, A review of the global climate change impacts, adaptation, and sustainable mitigation measures, *Environ. Sci. Pollut. Res.* 29 (2022) 42539–42559.
- [2] T. Searchinger, R. Waite, C. Hanson, J. Ranganathan, P. Dumas, E. Matthews, C. Klirs, Creating a sustainable food future: A menu of solutions to feed nearly 10 billion people by 2050, *World Resourc. Inst.* (2019).
- [3] K. Phasinam, T. Kassanuk, M. Shabaz, Applicability of internet of things in smart farming, *J. Food Qual.* 2022 (2022) 7692922.
- [4] L.F. Oliveira, A.P. Moreira, M.F. Silva, Advances in agriculture robotics: A state-of-the-art review and challenges ahead, *Robotics* 10 (2) (2021) 52.
- [5] R.K. Goel, C.S. Yadav, S. Vishnoi, R. Rastogi, Smart agriculture–Urgent need of the day in developing countries, *Sustain. Comput.: Inform. Syst.* 30 (2021) 100512.
- [6] A. Subeesh, C. Mehta, Automation and digitization of agriculture using artificial intelligence and internet of things, *Artif. Intell. Agric.* 5 (2021) 278–291.
- [7] E.S. Mohamed, A. Belal, S.K. Abd-Elmabod, M.A. El-Shirbeny, A. Gad, M.B. Zahran, Smart farming for improving agricultural management, *Egypt. J. Remote Sens. Space Sci.* 24 (2021) 971–981.
- [8] S. Meng, X. Wang, X. Hu, C. Luo, Y. Zhong, Deep learning-based crop mapping in the cloudy season using one-shot hyperspectral satellite imagery, *Comput. Electron. Agric.* 186 (2021) 106188.
- [9] A. Anagnostis, A.C. Tagarakis, D. Kateris, V. Moysiadis, C.G. Sørensen, S. Pearson, D. Bochtis, Orchard mapping with deep learning semantic segmentation, *Sensors* 21 (11) (2021) 3813.
- [10] C. Yang, J.H. Everitt, Q. Du, B. Luo, J. Chanussot, Using high-resolution airborne and satellite imagery to assess crop growth and yield variability for precision agriculture, *Proc. IEEE* 101 (3) (2012) 582–592.
- [11] E.R. Hunt Jr., C.S. Daughtry, What good are unmanned aircraft systems for agricultural remote sensing and precision agriculture? *Int. J. Remote Sens.* 39 (15–16) (2018) 5345–5376.
- [12] N. Gyagenda, J.V. Hatilima, H. Roth, V. Zhmud, A review of GNSS-independent UAV navigation techniques, *Robot. Auton. Syst.* (2022) 104069.
- [13] I.A. Hameed, A. la Cour-Harbo, O.L. Osen, Side-to-side 3D coverage path planning approach for agricultural robots to minimize skip/overlap areas between swaths, *Robot. Auton. Syst.* 76 (2016) 36–45.
- [14] D. Tiozzo Fasiolo, L. Scalera, E. Maset, A. Gasparetto, Recent trends in mobile robotics for 3D mapping in agriculture, in: International Conference on Robotics in Alpe-Adria Danube Region, Springer, 2022, pp. 428–435.
- [15] M. Ammoniaci, S.-P. Kartsios, R. Perria, P. Storchi, State of the art of monitoring technologies and data processing for precision viticulture, *Agriculture* 11 (3) (2021) 201.
- [16] A. Atefi, Y. Ge, S. Pitla, J. Schnable, Robotic technologies for high-throughput plant phenotyping: Contemporary reviews and future perspectives, *Front. Plant Sci.* 12 (2021) 611940.
- [17] A. Botta, P. Cavallone, L. Baglieri, G. Colucci, L. Tagliavini, G. Quaglia, A review of robots, perception, and tasks in precision agriculture, *Appl. Mech.* 3 (3) (2022) 830–854.
- [18] R.P. Sishodia, R.L. Ray, S.K. Singh, Applications of remote sensing in precision agriculture: A review, *Remote Sens.* 12 (19) (2020) 3136.
- [19] T. Duckett, S. Pearson, S. Blackmore, B. Grieve, W.-H. Chen, G. Cielniak, J. Cleaversmith, J. Dai, S. Davis, C. Fox, et al., Agricultural robotics: The future of robotic agriculture, UK-RAS Network, *Robot. Auton. Syst.* (2018).
- [20] S. Fountas, N. Mylonas, I. Malounas, E. Rodias, C. Hellmann Santos, E. Pekkeriet, Agricultural robotics for field operations, *Sensors* 20 (9) (2020) 2672.
- [21] S.G. Vougioukas, Agricultural robotics, *Ann. Rev. Control. Robot. Auton. Syst.* 2 (1) (2019) 365–392.
- [22] S.A. Magalhães, A.P. Moreira, F.N. dos Santos, J. Dias, Active perception fruit harvesting robots—A systematic review, *J. Intell. Robot. Syst.* 105 (1) (2022) 1–22.

- [23] J. Tardaguila, M. Stoll, S. Gutiérrez, T. Proffitt, M.P. Diago, Smart applications and digital technologies in viticulture: A review, *Smart Agric. Technol.* 1 (2021) 100005.
- [24] Q. Guo, Y. Su, T. Hu, H. Guan, S. Jin, J. Zhang, X. Zhao, K. Xu, D. Wei, M. Kelly, et al., LiDAR boosts 3D ecological observations and modelings: A review and perspective, *IEEE Geosci. Remote Sens. Mag.* 9 (1) (2020) 232–257.
- [25] A.S. Aguiar, F.N. dos Santos, J. Boaventura Cunha, H. Sobreira, A.J. Sousa, Localization and mapping for robots in agriculture and forestry: A survey, *Robotics* 9 (4) (2020) 97.
- [26] H. Ding, B. Zhang, J. Zhou, Y. Yan, G. Tian, B. Gu, Recent developments and applications of simultaneous localization and mapping in agriculture, *J. Field Robotics* 39 (2022) 956–983.
- [27] X. Gao, J. Li, L. Fan, Q. Zhou, K. Yin, J. Wang, C. Song, L. Huang, Z. Wang, Review of wheeled mobile robots' navigation problems and application prospects in agriculture, *IEEE Access* 6 (2018) 49248–49268.
- [28] L.C. Santos, F.N. Santos, E.S. Pires, A. Valente, P. Costa, S. Magalhães, Path planning for ground robots in agriculture: A short review, in: 2020 IEEE International Conference on Autonomous Robot Systems and Competitions, ICARSC, 2020, pp. 61–66.
- [29] X. Li, Q. Qiu, Autonomous navigation for orchard mobile robots: A rough review, in: 2021 36th Youth Academic Annual Conference of Chinese Association of Automation, YAC, IEEE, 2021, pp. 552–557.
- [30] I. Hrabar, J. Goričanec, Z. Kovačić, Towards autonomous navigation of a mobile robot in a steep slope vineyard, in: 2021 44th International Convention on Information, Communication and Electronic Technology, MIPRO, IEEE, 2021, pp. 1119–1124.
- [31] S. Bonadies, S.A. Gadsden, An overview of autonomous crop row navigation strategies for unmanned ground vehicles, *Eng. Agric., Environ. Food* 12 (1) (2019) 24–31.
- [32] J. Ferreira, A.P. Moreira, M. Silva, F. Santos, A survey on localization, mapping, and trajectory planning for quadruped robots in vineyards, in: 2022 IEEE International Conference on Autonomous Robot Systems and Competitions, ICARSC, IEEE, 2022, pp. 237–242.
- [33] H. Tian, T. Wang, Y. Liu, X. Qiao, Y. Li, Computer vision technology in agricultural automation—A review, *Inf. Process. Agric.* 7 (1) (2020) 1–19.
- [34] B. Darwin, P. Dharmaraj, S. Prince, D.E. Popescu, D.J. Hemanth, Recognition of bloom/yield in crop images using deep learning models for smart agriculture: A review, *Agronomy* 11 (4) (2021) 646.
- [35] M.T. Linaza, J. Posada, J. Bund, P. Eisert, M. Quartulli, J. Döllner, A. Pagani, I. G. Olaiola, A. Barriguinha, T. Moysiadis, et al., Data-driven artificial intelligence applications for sustainable precision agriculture, *Agronomy* 11 (6) (2021) 1227.
- [36] M. Pathan, N. Patel, H. Yagnik, M. Shah, Artificial cognition for applications in smart agriculture: A comprehensive review, *Artif. Intell. Agric.* 4 (2020) 81–95.
- [37] L. Santos, F. Santos, J. Mendes, P. Costa, J. Lima, R. Reis, P. Shinde, Path planning aware of robot's center of mass for steep slope vineyards, *Robotica* 38 (4) (2020) 684–698.
- [38] P. Gao, J. Jiang, J. Song, F. Xie, Y. Bai, Y. Fu, Z. Wang, X. Zheng, S. Xie, B. Li, Canopy volume measurement of fruit trees using robotic platform loaded LiDAR data, *IEEE Access* 9 (2021) 156246–156259.
- [39] D. Ball, B. Upcroft, G. Wyeth, P. Corke, A. English, P. Ross, T. Patten, R. Fitch, S. Sukkarieh, A. Bate, Vision-based obstacle detection and navigation for an agricultural robot, *J. Field Robotics* 33 (8) (2016) 1107–1130.
- [40] G. Bayar, M. Bergerman, A.B. Koku, E. İlhan Konukseven, Localization and control of an autonomous orchard vehicle, *Comput. Electron. Agric.* 115 (2015) 118–128.
- [41] A. Choudhary, Y. Kobayashi, F.J. Arjonilla, S. Nagasaka, M. Koike, Evaluation of mapping and path planning for non-holonomic mobile robot navigation in narrow pathway for agricultural application, in: 2021 IEEE/SICE International Symposium on System Integration, SII, 2021, pp. 17–22.
- [42] L.C. Santos, A. Santos, F.N. Santos, A. Valente, A case study on improving the software dependability of a ROS path planner for steep slope vineyards, *Robotics* 10 (3) (2021) 103.
- [43] H. Gan, W.S. Lee, Development of a navigation system for a smart farm, *IFAC-PapersOnLine* 51 (17) (2018) 1–4.
- [44] J. Iqbal, R. Xu, S. Sun, C. Li, Simulation of an autonomous mobile robot for LiDAR-based in-field phenotyping and navigation, *Robotics* 9 (2) (2020) 46.
- [45] S. Eiffert, N. Wallace, H. Kong, N. Pirmarzdashti, S. Sukkarieh, Resource and response aware path planning for long-term autonomy of ground robots in agriculture, *Field Robot.* 2 (2022) 1–33.
- [46] J.P. Fentanes, I. Gould, T. Duckett, S. Pearson, G. Cielniak, 3D soil compaction mapping through kriging-based exploration with a mobile robot, *IEEE Robot. Autom. Lett.* 3 (4) (2018) 3066–3072.
- [47] M.A. Post, A. Bianco, X.T. Yan, Autonomous navigation with ROS for a mobile robot in agricultural fields, in: 14th International Conference on Informatics in Control, Automation and Robotics, ICINCO, 2017.
- [48] T. Bak, H. Jakobsen, Agricultural robotic platform with four wheel steering for weed detection, *Biosyst. Eng.* 87 (2) (2004) 125–136.
- [49] R. Manish, Y.-C. Lin, R. Ravi, S.M. Hasheminasab, T. Zhou, A. Habib, Development of a miniaturized mobile mapping system for in-row, under-canopy phenotyping, *Remote Sens.* 13 (2) (2021) 276.
- [50] E.-T. Baek, D.-Y. Im, ROS-based unmanned mobile robot platform for agriculture, *Appl. Sci.* 12 (9) (2022) 4335.
- [51] M. Garrido, D.S. Parafos, D. Reiser, M. Vázquez Arellano, H.W. Griepentrog, C. Valero, 3D maize plant reconstruction based on georeferenced overlapping LiDAR point clouds, *Remote Sens.* 7 (12) (2015) 17077–17096.
- [52] N. Chebrolu, P. Lottes, A. Schaefer, W. Winterhalter, W. Burgard, C. Stachniss, Agricultural robot dataset for plant classification, localization and mapping on sugar beet fields, *Int. J. Robot. Res.* 36 (10) (2017) 1045–1052.
- [53] S. Cubero, E. Marco-Noales, N. Aleixos, S. Barbé, J. Blasco, Robhortic: A field robot to detect pests and diseases in horticultural crops by proximal sensing, *Agriculture* 10 (7) (2020) 276.
- [54] M.V. Gasparino, V.A. Higuti, A.E. Velasquez, M. Becker, Improved localization in a corn crop row using a rotated laser rangefinder for three-dimensional data acquisition, *J. Braz. Soc. Mech. Sci. Eng.* 42 (2020) 1–10.
- [55] T. Pire, M. Mujica, J. Civera, E. Kofman, The Rosario dataset: Multisensor data for localization and mapping in agricultural environments, *Int. J. Robot. Res.* 38 (6) (2019) 633–641.
- [56] J. Underwood, A. Wendel, B. Schofield, L. McMurray, R. Kimber, Efficient in-field plant phenomics for row-crops with an autonomous ground vehicle, *J. Field Robotics* 34 (6) (2017) 1061–1083.
- [57] M.F. Kragh, P. Christiansen, M.S. Laursen, M. Larsen, K.A. Steen, O. Green, H. Karstoft, R.N. Jørgensen, Fieldsafe: Dataset for obstacle detection in agriculture, *Sensors* 17 (11) (2017) 2579.
- [58] A. Krus, D. Van Apeldoorn, C. Valero, J.J. Ramirez, Acquiring plant features with optical sensing devices in an organic strip-cropping system, *Agronomy* 10 (2) (2020) 197.
- [59] L. Grimstad, P.J. From, The Thorvald II agricultural robotic system, *Robotics* 6 (2017) 24.
- [60] A. Shafeiekhani, S. Kadam, F.B. Fritsch, G.N. DeSouza, Vinobot and vinoculer: Two robotic platforms for high-throughput field phenotyping, *Sensors* 17 (1) (2017) 214.
- [61] R. de Silva, G. Cielniak, J. Gao, Towards agricultural autonomy: Crop row detection under varying field conditions using deep learning, 2021, arXiv preprint [arXiv:2109.08247](https://arxiv.org/abs/2109.08247).
- [62] I. Belovod, D. Kinaneva, G. Georgiev, G. Hristov, P. Zahariev, Artificial intelligence-driven autonomous robot for precision agriculture, *Acta Technol. Agric.* 24 (1) (2021) 48–54.
- [63] J. Gai, L. Xiang, L. Tang, Using a depth camera for crop row detection and mapping for under-canopy navigation of agricultural robotic vehicle, *Comput. Electron. Agric.* 188 (2021) 106301.
- [64] K. Wang, J. Zhou, W. Zhang, B. Zhang, Mobile LiDAR scanning system combined with canopy morphology extracting methods for tree crown parameters evaluation in orchards, *Sensors* 21 (2) (2021) 339.
- [65] P.M. Blok, K. van Boheemen, E.K. van Evert, J. IJsselmuiden, G.-H. Kim, Robot navigation in orchards with localization based on Particle filter and Kalman filter, *Comput. Electron. Agric.* 157 (2019) 261–269.
- [66] S. Marden, M. Whitty, GPS-free localisation and navigation of an unmanned ground vehicle for yield forecasting in a vineyard, in: Recent Advances in Agricultural Robotics, International Workshop Collocated with the 13th International Conference on Intelligent Autonomous Systems, IAS-13, 2014.
- [67] G. Reina, A. Milella, R. Galati, Terrain assessment for precision agriculture using vehicle dynamic modelling, *Biosyst. Eng.* 162 (2017) 124–139.
- [68] D. Aghi, V. Mazzia, M. Chiaberge, Local motion planner for autonomous navigation in vineyards with a RGB-D camera-based algorithm and deep learning synergy, *Machines* 8 (2) (2020) 27.
- [69] D. Aghi, S. Cerrato, V. Mazzia, M. Chiaberge, Deep semantic segmentation at the edge for autonomous navigation in vineyard rows, in: 2021 IEEE/RSJ International Conference on Intelligent Robots and Systems, IROS, IEEE, 2021, pp. 3421–3428.
- [70] S. Jiang, S. Wang, Z. Yi, M. Zhang, X. Lv, Autonomous navigation system of greenhouse mobile robot based on 3D LiDAR and 2D LiDAR SLAM, *Front. Plant Sci.* 13 (2022) 815218.
- [71] M. Fawakherji, C. Potena, A. Pretto, D.D. Bloisi, D. Nardi, Multi-spectral image synthesis for crop/weed segmentation in precision farming, *Robot. Auton. Syst.* 146 (2021) 103861.
- [72] M. Imperoli, C. Potena, D. Nardi, G. Grisetti, A. Pretto, An effective multi-cue positioning system for agricultural robotics, *IEEE Robot. Autom. Lett.* 3 (4) (2018) 3685–3692.
- [73] T. Le, J.G.O. Gjevestad, P.J. From, Online 3D mapping and localization system for agricultural robots, *IFAC-PapersOnLine* 52 (30) (2019) 167–172.

- [74] J. Weyler, A. Milioto, T. Falck, J. Behley, C. Stachniss, Joint plant instance detection and leaf count estimation for in-field plant phenotyping, *IEEE Robot. Autom. Lett.* 6 (2) (2021) 3599–3606.
- [75] W. Winterhalter, F. Fleckenstein, C. Dornhege, W. Burgard, Localization for precision navigation in agricultural fields—Beyond crop row following, *J. Field Robotics* 38 (3) (2021) 429–451.
- [76] A.S.P. Aguiar, F.N. dos Santos, L.C.F. dos Santos, V.M. de Jesus Filipe, A.J.M. de Sousa, Vineyard trunk detection using deep learning—An experimental device benchmark, *Comput. Electron. Agric.* 175 (2020) 105535.
- [77] A.S. Aguiar, F.N. dos Santos, H. Sobreira, J. Boaventura Cunha, A.J. Sousa, Particle filter refinement based on clustering procedures for high-dimensional localization and mapping systems, *Robot. Auton. Syst.* 137 (2021) 103725.
- [78] A.S. Aguiar, F.N. dos Santos, H. Sobreira, J. Boaventura Cunha, A.J. Sousa, Localization and mapping on agriculture based on point-feature extraction and semiplanes segmentation from 3D LiDAR data, *Front. Robot. AI* 9 (2022) 832165.
- [79] S. Dogru, L. Marques, Evaluation of an automotive short range radar sensor for mapping in orchards, in: 2018 IEEE International Conference on Autonomous Robot Systems and Competitions, ICARSC, IEEE, 2018, pp. 78–83.
- [80] N. Habibie, A.M. Nugraha, A.Z. Anshori, M.A. Ma'sum, W. Jatmiko, Fruit mapping mobile robot on simulated agricultural area in Gazebo simulator using simultaneous localization and mapping (SLAM), in: 2017 International Symposium on Micro-NanoMechatronics and Human Science, MHS, IEEE, 2017, pp. 1–7.
- [81] N. Ohi, K. Lassak, R. Watson, J. Strader, Y. Du, C. Yang, G. Hedrick, J. Nguyen, S. Harper, D. Reynolds, et al., Design of an autonomous precision pollination robot, in: 2018 IEEE/RSJ International Conference on Intelligent Robots and Systems, IROS, 2018, pp. 7711–7718.
- [82] L.C. Santos, A.S. Aguiar, F.N. Santos, A. Valente, J.B. Ventura, A.J. Sousa, Navigation stack for robots working in steep slope vineyard, in: Proceedings of SAI Intelligent Systems Conference, Springer, 2020, pp. 264–285.
- [83] L.C. Santos, F.N. Santos, A. Valente, H. Sobreira, J. Sarmento, M. Petry, Collision avoidance considering iterative Bézier based approach for steep slope terrains, *IEEE Access* 10 (2022) 25005–25015.
- [84] C. Yang, R.M. Watson, J.N. Gross, Y. Gu, Localization algorithm design and evaluation for an autonomous pollination robot, in: Proceedings of the 32nd International Technical Meeting of the Satellite Division of the Institute of Navigation, ION GNSS+ 2019, 2019, pp. 2702–2710.
- [85] L. Zhang, R. Li, Z. Li, Y. Meng, J. Liang, L. Fu, X. Jin, S. Li, A quadratic traversal algorithm of shortest weeding path planning for agricultural mobile robots in cornfield, *J. Robot.* 2021 (2021) 6633139.
- [86] S. Cerrato, V. Mazzia, F. Salvetti, M. Chiaberge, A deep learning driven algorithmic pipeline for autonomous navigation in row-based crops, 2021, arXiv preprint [arXiv:2112.03816](https://arxiv.org/abs/2112.03816).
- [87] J. Pak, J. Kim, Y. Park, H.I. Son, Field evaluation of path-planning algorithms for autonomous mobile robot in smart farms, *IEEE Access* 10 (2022) 60253–60266.
- [88] N. Shalal, T. Low, C. McCarthy, N. Hancock, Orchard mapping and mobile robot localisation using on-board camera and laser scanner data fusion—Part B: Mapping and localisation, *Comput. Electron. Agric.* 119 (2015) 267–278.
- [89] T. Clamens, G. Alexakis, R. Duverne, R. Seulin, E. Fauvet, D. Fofi, Real-time multispectral image processing and registration on 3D point cloud for vineyard analysis, in: 16th International Conference on Computer Vision Theory and Applications, 2021.
- [90] R. Guzmán, J. Ariño, R. Navarro, C. Lopes, J. Graça, M. Reyes, A. Barriguinha, R. Braga, Autonomous hybrid GPS/reactive navigation of an unmanned ground vehicle for precision viticulture-VINBOT, *Intervitis Interfructa Hortitechnica-Technol. Wine, Juice Spec. Crops* (2016).
- [91] I. Hroob, R. Polvara, S. Molina, G. Cieliak, M. Hanheide, Benchmark of visual and 3D LiDAR SLAM systems in simulation environment for vineyards, in: Annual Conference Towards Autonomous Robotic Systems, Springer, 2021, pp. 168–177.
- [92] M. Halstead, A. Ahmadi, C. Smitt, O. Schmittmann, C. McCool, Crop agnostic monitoring driven by deep learning, *Front. Plant Sci.* 12 (2021) 786702.
- [93] L. Emmi, E. Le Flécher, Cadenat, Devy, A hybrid representation of the environment to improve autonomous navigation of mobile robots in agriculture, *Precis. Agric.* 22 (2) (2021) 524–549.
- [94] M. Duarte, F.N. dos Santos, A. Sousa, R. Morais, Agricultural wireless sensor mapping for robot localization, in: Robot 2015: Second Iberian Robotics Conference, Springer, 2016, pp. 359–370.
- [95] F.B. Malavazi, R. Guyonneau, J.-B. Fasquel, S. Lagrange, F. Mercier, LiDAR-only based navigation algorithm for an autonomous agricultural robot, *Comput. Electron. Agric.* 154 (2018) 71–79.
- [96] Y. Yamasaki, M. Morie, N. Noguchi, Development of a high-accuracy autonomous sensing system for a field scouting robot, *Comput. Electron. Agric.* 193 (2022) 106630.
- [97] J. Jackson, B. Davis, D. Gebre-Egziabher, A performance assessment of low-cost RTK GNSS receivers, in: IEEE/ION Position, Location and Navigation Symposium, PLANS, 2018, pp. 642–649.
- [98] J. Guo, X. Li, Z. Li, L. Hu, G. Yang, C. Zhao, D. Fairbairn, D. Watson, M. Ge, Multi-GNSS precise point positioning for precision agriculture, *Precis. Agric.* 19 (5) (2018) 895–911.
- [99] H. Kaartinen, J. Hyppä, M. Vastaranta, A. Kukko, A. Jaakkola, X. Yu, J. Pyörälä, X. Liang, J. Liu, Y. Wang, R. Kaijaluoto, T. Melkas, M. Holopainen, H. Hyppä, Accuracy of kinematic positioning using global satellite navigation systems under forest canopies, *Forests* 6 (9) (2015) 3218–3236.
- [100] R. Hirokawa, T. Ebinuma, A low-cost tightly coupled GPS/INS for small UAVs augmented with multiple GPS antennas, *Navigation* 56 (1) (2009) 35–44.
- [101] B. Grocholsky, S. Nuske, M. Aasted, S. Achar, T. Bates, A camera and laser system for automatic vine balance assessment, in: 2011 Louisville, Kentucky, August 7–10, 2011, American Society of Agricultural and Biological Engineers, 2011, p. 1.
- [102] H. Lan, M. Elsheikh, W. Abdelfatah, A. Wahdan, N. El-Sheimy, Integrated RTK/INS navigation for precision agriculture, in: 32nd International Technical Meeting of the Satellite Division of the Institute of Navigation, 2019, pp. 4076–4086.
- [103] T. Lowe, P. Moghadam, E. Edwards, J. Williams, Canopy density estimation in perennial horticulture crops using 3D spinning LiDAR SLAM, *J. Field Robotics* 38 (4) (2021) 598–618.
- [104] R.V. Vitali, R.S. McGinnis, N.C. Perkins, Robust error-state Kalman filter for estimating IMU orientation, *IEEE Sensors J.* 21 (3) (2020) 3561–3569.
- [105] H. Masuzawa, J. Miura, S. Oishi, Development of a mobile robot for harvest support in greenhouse horticulture—Person following and mapping, in: 2017 IEEE/SICE International Symposium on System Integration, SII, IEEE, 2017, pp. 541–546.
- [106] I. del Moral-Martínez, J.R. Rosell-Polo, J. Company, R. Sanz, A. Escalà, J. Masip, J.A. Martínez-Casasnovas, J. Arno, Mapping vineyard leaf area using mobile terrestrial laser scanners: Should rows be scanned on-the-go or discontinuously sampled? *Sensors* 16 (1) (2016) 119.
- [107] H. Moreno, C. Valero, J.M. Bengoechea-Guevara, Á. Ribeiro, M. Garrido-Izard, D. Andújar, On-ground vineyard reconstruction using a LiDAR-based automated system, *Sensors* 20 (4) (2020) 1102.
- [108] A. Pagliai, M. Ammoniaci, D. Sarri, R. Lisci, R. Perria, M. Vieri, M.E.M. D'Arcangelo, P. Storchi, S.-P. Kartsiotis, Comparison of aerial and ground 3D point clouds for canopy size assessment in precision viticulture, *Remote Sens.* 14 (5) (2022) 1145.
- [109] G. Riggio, C. Fantuzzi, C. Secchi, A low-cost navigation strategy for yield estimation in vineyards, in: 2018 IEEE International Conference on Robotics and Automation, ICRA, 2018, pp. 2200–2205.
- [110] V. Saiz-Rubio, F. Rovira-Más, A. Cuenca-Cuenca, F. Alves, Robotics-based vineyard water potential monitoring at high resolution, *Comput. Electron. Agric.* 187 (2021) 106311.
- [111] F.N. dos Santos, H. Sobreira, D. Campos, R. Morais, A. Paulo Moreira, O. Contente, Towards a reliable robot for steep slope vineyards monitoring, *J. Intell. Robot. Syst.* 83 (3) (2016) 429–444.
- [112] R. Sanz, J. Rosell, J. Llorens, E. Gil, S. Planas, Relationship between tree row LiDAR-volume and leaf area density for fruit orchards and vineyards obtained with a LiDAR 3D dynamic measurement system, *Agric. Forest Meteorol.* 171 (2013) 153–162.
- [113] M.H. Siebers, E.J. Edwards, J.A. Jimenez-Berni, M.R. Thomas, M. Salim, R.R. Walker, Fast phenomics in vineyards: Development of GRover, the grapevine rover, and LiDAR for assessing grapevine traits in the field, *Sensors* 18 (9) (2018) 2924.
- [114] A. Silwal, F. Yandun, A. Nellithimaru, T. Bates, G. Kantor, Bumblebee: A path towards fully autonomous robotic vine pruning, 2021, arXiv preprint [arXiv:2112.00291](https://arxiv.org/abs/2112.00291).
- [115] P. Lepej, J. Rakun, Simultaneous localisation and mapping in a complex field environment, *Biosyst. Eng.* 150 (2016) 160–169.
- [116] J. Zhang, G. Kantor, M. Bergerman, S. Singh, Monocular visual navigation of an autonomous vehicle in natural scene corridor-like environments, in: 2012 IEEE/RSJ International Conference on Intelligent Robots and Systems, IEEE, 2012, pp. 3659–3666.
- [117] W. Mao, H. Liu, W. Hao, F. Yang, Z. Liu, Development of a combined orchard harvesting robot navigation system, *Remote Sens.* 14 (3) (2022) 675.
- [118] G. Ristorto, R. Gallo, A. Gasparetto, L. Scalera, R. Vidoni, F. Mazzetto, A mobile laboratory for orchard health status monitoring in precision farming, *Chem. Eng. Trans.* 58 (2017) 661–666.
- [119] R. Vidoni, R. Gallo, G. Ristorto, G. Carabin, F. Mazzetto, L. Scalera, A. Gasparetto, ByeLab: An agricultural mobile robot prototype for proximal sensing and precision farming, in: ASME International Mechanical Engineering Congress and Exposition, vol. 58370, American Society of Mechanical Engineers, 2017.

- [120] J. Zhang, S. Maeta, M. Bergerman, S. Singh, Mapping orchards for autonomous navigation, in: Proc. ASABE Annu. Int. Meeting, Montreal, Quebec Canada, American Society of Agricultural and Biological Engineers, 2014, 141838567.
- [121] Z. Al-Mashhadani, M. Mainampati, B. Chandrasekaran, Autonomous exploring map and navigation for an agricultural robot, in: 2020 3rd International Conference on Control and Robots, ICCR, IEEE, 2020, pp. 73–78.
- [122] E.H.C. Harik, A. Korsaeth, Combining Hector SLAM and artificial potential field for autonomous navigation inside a greenhouse, *Robotics* 7 (2018) 22.
- [123] C.C. Ulloa, A. Krus, A. Barrientos, J. del Cerro, C. Valero, Robotic fertilization in strip cropping using a CNN vegetables detection-characterization method, *Comput. Electron. Agric.* 193 (2022) 106684.
- [124] F.A.A. Cheein, J. Guivant, SLAM-based incremental convex hull processing approach for treetop volume estimation, *Comput. Electron. Agric.* 102 (2014) 19–30.
- [125] A.F. Colaco, R.G. Trevisan, J.P. Molin, J.R. Rosell-Polo, A. Escolà, A method to obtain orange crop geometry information using a mobile terrestrial laser scanner and 3D modeling, *Remote Sens.* 9 (8) (2017) 763.
- [126] J.A. Martínez-Casasnovas, J. Rufat, J. Arnó, A. Arbonés, F. Sebé, M. Pasqual, E. Gregorio, J.R. Rosell-Polo, et al., Mobile terrestrial laser scanner applications in precision fruticulture/horticulture and tools to extract information from canopy point clouds, *Precis. Agric.* 18 (1) (2017) 111–132.
- [127] M. Bietresato, G. Carabin, R. Vidoni, A. Gasparetto, F. Mazzetto, Evaluation of a LiDAR-based 3D-stereoscopic vision system for crop-monitoring applications, *Comput. Electron. Agric.* 124 (2016) 1–13.
- [128] M. Wichmann, M. Kamil, A. Frederiksen, S. Kotzur, M. Scherl, Long-term investigations of weather influence on direct time-of-flight LiDAR at 905nm, *IEEE Sens. J.* 22 (3) (2021) 2024–2036.
- [129] R. Rouveure, P. Faure, M. Monod, Description and experimental results of a panoramic k-band radar dedicated to perception in mobile robotics applications, *J. Field Robotics* 35 (5) (2018) 678–704.
- [130] Y. Cheng, P. Changsong, J. Mengxin, L. Yimin, Relocalization based on millimeter wave radar point cloud for visually degraded environments, *J. Field Robot.* (2023) <http://dx.doi.org/10.1002/rob.22162>.
- [131] A. Velasquez, V. Higuti, H. Guerrero, D. Milori, D. Magalhães, M. Becker, Helvis-a small-scale agricultural mobile robot prototype for precision agriculture, in: 13th International conference of precision agriculture, International Society of Precision Agriculture, St. Louis, Missouri, USA, vol. 17, 2016.
- [132] J.-E. Blanquart, E. Sirignano, B. Lenaerts, W. Saeys, Online crop height and density estimation in grain fields using LiDAR, *Biosyst. Eng.* 198 (2020) 1–14.
- [133] F.A. Cheein, G.M. Steiner, G.P. Paina, R. Carelli, Optimized EIF-SLAM algorithm for precision agriculture mapping based on stems detection, *Comput. Electron. Agric.* 78 (2) (2011) 195–207.
- [134] G. Daglio, R. Gallo, S. Petrucci, C. Andergassen, M. Kelderer, F. Mazzetto, Automated crop monitoring solutions to assess the blooming charge in orchards: Preliminary results achieved by a prototype mobile lab used on apple trees, in: IOP Conference Series: Earth and Environmental Science, vol. 275, IOP Publishing, 2019, 012019.
- [135] A.N. French, M.A. Gore, A. Thompson, Cotton phenotyping with LiDAR from a track-mounted platform, in: Autonomous Air and Ground Sensing Systems for Agricultural Optimization and Phenotyping, vol. 9866, International Society for Optics and Photonics, 2016, p. 98660B.
- [136] G. Freitas, J. Zhang, B. Hamner, M. Bergerman, G. Kantor, A low-cost, practical localization system for agricultural vehicles, in: International Conference on Intelligent Robotics and Applications, Springer, 2012, pp. 365–375.
- [137] M. Pérez-Ruiz, A. Prior, J. Martínez-Guanter, O. Apolo-Apolo, P. Andrade-Sánchez, G. Egea, Development and evaluation of a self-propelled electric platform for high-throughput field phenotyping in wheat breeding trials, *Comput. Electron. Agric.* 169 (2020) 105237.
- [138] S. Sun, C. Li, A.H. Paterson, Y. Jiang, R. Xu, J.S. Robertson, J.L. Snider, P.W. Chee, In-field high throughput phenotyping and cotton plant growth analysis using LiDAR, *Front. Plant Sci.* 9 (2018) 16.
- [139] Y. Arita, E. di Maria, R. Gallone, L. Capodieci, M. Morita, K. Okubo, N.I. Giannoccaro, M. Shige-Eda, T. Nishida, Development of a mobile robot platform for 3D measurement of forest environments, 2016, ICT-ROBOT2016.
- [140] U. Weiss, P. Biber, Plant detection and mapping for agricultural robots using a 3D LiDAR sensor, *Robot. Auton. Syst.* 59 (5) (2011) 265–273.
- [141] H. Nehme, C. Aubry, T. Solatges, X. Savatier, R. Rossi, R. Boutteau, LiDAR-based structure tracking for agricultural robots: Application to autonomous navigation in vineyards, *J. Intell. Robot. Syst.* 103 (4) (2021) 1–16.
- [142] N. Dong, R. Chi, W. Zhang, LiDAR odometry and mapping based on semantic information for maize field, *Agronomy* 12 (12) (2022) 3107.
- [143] M. Chakraborty, L.R. Khot, S. Sankaran, P.W. Jacoby, Evaluation of mobile 3D light detection and ranging based canopy mapping system for tree fruit crops, *Comput. Electron. Agric.* 158 (2019) 284–293.
- [144] A. Wendel, J. Underwood, K. Walsh, Maturity estimation of mangoes using hyperspectral imaging from a ground based mobile platform, *Comput. Electron. Agric.* 155 (2018) 298–313.
- [145] P. Astolfi, A. Gabrielli, L. Bascetta, M. Matteucci, Vineyard autonomous navigation in the echord++ grape experiment, *IFAC-PapersOnLine* 51 (2018) 704–709.
- [146] H. Durmuş, E.O. Güneş, M. Kirci, B.B. Üstündag, The design of general purpose autonomous agricultural mobile-robot: "AGROBOT", in: 2015 Fourth International Conference on Agro-Geoinformatics, Agro-Geoinformatics, IEEE, 2015, pp. 49–53.
- [147] W.S. Barbosa, A.I. Oliveira, G.B. Barbosa, A.C. Leite, K.T. Figueiredo, M.M. Vellasco, W. Caarls, Design and development of an autonomous mobile robot for inspection of soy and cotton crops, in: 2019 12th International Conference on Developments in ESystems Engineering, DeSE, IEEE, 2019, pp. 557–562.
- [148] C. Smitt, M. Halstead, T. Zaenker, M. Bennewitz, C. McCool, Pathobot: A robot for glasshouse crop phenotyping and intervention, in: IEEE International Conference on Robotics and Automation, ICRA, 2021, pp. 2324–2330.
- [149] P. Kurtsen, O. Ringdahl, N. Rotstein, R. Berenstein, Y. Edan, In-field grape cluster size assessment for vine yield estimation using a mobile robot and a consumer level RGB-D camera, *IEEE Robot. Autom. Lett.* 5 (2) (2020) 2031–2038.
- [150] F. Vulpi, R. Marani, A. Petitti, G. Reina, A. Milella, An RGB-D multi-view perspective for autonomous agricultural robots, *Comput. Electron. Agric.* 202 (2022) 107419.
- [151] S. Matsuzaki, H. Masuzawa, J. Miura, S. Oishi, 3D semantic mapping in greenhouses for agricultural mobile robots with robust object recognition using robots' trajectory, in: 2018 IEEE International Conference on Systems, Man, and Cybernetics, SMC, IEEE, 2018, pp. 357–362.
- [152] J.R. Rosell-Polo, E. Gregorio, J. Gené, J. Llorens, X. Torrent, J. Arnó, A. Escola, Kinect V2 sensor-based mobile terrestrial laser scanner for agricultural outdoor applications, *IEEE/ASME Trans. Mechatronics* 22 (6) (2017) 2420–2427.
- [153] M.S.A. Khan, D. Hussain, S. Khan, F.U. Rehman, A.B. Aqeel, U.S. Khan, Implementation of SLAM by using a mobile agribot in a simulated indoor environment in Gazebo, in: 2021 International Conference on Robotics and Automation in Industry, ICRAI, IEEE, 2021, pp. 1–4.
- [154] S. Jay, G. Rabatel, X. Hadoux, D. Moura, N. Gorretta, In-field crop row phenotyping from 3D modeling performed using structure from motion, *Comput. Electron. Agric.* 110 (2015) 70–77.
- [155] D.I. Patrício, R. Rieder, Computer vision and artificial intelligence in precision agriculture for grain crops: A systematic review, *Comput. Electron. Agric.* 153 (2018) 69–81.
- [156] S. Zaman, L. Comba, A. Biglia, D.R. Aimonino, P. Barge, P. Gay, Cost-effective visual odometry system for vehicle motion control in agricultural environments, *Comput. Electron. Agric.* 162 (2019) 82–94.
- [157] M. Lv, H. Wei, X. Fu, W. Wang, D. Zhou, A loosely coupled Extended Kalman Filter algorithm for agricultural scene-based multi-sensor fusion, *Front. Plant Sci.* 13 (2022) 849260.
- [158] A. Durand-Petiteville, E. Le Flecher, V. Cadene, T. Sentenac, S. Vougioukas, Tree detection with low-cost three-dimensional sensors for autonomous navigation in orchards, *IEEE Robot. Autom. Lett.* 3 (4) (2018) 3876–3883.
- [159] A.C. Tagarakis, E. Filippou, D. Kalaitzidis, L. Benos, P. Busato, D. Bochtis, Proposing UGV and UAV systems for 3D mapping of orchard environments, *Sensors* 22 (2022) 1571.
- [160] J. Fernández-Novales, V. Saiz-Rubio, I. Barrio, F. Rovira-Más, A. Cuenc-Cuena, F. Santos Alves, J. Valente, J. Tardaguila, M.P. Diago, Monitoring and mapping vineyard water status using non-invasive technologies by a ground robot, *Remote Sens.* 13 (14) (2021) 2830.
- [161] A. Bannari, D. Morin, F. Bonn, A. Huete, A review of vegetation indices, *Remote Sens. Rev.* 13 (1–2) (1995) 95–120.
- [162] N. Pettorelli, J.O. Vik, A. Mysterud, J.-M. Gaillard, C.J. Tucker, N.C. Stenseth, Using the satellite-derived NDVI to assess ecological responses to environmental change, *Trends Ecol. Evol.* 20 (9) (2005) 503–510.
- [163] C.N. Thompson, W. Guo, B. Sharma, G.L. Ritchie, Using normalized difference red edge index to assess maturity in cotton, *Crop Sci.* 59 (5) (2019) 2167–2177.
- [164] I. Pôças, A. Calera, I. Campos, M. Cunha, Remote sensing for estimating and mapping single and basal crop coefficients: A review on spectral vegetation indices approaches, *Agricul. Water Manag.* 233 (2020) 106081.
- [165] T. Dong, J. Liu, J. Shang, B. Qian, B. Ma, J.M. Kovacs, D. Walters, X. Jiao, X. Geng, Y. Shi, Assessment of red-edge vegetation indices for crop leaf area index estimation, *Remote Sens. Environ.* 222 (2019) 133–143.

- [166] M. Bietresato, G. Carabin, D. D'Auria, R. Gallo, G. Ristorto, F. Mazzetto, R. Vidoni, A. Gasparetto, L. Scalera, A tracked mobile robotic lab for monitoring the plants volume and health, in: 2016 12th IEEE/ASME International Conference on Mechatronic and Embedded Systems and Applications, MESA, 2016, pp. 1–6.
- [167] S. Khanal, J. Fulton, S. Shearer, An overview of current and potential applications of thermal remote sensing in precision agriculture, *Comput. Electron. Agric.* 139 (2017) 22–32.
- [168] C. Peng, Z. Fei, S.G. Vougioukas, Depth camera based row end detection and headland maneuvering in orchard navigation without GNSS, in: 30th Mediterranean Conference on Control and Automation, Athens, Greece, IEEE, 2022, pp. 538–544.
- [169] J. Chen, H. Qiang, J. Wu, G. Xu, Z. Wang, Navigation path extraction for greenhouse cucumber-picking robots using the prediction-point Hough transform, *Comput. Electron. Agric.* 180 (2021) 105911.
- [170] G. Colucci, A. Botta, L. Tagliavini, P. Cavallone, L. Baglieri, G. Quaglia, Kinematic modeling and motion planning of the mobile manipulator AgriQ for precision agriculture, *Machines* 10 (5) (2022) 321.
- [171] Z. Fei, S. Vougioukas, Row-sensing templates: A generic 3D sensor-based approach to robot localization with respect to orchard row centerlines, *J. Field Robotics* 39 (2022) 712–738.
- [172] M. Kragh, R.N. Jørgensen, H. Pedersen, Object detection and terrain classification in agricultural fields using 3D LiDAR data, in: International Conference on Computer Vision Systems, Springer, 2015, pp. 188–197.
- [173] Q. Li, Y. Xu, Minimum-time row transition control of a vision-guided agricultural robot, *J. Field Robotics* 39 (2022) 335–354.
- [174] F.Y. Narváez, E. Gregorio, A. Escolà, J.R. Rosell-Polo, M. Torres-Torriti, F.A. Cheein, Terrain classification using ToF sensors for the enhancement of agricultural machinery traversability, *J. Terramech.* 76 (2018) 1–13.
- [175] M. Chen, Y. Tang, X. Zou, Z. Huang, H. Zhou, S. Chen, 3D global mapping of large-scale unstructured orchard integrating eye-in-hand stereo vision and SLAM, *Comput. Electron. Agric.* 187 (2021) 106237.
- [176] M. Skoczeń, M. Ochman, K. Spyra, M. Nikodem, D. Krata, M. Panek, A. Pawłowski, Obstacle detection system for agricultural mobile robot application using RGB-D cameras, *Sensors* 21 (16) (2021) 5292.
- [177] F. Yandun, T. Parhar, A. Silwal, D. Clifford, Z. Yuan, G. Levine, S. Yaroshenko, G. Kantor, Reaching pruning locations in a vine using a deep reinforcement learning policy, in: 2021 IEEE International Conference on Robotics and Automation, ICRA, IEEE, 2021, pp. 2400–2406.
- [178] X. Zhang, Y. Guo, J. Yang, D. Li, Y. Wang, R. Zhao, Many-objective evolutionary algorithm based agricultural mobile robot route planning, *Comput. Electron. Agric.* 200 (2022) 107274.
- [179] D. Reiser, J.M. Martín-López, E. Memic, M. Vázquez-Arellano, S. Brandner, H.W. Grieppentrog, 3D imaging with a sonar sensor and an automated 3-axes frame for selective spraying in controlled conditions, *J. Imaging* 3 (1) (2017) 9.
- [180] J.P. Simões, P.D. Gaspar, E. Assunção, R. Mesquita, M.P. Simões, Navigation system of autonomous multitask robotic rover for agricultural activities on peach orchards based on computer vision through tree trunk detection, in: X International Peach Symposium 1352, 2022, pp. 593–600.
- [181] S.P. Adhikari, G. Kim, H. Kim, Deep neural network-based system for autonomous navigation in paddy field, *IEEE Access* 155 (2020) 71272–71278.
- [182] A.S. Aguiar, N.N. Monteiro, F.N. dos Santos, E.J. Solteiro Pires, D. Silva, A.J. Sousa, J. Boaventura Cunha, Bringing semantics to the vineyard: An approach on deep learning-based vine trunk detection, *Agriculture* 11 (2021) 131.
- [183] V. Mazzia, A. Khaliq, F. Salvetti, M. Chiaberge, Real-time apple detection system using embedded systems with hardware accelerators: An edge AI application, *IEEE Access* 8 (2020) 9102–9114.
- [184] P.K. Panigrahi, S.K. Bisoy, Localization strategies for autonomous mobile robots: A review, *J. King Saud Univ. - Comput. Inf. Sci.* 34 (8, Part B) (2022) 6019–6039.
- [185] S. Cerrato, D. Aghi, V. Mazzia, F. Salvetti, M. Chiaberge, An adaptive row crops path generator with deep learning synergy, in: 2021 6th Asia-Pacific Conference on Intelligent Robot Systems, ACIRS, IEEE, 2021, pp. 6–12.
- [186] P. Gao, H. Lee, C.-W. Jeon, C. Yun, H.-J. Kim, W. Wang, G. Liang, Y. Chen, Z. Zhang, X. Han, Improved position estimation algorithm of agricultural mobile robots based on multisensor fusion and autoencoder neural network, *Sensors* 22 (4) (2022) 1522.
- [187] C. Debeunne, D. Vivet, A review of visual-LiDAR fusion based simultaneous localization and mapping, *Sensors* 20 (7) (2020) 2068.
- [188] S. Se, D. Lowe, J. Little, Vision-based mobile robot localization and mapping using scale-invariant features, in: IEEE International Conference on Robotics and Automation, vol. 2, IEEE, 2001, pp. 2051–2058.
- [189] J. Dong, J.G. Burnham, B. Boots, G. Rains, F. Dellaert, 4D crop monitoring: Spatio-temporal reconstruction for agriculture, in: 2017 IEEE International Conference on Robotics and Automation, ICRA, IEEE, 2017, pp. 3878–3885.
- [190] R. Mur-Artal, J.M.M. Montiel, J.D. Tardos, ORB-SLAM: A versatile and accurate monocular SLAM system, *IEEE Trans. Robot.* 31 (5) (2015) 1147–1163.
- [191] R. Mur-Artal, J.D. Tardos, ORB-SLAM2: An open-source SLAM system for monocular, stereo and RGB-D cameras, *IEEE Trans. Robot.* 33 (5) (2017) 1255–1262.
- [192] F. Shu, P. Lesur, Y. Xie, A. Pagani, D. Stricker, SLAM in the field: An evaluation of monocular mapping and localization on challenging dynamic agricultural environment, in: IEEE/CVF Winter Conference on Applications of Computer Vision, 2021, pp. 1761–1771.
- [193] W. Zhao, X. Wang, B. Qi, T. Runge, Ground-level mapping and navigating for agriculture based on IoT and computer vision, *IEEE Access* 8 (2020) 221975–221985.
- [194] C. Campos, R. Elvira, J.J.G. Rodríguez, J.M. Montiel, J.D. Tardós, ORB-SLAM3: An accurate open-source library for visual, visual-inertial, and multimap SLAM, *IEEE Trans. Robot.* 37 (6) (2021) 1874–1890.
- [195] J. Cremona, R. Comelli, T. Pire, Experimental evaluation of visual-inertial odometry systems for arable farming, *J. Field Robot.* 39 (7) (2022) 1121–1135.
- [196] M. Labbé, F. Michaud, RTAB-Map as an open-source LiDAR and visual simultaneous localization and mapping library for large-scale and long-term online operation, *J. Field Robotics* 36 (2) (2019) 416–446.
- [197] R. Comelli, T. Pire, E. Kofman, Evaluation of visual SLAM algorithms on agricultural dataset, *Reunión de Trabajo en Procesamiento de la Información y Control* (2019) 1–6.
- [198] S. Thrun, Probabilistic robotics, *Commun. ACM* 45 (3) (2002) 52–57.
- [199] G. Grisetti, C. Stachniss, W. Burgard, Improving grid-based SLAM with Rao-Blackwellized particle filters by adaptive proposals and selective resampling, in: Proceedings of the 2005 IEEE International Conference on Robotics and Automation, 2005, pp. 2432–2437.
- [200] G. Grisetti, C. Stachniss, W. Burgard, Improved techniques for grid mapping with Rao-Blackwellized particle filters, *IEEE Trans. Robot.* 23 (1) (2007) 34–46.
- [201] D.W. Marquardt, An algorithm for least-squares estimation of nonlinear parameters, *J. Soc. Ind. Appl. Math.* 11 (2) (1963) 431–441.
- [202] P.J. Besl, N.D. McKay, Method for registration of 3D shapes, in: Sensor Fusion IV: Control Paradigms and Data Structures, vol. 1611, Spie, 1992, pp. 586–606.
- [203] F. Dellaert, Factor Graphs and GTSAM: A Hands-On Introduction, Tech. Rep., Georgia Institute of Technology, 2012.
- [204] J. Zhang, S. Singh, LOAM: Lidar odometry and mapping in real-time, in: *Robotics: Science and System*, vol. 2, Berkeley, CA, 2014, pp. 1–9.
- [205] T. Shan, B. Englot, LeGO-LOAM: Lightweight and ground-optimized LiDAR odometry and mapping on variable terrain, in: 2018 IEEE/RSJ International Conference on Intelligent Robots and Systems, IROS, 2018, pp. 4758–4765.
- [206] T. Shan, B. Englot, D. Meyers, W. Wang, C. Ratti, D. Rus, LIO-SAM: Tightly-coupled LiDAR inertial odometry via smoothing and mapping, in: 2020 IEEE/RSJ International Conference on Intelligent Robots and Systems, IROS, 2020, pp. 5135–5142.
- [207] E. Liu, Static mapping, 2020, <https://github.com/EdwardLiuyc/StaticMapping>.
- [208] H. Ye, Y. Chen, M. Liu, Tightly coupled 3D LiDAR inertial odometry and mapping, in: 2019 IEEE International Conference on Robotics and Automation, ICRA, IEEE, 2019, pp. 3144–3150.
- [209] P. Biber, W. Straßer, The normal distributions transform: A new approach to laser scan matching, in: IEEE/RSJ International Conference on Intelligent Robots and Systems, vol. 3, IROS 2003, 2003, pp. 2743–2748.
- [210] K. Koide, J. Miura, E. Menegatti, A portable three-dimensional LiDAR-based system for long-term and wide-area people behavior measurement, *Int. J. Adv. Robot. Syst.* 16 (2) (2019) 1729881419841532.
- [211] J. Radcliffe, J. Cox, D.M. Bulanon, Machine vision for orchard navigation, *Comput. Ind.* 98 (2018) 165–171.
- [212] M. Mammarella, L. Comba, A. Biglia, F. Dabbene, P. Gay, Cooperation of unmanned systems for agricultural applications: A case study in a vineyard, *Biosyst. Eng.* 223 (2022) 81–102.
- [213] S.N.A. Ahmed, Y. Zeng, UWB positioning accuracy and enhancements, in: TENCON 2017-2017 IEEE Region 10 Conference, IEEE, 2017, pp. 634–638.
- [214] L. Yao, D. Hu, C. Zhao, Z. Yang, Z. Zhang, Wireless positioning and path tracking for a mobile platform in greenhouse, *Int. J. Agric. Biol. Eng.* 14 (1) (2021) 216–223.
- [215] M.L. Fung, M.Z. Chen, Y.H. Chen, Sensor fusion: A review of methods and applications, in: 2017 29th Chinese Control and Decision Conference, CCDC, IEEE, 2017, pp. 3853–3860.
- [216] S. Hansen, E. Bayramoglu, J.C. Andersen, O. Ravn, N. Andersen, N.K. Poulsen, Orchard navigation using derivative free Kalman filtering, in: Proceedings of the 2011 American Control Conference, IEEE, 2011, pp. 4679–4684.
- [217] J. Iqbal, R. Xu, H. Halloran, C. Li, Development of a multi-purpose autonomous differential drive mobile robot for plant phenotyping and soil sensing, *Electronics* 9 (2020) 1550.
- [218] F.R. Kschischang, B.J. Frey, H.-A. Loeliger, Factor graphs and the sum-product algorithm, *IEEE Trans. Inform. Theory* 47 (2) (2001) 498–519.

- [219] H.-A. Loeliger, An introduction to factor graphs, *IEEE Signal Process. Mag.* 21 (1) (2004) 28–41.
- [220] V. Indelman, S. Williams, M. Kaess, F. Dellaert, Factor graph based incremental smoothing in inertial navigation systems, in: 15th International Conference on Information Fusion, IEEE, 2012, pp. 2154–2161.
- [221] D. Tiozzo Fasiolo, L. Scalera, E. Maset, Comparing LiDAR and IMU-based SLAM approaches for 3D robotic mapping, *Robotica* (2023) 1–17.
- [222] F.Y. Narvaez, G. Reina, M. Torres-Torriti, G. Kantor, F.A. Cheein, A survey of ranging and imaging techniques for precision agriculture phenotyping, *IEEE/ASME Trans. Mechatronics* 22 (6) (2017) 2428–2439.
- [223] M.A. Fischler, R.C. Bolles, Random sample consensus: A paradigm for model fitting with applications to image analysis and automated cartography, *Commun. ACM* 24 (6) (1981) 381–395.
- [224] W. Zhang, J. Qi, P. Wan, H. Wang, D. Xie, X. Wang, G. Yan, An easy-to-use airborne LiDAR data filtering method based on cloth simulation, *Remote Sens.* 8 (6) (2016) 501.
- [225] S.O. Ihuoma, C.A. Madramootoo, Recent advances in crop water stress detection, *Comput. Electron. Agric.* 141 (2017) 267–275.
- [226] D.J. Watson, Comparative physiological studies on the growth of field crops: I. Variation in net assimilation rate and leaf area between species and varieties, and within and between years, *Ann. Botany* 11 (41) (1947) 41–76.
- [227] J. Xue, S. Zhang, et al., Navigation of an agricultural robot based on laser radar, *Trans. Chin. Soc. Agric. Mach.* 45 (9) (2014) 55–60.
- [228] B. Siciliano, L. Sciavicco, L. Villani, G. Oriolo, Motion planning, *Robot.: Model., Plan., Control* (2009) 523–559.
- [229] M. Phillips, SBPL_Lattice_Planner, 2018, http://wiki.ros.org/sbpl_lattice_planner.
- [230] M.S.A. Mahmud, M.S.Z. Abidin, Z. Mohamed, M.K.I. Abd Rahman, M. Iida, Multi-objective path planner for an agricultural mobile robot in a virtual greenhouse environment, *Comput. Electron. Agric.* 157 (2019) 488–499.
- [231] C.-W. Jeon, H.-J. Kim, C. Yun, M. Gang, X. Han, An entry-exit path planner for an autonomous tractor in a paddy field, *Comput. Electron. Agric.* 191 (2021) 106548.
- [232] D. Fox, W. Burgard, S. Thrun, The dynamic window approach to collision avoidance, *IEEE Robot. Autom. Mag.* 4 (1) (1997) 23–33.
- [233] S. Quinlan, O. Khatib, Elastic bands: Connecting path planning and control, in: Proceedings IEEE International Conference on Robotics and Automation, 1993, pp. 802–807.
- [234] J. Reeds, L. Shepp, Optimal paths for a car that goes both forwards and backwards, *Pacific J. Math.* 145 (2) (1990) 367–393.
- [235] N.T. Dang, N.T. Luy, et al., LiDAR-based online navigation algorithm for an autonomous agricultural robot, *J. Control Eng. Appl. Inf.* 24 (2022) 90–100.
- [236] H. Isack, Y. Boykov, Energy-based geometric multi-model fitting, *Int. J. Comput. Vis.* 97 (2) (2012) 123–147.
- [237] A. Danton, J.-C. Roux, B. Dance, C. Cariou, R. Lenain, Development of a spraying robot for precision agriculture: An edge following approach, in: 2020 IEEE Conference on Control Technology and Applications, CCTA, IEEE, 2020, pp. 267–272.
- [238] D. Iberraken, F. Gaurier, J.-C. Roux, C. Chaballier, R. Lenain, Autonomous vineyard tracking using a four-wheel-steering mobile robot and a 2D LiDAR, *AgriEngineering* 4 (4) (2022) 826–846.
- [239] R.O. Duda, P.E. Hart, Use of the Hough transformation to detect lines and curves in pictures, *Commun. ACM* 15 (1) (1972) 11–15.
- [240] J. Canny, A computational approach to edge detection, *IEEE Trans. Pattern Anal. Mach. Intell.* (1986) 679–698.
- [241] M. Sharifi, X. Chen, A novel vision based row guidance approach for navigation of agricultural mobile robots in orchards, in: 2015 6th International Conference on Automation, Robotics and Applications, ICARA, IEEE, 2015, pp. 251–255.
- [242] X. Liang, B. Chen, C. Wei, X. Zhang, Inter-row navigation line detection for cotton with broken rows, *Plant Methods* 18 (2022) 1–12.
- [243] P. Ruangurai, M.N. Dailey, M. Ekpanyapong, P. Soni, Optimal vision-based guidance row locating for autonomous agricultural machines, *Precis. Agric.* (2022) 1–21.
- [244] Y. Hu, H. Huang, Extraction method for centerlines of crop row based on improved lightweight YoloV4, in: 2021 6th International Symposium on Computer and Information Processing Technology, ISCIPT, IEEE, 2021, pp. 127–132.
- [245] R. Bajcsy, Active perception, *Proc. IEEE* 76 (1988) 966–1005.
- [246] I. Lluvia, E. Lazcano, A. Ansuaegi, Active mapping and robot exploration: A survey, *Sensors* 21 (2021) 2445.
- [247] B. Yamauchi, A frontier-based approach for autonomous exploration, in: Proceedings 1997 IEEE International Symposium on Computational Intelligence in Robotics and Automation, CIRA, IEEE, 1997, pp. 146–151.
- [248] B. Yamauchi, A. Schultz, W. Adams, Mobile robot exploration and map-building with continuous localization, in: Proceedings 1998 IEEE International Conference on Robotics and Automation, vol. 4, IEEE, 1998, pp. 3715–3720.
- [249] M. Keidar, G.A. Kaminka, Efficient frontier detection for robot exploration, *Int. J. Robot. Res.* 33 (2014) 215–236.
- [250] C. Dornhege, A. Kleiner, A frontier-void-based approach for autonomous exploration in 3D, *Adv. Robot.* 27 (2013) 459–468.
- [251] P. Senarathne, D. Wang, Towards autonomous 3D exploration using surface frontiers, in: 2016 IEEE International Symposium on Safety, Security, and Rescue Robotics, SSRR, 2016, pp. 34–41.
- [252] A. Bircher, M. Kamel, K. Alexis, H. Oleynikova, R. Siegwart, Receding horizon “next-best-view” planner for 3D exploration, in: 2016 IEEE International Conference on Robotics and Automation, ICRA, 2016, pp. 1462–1468.
- [253] R. Polvara, F. Del Dutto, G. Neumann, M. Hanheide, Navigate-and-seek: A robotics framework for people localization in agricultural environments, *IEEE Robot. Automat. Lett.* 6 (2021) 6577–6584.
- [254] D. Holz, N. Basilico, F. Amigoni, S. Behnke, Evaluating the efficiency of frontier-based exploration strategies, in: ISR 2010 (41st International Symposium on Robotics) and ROBOTIK 2010 (6th German Conference on Robotics), VDE, 2010, pp. 1–8.
- [255] C. Stachniss, D. Hahnel, W. Burgard, Exploration with active loop-closing for FastSLAM, in: 2004 IEEE/RSJ International Conference on Intelligent Robots and Systems, vol. 2, IROS, 2004, pp. 1505–1510.
- [256] V.A. Metre, S.D. Sawarkar, Reviewing important aspects of plant leaf disease detection and classification, in: 2022 International Conference for Advancement in Technology, ICONAT, IEEE, 2022, pp. 1–8.
- [257] A. Ahmadi, M. Halstead, C. McCool, Virtual temporal samples for recurrent neural networks: Applied to semantic segmentation in agriculture, in: DAGM German Conference on Pattern Recognition, vol. 13024, Springer, 2021, pp. 574–588.
- [258] E. Maset, B. Padova, A. Fusielo, Efficient large-scale airborne LiDAR data classification via fully convolutional network, *Int. Arch. Photogram., Remote Sens. Spat. Inf. Sci.* 43 (2020) 527–532.
- [259] R. Girshick, I. Radosavovic, G. Gkioxari, P. Dollár, K. He, Detectron, 2018, <https://github.com/facebookresearch/detectron>.
- [260] K. He, G. Gkioxari, P. Dollár, R. Girshick, Mask R-CNN, in: Proceedings of the IEEE International Conference on Computer Vision, 2017, pp. 2961–2969.
- [261] J. Redmon, A. Farhadi, YOLO9000: Better, faster, stronger, in: Proceedings of the IEEE Conference on Computer Vision and Pattern Recognition, 2017, pp. 7263–7271.
- [262] J. Redmon, A. Farhadi, Yolov3: An incremental improvement, 2018, arXiv preprint [arXiv:1804.02767](https://arxiv.org/abs/1804.02767).
- [263] M. Tan, Q. Le, Efficientnet: Rethinking model scaling for convolutional neural networks, in: International Conference on Machine Learning, PMLR, 2019, pp. 6105–6114.
- [264] L. Fu, Y. Feng, J. Wu, Z. Liu, F. Gao, Y. Majeed, A. Al-Mallahi, Q. Zhang, R. Li, Y. Cui, Fast and accurate detection of kiwifruit in orchard using improved YOLOv3-tiny model, *Precis. Agric.* 22 (3) (2021) 754–776.
- [265] X. Xia, C. Xu, B. Nan, Inception-v3 for flower classification, in: 2017 2nd International Conference on Image, Vision and Computing, ICIVC, IEEE, 2017, pp. 783–787.
- [266] L.-C. Chen, Y. Zhu, G. Papandreou, F. Schroff, H. Adam, Encoder-decoder with atrous separable convolution for semantic image segmentation, in: Proceedings of the European Conference on Computer Vision, ECCV, 2018, pp. 801–818.
- [267] D. Bolya, C. Zhou, F. Xiao, Y.J. Lee, Yolact: Real-time instance segmentation, in: IEEE/CVF International Conference on Computer Vision, 2019, pp. 9157–9166.
- [268] O. Ronneberger, P. Fischer, T. Brox, U-net: Convolutional networks for biomedical image segmentation, in: International Conference on Medical Image Computing and Computer-Assisted Intervention, Springer, 2015, pp. 234–241.
- [269] A. Howard, M. Sandler, G. Chu, L.-C. Chen, B. Chen, M. Tan, W. Wang, Y. Zhu, R. Pang, V. Vasudevan, et al., Searching for MobilenetV3, in: Proceedings of the IEEE/CVF International Conference on Computer Vision, 2019, pp. 1314–1324.
- [270] L.C. Santos, A.S. Aguiar, F.N. Santos, A. Valente, M. Petry, Occupancy grid and topological maps extraction from satellite images for path planning in agricultural robots, *Robotics* 9 (2020) 77.
- [271] S. Matsuzaki, J. Miura, H. Masuzawa, Multi-source pseudo-label learning of semantic segmentation for the scene recognition of agricultural mobile robots, *Adv. Robot.* (2022) 1–19.
- [272] T. Zaenker, C. Smitt, C. McCool, M. Bennewitz, Viewpoint planning for fruit size and position estimation, in: 2021 IEEE/RSJ International Conference on Intelligent Robots and Systems, IROS, IEEE, 2021, pp. 3271–3277.
- [273] T. Sipola, J. Alatalo, T. Kokkonen, M. Rantonen, Artificial intelligence in the IoT era: A review of edge AI hardware and software, in: 2022 31st Conference of Open Innovations Association, FRUCT, IEEE, 2022, pp. 320–331.
- [274] M. Gonzalez-de Soto, L. Emmi, P. Gonzalez-de Santos, Hybrid-powered autonomous robots for reducing both fuel consumption and pollution in precision agriculture tasks, *Agric. Robots-Fund. Appl.* (2018).

- [275] T. Dharmasena, R. de Silva, N. Abhayasingha, P. Abeygunawardhana, Autonomous cloud robotic system for smart agriculture, in: 2019 Moratuwa Engineering Research Conference, MERCon, IEEE, 2019, pp. 388–393.
- [276] D. Albiero, A.P. Garcia, C.K. Umez, R.L. de Paulo, Swarm robots in mechanized agricultural operations: A review about challenges for research, Comput. Electronic. Agric. 193 (2022) 106608.
- [277] K. Chen, B.T. Lopez, A.-a. Agha-mohammadi, A. Mehta, Direct LiDAR odometry: Fast localization with dense point clouds, IEEE Robot. Autom. Lett. 7 (2) (2022) 2000–2007.
- [278] R.A. Newcombe, S.J. Lovegrove, A.J. Davison, DTAM: Dense tracking and mapping in real-time, in: 2011 International Conference on Computer Vision, IEEE, 2011, pp. 2320–2327.
- [279] W. Wang, J. Liu, C. Wang, B. Luo, C. Zhang, DV-LOAM: Direct visual LiDAR odometry and mapping, Remote Sens. 13 (16) (2021) 3340.
- [280] H. Wang, C. Wang, C.-L. Chen, L. Xie, F-LOAM: Fast LiDAR odometry and mapping, in: 2021 IEEE/RSJ International Conference on Intelligent Robots and Systems, IROS, 2021, pp. 4390–4396.
- [281] E. Garcia-Fidalgo, J.P. Company-Corcoles, F. Bonnin-Pascual, A. Ortiz, LiODOM: Adaptive local mapping for robust LiDAR-only odometry, Robot. Auton. Syst. 156 (2022) 104226.
- [282] T. Shan, B. Englot, C. Ratti, D. Rus, LVI-SAM: Tightly-coupled LiDAR-visual-inertial odometry via smoothing and mapping, in: 2021 IEEE International Conference on Robotics and Automation, ICRA, 2021, pp. 5692–5698.
- [283] J. Engel, T. Schöps, D. Cremers, LSD-SLAM: Large-scale direct monocular SLAM, in: European Conference on Computer Vision, Springer, 2014, pp. 834–849.
- [284] Y. He, J. Zhao, Y. Guo, W. He, K. Yuan, PL-VIO: Tightly-coupled monocular visual-inertial odometry using point and line features, Sensors 18 (4) (2018) 1159.
- [285] R. Wang, M. Schworer, D. Cremers, Stereo DSO: Large-scale direct sparse visual odometry with stereo cameras, in: Proceedings of the IEEE International Conference on Computer Vision, 2017, pp. 3903–3911.
- [286] C. Forster, M. Pizzoli, D. Scaramuzza, SVO: Fast semi-direct monocular visual odometry, in: 2014 IEEE International Conference on Robotics and Automation, ICRA, IEEE, 2014, pp. 15–22.
- [287] A. Vaswani, N. Shazeer, N. Parmar, J. Uszkoreit, L. Jones, A.N. Gomez, L. Kaiser, I. Polosukhin, Attention is all you need, Adv. Neural Inf. Process. Syst. 30 (2017).



Diego Tiozzo Fasiolo studied Mechanical Engineering at the University of Padova (Italy), received his Bachelor's Degree in 2019, and his Master's Degree in 2021. Since 2021, he is working at University of Udine (Italy) as a Ph.D. student of the Italian National Doctorate in Artificial Intelligence for Agriculture (Agrifood) and Environment coordinated by the University of Naples Federico II (Italy). His research interests are in the fields of mobile robotics, autonomous navigation, and 3D mapping.



Lorenzo Scalera achieved the Master's Degree in Mechanical Engineering (cum laude) at University of Trieste (Italy) in 2015, and the Ph.D. Degree in Industrial and Information Engineering at University of Udine (Italy) in 2019. In 2018 he was a visiting Ph.D. student at the Stevens Institute of Technology in Hoboken (NJ, USA). In 2019 he was a Post Doc Research Fellow at Free University of Bozen-Bolzano (Italy). Since 2020 he is Assistant Professor of Mechanics Applied to Machines at the Polytechnic Department of Engineering and Architecture of the University of Udine. His research interests include dynamic modeling of robotic systems, trajectory planning, collaborative robotics, human-machine interfaces, and mobile robotics.



Eleonora Maset received the Master's Degree in Environmental Engineering (cum laude) in 2015, and the Ph.D. degree in Industrial and Information Engineering from the University of Udine (Italy), in 2019. She currently holds a post-doctoral position at the Polytechnic Department of Engineering and Architecture, University of Udine. Her research interests include image orientation, point cloud processing, indoor modeling, and mobile robotics.



Alessandro Gasparetto (Rovigo - Italy, 26 October 1968) received the M.Sc. in Electronic Engineering from the University of Padova, Italy, in 1992; the M.Sc. in Mathematics from University of Padova, Italy, in 2003; the Ph.D. in Mechanics of Machines from University of Brescia, Italy, in 1996. He is Full Professor of Mechanics of Machines at the Polytechnic Department of Engineering and Architecture, University of Udine (Udine, Italy), where he is the head of the research group in Mechatronics and Robotics, as well as the Head of the Department (since 2021). He has been included in the ranking of the top 2% most quoted and authoritative scientists in the world, published by researchers at Stanford University (2019 and 2021). Since 2017, he is the Chair of IFToMM Italy, the Italian branch of IFToMM (the International Federation for the Promotion of Mechanism and Machine Science). Since 2018, he is the Chair of the IFToMM Permanent Commission for the History of Mechanism and Machine Science. His research interests are in the fields of modeling and control of mechatronic systems, robotics, mechanical design, industrial automation, mechanical vibrations. He is author of more than 200 international publications and has been involved in the scientific and organizing committees of several conferences, as well as in many research projects, at the regional, national and European level.